Report

Nord2000. Comprehensive Outdoor Sound Propagation Model. Part 1: Propagation in an Atmosphere without Significant Refraction.

Client: Nordic Noise Group & Nordic Road Directorates

AV 1849/00
Page 1 of 127

31 December 2000
Revised 31 December 2001
Revised 31 March 2006

DELTA
Danish Electronics,
Light & Acoustics

Venlighedsvej 4
2970 Hørsholm
Danmark

Tlf. (+45) 72 19 40 00
Fax (+45) 72 19 40 01
www.delta.dk

Title
Nord2000. Comprehensive Outdoor Sound Propagation Model. Part 1: Propagation in an Atmosphere without Significant Refraction.

Journal no.	**Project no.**	**Our ref.**
AV 1849/00	A550054	BP\JK\lm

Client
Nordic Noise Group & Nordic Road Directorates

Summary

See page 9.

DELTA, 31 March 2006

Birger Plovsing
Noise & Vibraton

Contents

List of Symbols

j	Complex unit ($=\sqrt{-1}$)
f	Frequency (at the centre frequency in case of 1/3 octave bands)
k	Wave number ($=2\pi f/c \quad =2\pi/\lambda$)
ω	Angular frequency ($=2\pi f$)
c	Speed of sound ($=20.05\sqrt{t+273.15}$)
λ	Wave length ($=c/f$)
L	Sound pressure level
L_W	Sound power level
A	Attenuation
ΔL	Propagation effect (ΔL=-A)
ΔL_d	Propagation effect of spherical divergence
ΔL_a	Propagation effect of air absorption
ΔL_t	Propagation effect of terrain (ground and barriers)
ΔL_s	Propagation effect of scattering zones
ΔL_r	Propagation effect of reflecting obstacle
p	Complex pressure
p_{diffr}	Complex pressure from a diffracted path
p_0	Complex pressure from free field wave
α	Phase angle
x,y,z	Spatial coordinates
P	Point (1-D, 2-D and 3-D)
d	Horizontal distance
h	Vertical height
h_S	Height of source above local ground
h_R	Height of receiver above local ground
R	Distance between to points
ℓ	Path length
$\Delta\ell$	Path length difference
θ	Angle (of incidence or diffraction)
ψ_G	Grazing angle (=π/2-θ)
S	Surface area
β	Wedge angle

Q	Spherical wave reflection coefficient
$\Re_p$	Plane wave reflection coefficient
$\Re$	Pressure-amplitude reflection coefficient based on the random incidence absorption coefficient
ρ_E	Energy reflection coefficient (= $\lvert\Re\rvert^2$)
Z	Acoustic impedance (normalised, specific)
σ	Flow resistivity
σ_r	Roughness parameter
D	Diffraction coefficient
R_{ve}	Transmission loss from diffraction of a vertical edge
F_λ	Fraction of the wavelength (used in determination of Fresnel-zones)
w	Fresnel-zone weight

F	Fraction of coherent sound
F_f	Fraction of coherent sound, frequency band averaging
$F_{\Delta\tau}$	Fraction of coherent sound, fluctuating refraction
F_c	Fraction of coherent sound, turbulence
F_r	Fraction of coherent sound, surface roughness
F_s	Fraction of coherent sound, scattering zones

u	Average wind speed component in the direction of propagation
σ_u	Standard deviation of the wind speed component in the direction of propagation
t	Temperature in °C
dt/dz	Average temperature gradient
$\sigma_{dt/dz}$	Standard deviation of the temperature gradient
z_0	Roughness length
τ	Travel time along a sound ray
C_v^2	Structure parameter of turbulent wind speed fluctuations
C_T^2	Structure parameter of turbulent temperature fluctuations

Subscripts

S	Source
R	Receiver
SCR	Screen

Functions

ln	Natural logarithm (base e)
log	Logarithm to base 10
H(x)	Heavisides' step function (H = 1 for $x \geq 0$ and H = 0 for $x < 0$)
sign(x)	Signum function (sign = 1 for $x > 0$, sign = 0 for $x = 0$, sign = -1 for $x < 0$)

Preface

This prediction method has been developed within the frame of a Nordic project, Nord 2000. It would not have been possible without the generous support from authorities and research councils throughout the Nordic countries. The main financial support has come from the Nordic Council of Ministers but additional support, both to the main project and to related projects, has come from the following organizations:

- Miljøstyrelsen, Denmark
- Danish Road Directorate
- Danish National Railways
- Ministry of the Environment, Finland
- The Finnish Road Administration
- The Norwegian Road Administration
- Norwegian State Pollution Authority
- The Swedish Rail Administration
- The Swedish Road Administration
- The National Board of Health and Welfare, Sweden
- The Swedish Transport & Communications Research Board
- Nordtest

The prediction method was developed by a joint Nordic project group consisting of Jørgen Kragh and Birger Plovsing, DELTA Danish Electronics, Light & Acoustics, Denmark, Svein Storeheier, Sintef Telecom and Informatics, Norway, and Hans Jonasson, Mikael Ögren and Xuetao Zhang, SP Swedish National Testing and Research Institute. Juhani Parmanen, VTT Building Technology, Finland has been an observer.

The support of the above organisations and individuals is gratefully acknowledged.

Valuable contributions have furthermore been received from Jens Forssén, Dept. of Applied Acoustics, Chalmers University of Technology, Sweden concerning the effect of atmospheric turbulence and from Susana Quirós-Alpera, Departamento de Física, E.T.S. de Arquitectura de Valladolid, Spain who has been doing calculations by the Boundary Element Method used to validate the propagation model.

In 2005-2006, the prediction method has been revised with financial support from Nordic Road Administrations mentioned above. The present report is replacing the earlier version of the report AV 1849/00. The revision has been carried out by a joint Nordic project

group consisting of Jørgen Kragh and Birger Plovsing, DELTA (Denmark), Svein Storeheier and Gunnar Taraldsen, SINTEF (Norway), Hans Jonasson, SP (Sweden), and Ari Saarinen, VTT (Finland).

The changes in the Nord2000 method which have taken place since 2001 have been summarized in the report AV 1307/06: “Changes in the Nord2000 method since year 2001”.

Validation of the model has been described in the report AV 1117/06: “Nord2000. Validation of the Propagation Model”.

Summary

The present report contains a full description of the new Nordic comprehensive model for sound propagating outdoors in an atmosphere without significant refraction. The model is based on geometrical ray theory and theory of diffraction and calculations are carried out in one-third octave bands. The model is applicable for any non-flat terrain approximated by a segmented terrain shape (a number of straight line segments) with or without screens. The effect of scattering by objects such as housing areas or forests can be included in the model using a statistical approach. In the model ground surface properties is characterised by its impedance and roughness (unevenness) and may vary along the propagation path. The model may also include the effect of reflection from obstacles.

The model has in approximate manner been extended to include propagation in moderately refracting atmospheres which is described in a companion report AV 1851/00: "Nord2000. Comprehensive Outdoor Sound Propagation Model. Part 2: Propagation in an Atmosphere with Refraction".

The comprehensive sound propagation model will be used in new Nordic prediction models for various types of sources.

During the elaboration of the model a number of subtasks has been carried out and reported in a number of background reports.

1. Introduction

The present report contains a detailed description of the new Nordic comprehensive model for sound propagating outdoors in an atmosphere without significant refraction. The model is based on geometrical ray theory and theory of diffraction and calculations are carried out in one-third octave bands. The model is applicable for any non-flat terrain approximated by a segmented shape (a number of straight line segments) with or without screens. The effect of scattering by objects such as housing areas or forests can be included in the model. In the model ground surface properties is characterised by its impedance and roughness (unevenness) and may vary along the propagation path. The model may also include the effect of reflection from obstacles. The model has in approximate manner been extended to include propagation in moderately refracting atmospheres which has been described in a companion report [20].

The elaborated comprehensive model will be used in new Nordic prediction models for various types of sources. A general overview of the work with the Nordic prediction models can be found in [12].

The elaboration of the comprehensive model has been carried out since 1996 and subtasks within the project have along the way been reported in a number of background reports. Contrary to the present report these reports contain a discussion of the solutions and comparison of prediction results with measurements or with results obtained by other prediction models. The background reports are:

- [31] describes the chosen basic geometrical ray theory model and the diffraction model and contains an evaluation of the chosen diffraction model in comparison with other theoretical models.

- [16] describes a method elaborated for predicting propagation over flat terrain with varying ground surface properties. The method is based on a Fresnel-zone approach.

- [17] describes a method elaborated for predicting propagation over non-flat valley-shaped terrain. The method is similarly based on a Fresnel-zone approach.

- [18] describes a method elaborated for predicting propagation over non-flat terrain with one screen. The report also contains a first proposal for a comprehensive model which introduces incoherent effects and combine available models for different kind of terrain.

- [19] describes a method elaborated for predicting propagation over non-flat terrain with more than one screen.

- [32] describes a method for calculating the effect of scattering from turbulence in the shadow zone of a screen.

- [33] describes a method for including finite length of screens.

- [25] describes methods for including the effect of terrain roughness.

- [26] and [27] describe a statistical method for prediction of the effect of scattering object along the propagation path. The method is used for propagation through housing areas and forests.

- [28] contains acoustical classification of ground surface types.

- [29] and [30] describe methods to include reflections from obstacles

The comprehensive model outlined in the present report may reflect changes that have taken place in the principles since the background reports have been published.

In the development of the comprehensive model two of the main demands have been

- to avoid discontinuities whenever possible

- and to organise the model so that is not sensitive to terrain segmentation in the sense that the model produces the same result for two different segmented terrains which virtually are the same.

In some parts of the model, it has not been possible to find solutions with a physical foundation. In such cases a logical solution has been chosen with respect to these two demands.

2. Basic Components

2.1 Point Source

The propagation model predicts the sound pressure level at the receiver in one-third octave bands from 25 Hz to 10 kHz. The propagation model is valid for a point source and predictions are based on the sound power level of the source in one-third octave bands. The sound pressure level L_R at the receiver is for each frequency band predicted according to Eq. (1).

$$L_R = L_W + \Delta L_d + \Delta L_a + \Delta L_t + \Delta L_s + \Delta L_r \qquad (1)$$

where

L_W is the sound power level within the considered frequency band,

ΔL_d is the propagation effect of spherical divergence of the sound energy,

ΔL_a is the propagation effect of air absorption,

ΔL_t is the propagation effect of the terrain (ground and barriers),

ΔL_s is the propagation effect of scattering zones,

ΔL_r is the propagation effect of obstacle dimensions and surface properties when calculating a contribution from sound reflected by an obstacle.

The propagation effects mentioned above are assumed to be independent and can therefore be predicted separately. The only exception is the effect of the terrain ΔL_t and the effect of scattering zones ΔL_s which may interact to some extent as a decrease in coherence introduced by the latter effect may affect the prediction of the former effect.

The propagation effects in Eq. (1) are determined on basis of propagation parameters measured along the propagation path from the source to the receiver. The propagation path is in this connection the projection of the source-receiver line onto the horizontal plane. Normally the propagation path is a straight line between the source and the receiver. However, when sound is diffracted around the vertical edge of a screen with a finite length (see Section 4.6) or reflected by an obstacle (see Section 6) the propagation path will be a broken line.

If a real source cannot be approximated by a single point source, the real source (denoted the extended source in the following) has to be approximated by a number of incoherent point sources. Eq. (1) is used for each point source and L_R for each point source are added incoherently.

If the point source is not omnidirectional but has a directivity pattern, L_W is determined as the sound power level of the equivalent monopole which produce the same sound pressure level in the direction of the propagation path as the directivity dependent source. L_W should therefore be interpreted as the combination of the sound power level and the directivity correction.

ΔL_d which is independent of the frequency is calculated by Eq. (2). R is the distance between source and receiver.

$$\Delta L_d = -10 \log \left(4 \pi R^2\right) \tag{2}$$

The remaining effects in Eq. (1) which all depend on the frequency will be described in the following sections of this report.

2.2 Moving Source

The propagation model outlined in the present report is basically developed for calculating the sound pressure level at the receiver from a stationary extended source. In case of moving sources the straight forward approach when using the model will be to approximate the movement by a number of extended source points on the source track. A suitable incremental distance or time spacing between points must be chosen to ensure that the point is representative to the propagation condition of any point on the small track segment where the source point is placed in the middle. By this approach often called simulation, it is possible to calculate the sound pressure level time history and from that determine different noise metrics such as the sound exposure level L_{AE} or the maximum level L_{Amax} from a pass-by.

In a simulation approach it is only considered necessary to include the third dimension when determining the contribution from reflecting obstacles. Due to averaging from the movement the effect of diffraction around vertical edges of a finite screen (see Section 4.6) can be ignored and for the same reason only the mix of surface properties determined along the propagation path has to be considered (see Section 4.4.1.2).

However, the use of simulation with small space increments between source positions is very costly from a time consumption point of view. Therefore, for the calculation of time integrated noise levels larger track segments can be allowed in case of a simple propagation environment. Each segment is represented by one equivalent extended source placed at the acoustic mean point of the segment. The mean point is determined by the line from the source dividing the angle of view of the track segment under consideration into two equally large angles as shown in Figure 1.

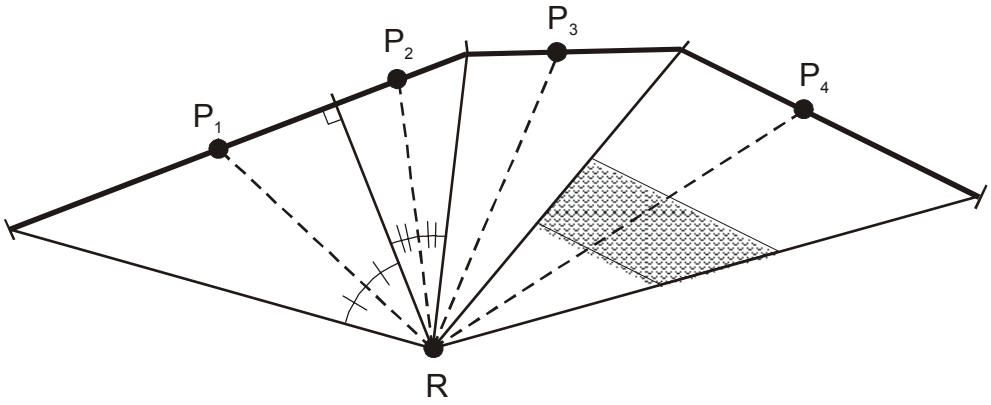

Figure 1
Line source segments.

The definition of track segments has to follow certain requirements:

1. The track segment must have a limited size compared to the shortest distance from the receiver to the track.
2. The point on the track where the normal to the track goes through the receiver (closest point) must always be used as a segment end point to ensure that the mean point represents average propagation within the segment.
3. The terrain cross-section between any point on the track segment and the receiver with respect to terrain shape and surface properties must only show small deviations from the cross-section between the equivalent source and the receiver when scaled to the same the propagation distance.
4. Source emission properties and source speed are only allowed to vary insignificantly within a track segment.

Rules for subdividing the track of a moving source into track segments can be found in the prediction methods [10] and [11].

As in the case of simulation the effect of diffraction around vertical edges of a finite screen is again ignored in the calculation of the propagation effect but due to rule no. 3 vertical edges of finite screens will normally lead to subdividing of track segments.

Rule no. 3 also states that only moderate changes in surface properties may take place compared to the surface properties for the propagation line between the equivalent source and the receiver. However, as some variation is allowed the mix of surface properties should not be determined along the propagation line alone as prescribed for simulation but within an area on each side of the propagation line (the cross-hatched area shown in Figure 1). The area is determined by the angle of view and lines parallel to the track segment through terrain profile segment end points (see Section 4.1).

3. Effect of Air Absorption

The propagation effect of air absorption is calculated on the basis of ISO 9613-1 [7]. It predicts pure-tone attenuation from 50 Hz to 10,000 Hz.

However, pure-tone attenuation coefficients cannot always be applied accurately to determine the attenuation of broadband sound analysed by one-third octave band filters. The band attenuation depends on the finite width and shape of the bandpass filters and the strong frequency-dependent characteristics of atmospheric attenuation.

A method for taking into account these effects is described in [8]. The method is founded on theoretical considerations but adjusted empirically. According to the method the one-third octave band attenuation is determined from the pure-tone attenuation A_0 over the propagation path at the exact centre frequency as shown in Eq. (3).

$$\Delta L_a = -A_0 \left(1.0053255 - 0.00122622\ A_0\right)^{1.6} \tag{3}$$

According to Eq. (3) the band attenuation will be reduced compared to the attenuation at the centre frequency and the reduction is increasing with increasing centre frequency attenuation as shown in Figure 2.

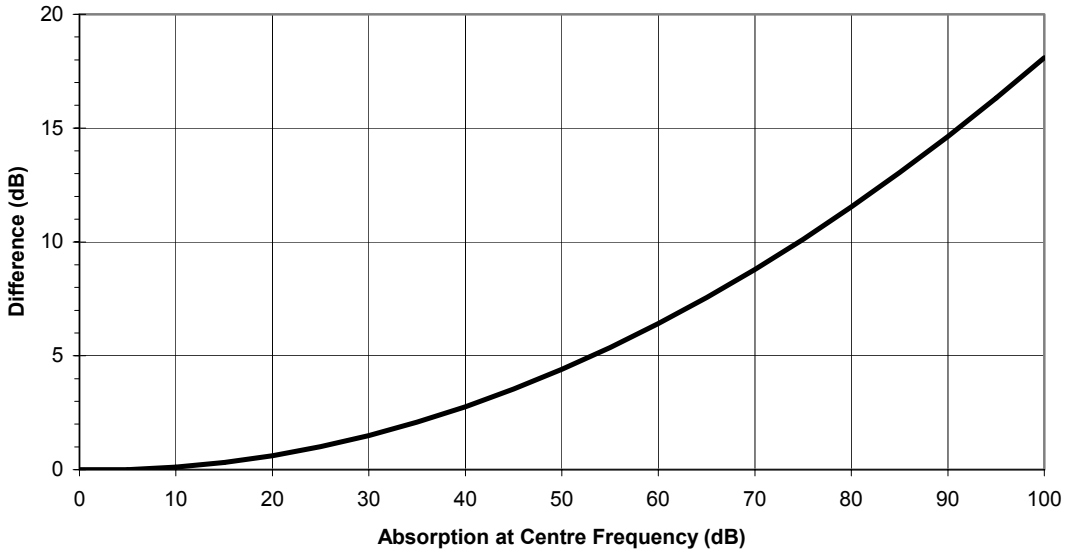

Figure 2
Difference between the absorption at the centre frequency of the one-third octave band and the band absorption as a function of the absorption at the centre frequency.

The figure shows that there is no significant difference (within 0.1 dB) if the attenuation due to air absorption is less than 10 dB. At 20 dB the difference becomes significant (0.6 dB) and at high attenuation substantial differences are found.

In the comprehensive model the effect of air absorption is predicted by Eq. (3). The attenuation A_0 at the centre frequency is determined according to ISO 9613-1 for the propagation distance R between source and receiver.

4. Effect of Terrain and Screens

When sound propagates over a terrain surface the sound pressure level at the receiver is highly affected by reflections from the terrain surface. When the receiver is in a shadow zone behind a barrier sound is diffracted into the shadow zone and the sound pressure level at the receiver is affected by the diffraction of the barrier combined with reflections from the terrain surface.

When taking into account the effect of a barrier it is in principle not necessary to distinguish between man-made structures such as screens or embankments and natural barriers which are a part of the terrain surface. However, for practical reasons it is recommend in an implementation of the comprehensive model to distinguish between “natural” screens and “artificial” screens added to the terrain by man. One reason is that man-made screens have a well-defined finite length which terrain screens have not. Another reason is that it is appropriate in the procedure for determining the equivalent flat terrain (see Section 4.4.4.1) to disregard screens. Finally, in the future terrain information will probably be obtained from digital elevation data or other kind of topographical maps but such data will have a resolution that is too small for defining screening and reflecting obstacles with a sufficient accuracy.

The model for including the effect of terrain and screens is basically a two-dimensional model where the terrain shape used in the calculations is determined by a vertical cross section along the propagation path from source to receiver. However, in a few cases the third dimension has to be taken into account without this making the model truly three-dimensional. These cases concern screen with finite length and reflecting obstacles as well as surface areas for determining ground surface properties.

In the prediction model it is assumed that the 2D terrain profile can be approximated by a number of straight line segments also denoted a broken line. The method for approximating a terrain by a broken line is described in Section 4.1. It is assumed that each line segment is characterised by its surface impedance and roughness as described in Section 4.3. Screens are also approximated by broken lines.

The method for predicting the combined coherent effect of terrain and screens is described in Section 4.4. In this description of the model it is assumed that only the two most efficient edges are taken into account (may be two screens with one edge each or one screen with two edges). In principle the method outlined below can be extended to any number of screens and diffracting edges but the complexity of the implementation would increase substantially and most likely without a resulting significant gain in accuracy. The method described in Section 4.4, as well as other parts of the comprehensive prediction model, is largely based on the concept of Fresnel-zones. Fresnel-zones are described in details in Section 4.2.

Effects of frequency bandwidth, fluctuating atmospheric refraction, turbulence, surface roughness and scattering zones will reduce the coherence between rays, especially at high frequencies. The introduction of incoherent effects in the comprehensive model is described in Section 4.5.

4.1 Simplification of Terrain

Before outlining the principles for simplifying the terrain shape it will be practical to introduce a few definitions.

The terrain baseline is defined as the line between the ground point P_S vertically below the source and the ground point P_R vertically below the receiver as shown in Figure 3. The source ground point S_G is the ground point outside the ground shape from P_S to P_R which is closest to source S. Correspondingly, the receiver ground point R_G is the ground point outside P_S to P_R which is closest to receiver R. If the terrain is flat the baseline will be identical to the ground surface and S_G and R_G will be identical to P_S and P_R, respectively. If the ground surface has a circular convex shape S_G and R_G will also be identical to P_S and P_R.

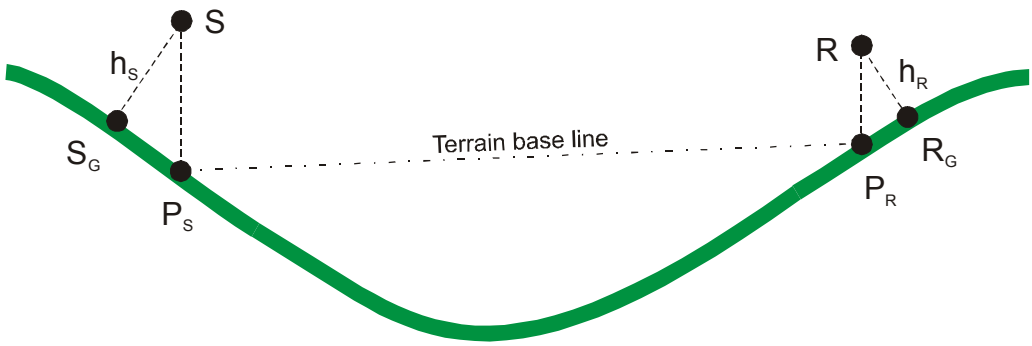

Figure 3
Definition of terrain base line P_SP_R and source and receiver ground points S_G and R_G.

In the method for predicting the ground effect of non-flat terrain the terrain has to be approximated by a broken line as shown in Figure 4 for three categories of non-flat terrain.

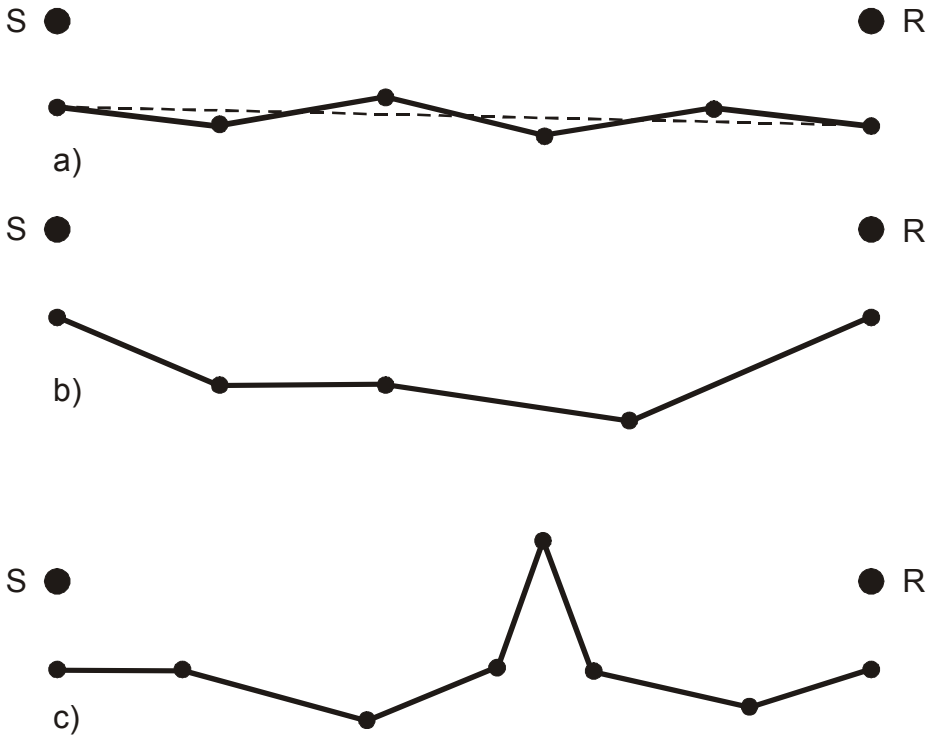

Figure 4
Examples of segmented terrain: a) virtually flat terrain, b) valley-shaped terrain, c) hill-shaped terrain.

A method has been developed [17] for approximating any real terrain shapes possibly defined on basis of digital elevation data by such segmented terrain. When using the method, artificial screens should be ignored.

The method is based on "the maximum deviation principle" in which the ground point P having the maximum perpendicular distance r_{max} to the line between the first and the last ground point P_1 and P_2 will become a new ground point in the segmented terrain. The principle is illustrated in

Figure 5.

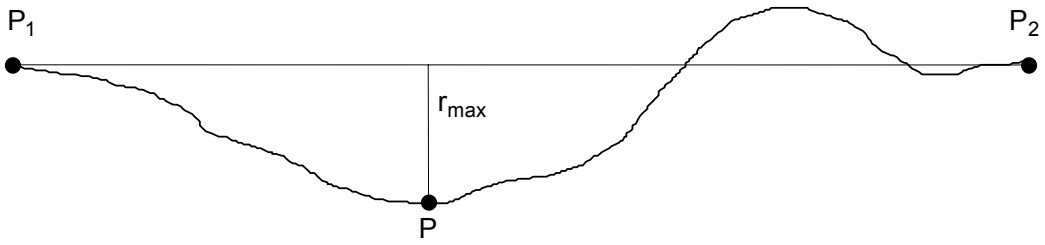

Figure 5
"Maximum deviation principle" used to determine a new ground point.

In the first step the ground point P between P_1 (equal to the source ground point S_G) and P_2 (equal to the receiver ground point R_G) is determined according to the maximum deviation principle. If r_{max} is below a specified limit the terrain is defined as being flat but if not, P will become a new ground point in the simplified terrain shape which now consists of two straight segments P_1P and PP_2.

In the next step the process is repeated for the two ground shapes P_1 to P and P to P_2. r_{max} is determined for each of these two shapes and the point corresponding to the largest value of r_{max} will become the next ground point in the simplified shape which now consists of three segments.

This process may be repeated to any degree of perfection but each time a new point is added, an existing segment is replaced by two new segments. As the calculation time of the comprehensive propagation model will increase strongly with the number of segments this should only be repeated until deviations between the real and the segmented terrain are within acceptable limits. It is recommended that additional extra ground points are added to the segmented terrain until the following requirements are fulfilled:

- The maximum deviation r_{max} fulfils Eq. (4)
- The length of a segment d_{segm} fulfils Eq. (5)
- The maximum number of segments is 10

$$r_{max} \leq \begin{cases} 0.1 & d \leq 50 \\ 0.002\,d & 50 < d < 500 \\ 1 & d \geq 500 \end{cases} \qquad (4)$$

$$d_{segm} \leq \begin{cases} 1 & d \leq 20 \\ 0.05\,d & 20 < d < 200 \\ 10 & d \geq 200 \end{cases} \qquad (5)$$

***Note**: The outlined procedure for approximating a real terrain by a segmented terrain shall only be considered a proposal. If a more efficient procedure can be developed, such a method should be used instead. The values given in the 3 requirements are the result of best judgement taking into account the impact on calculation time. Use of the method may therefore reveal a need for adjusting the requirements and it is possible that the maximum number of segments has to be increased.*

Artificial screens are also approximated by straight line segments but in this case the number and size of the segments can be determined by the user. However, if a screen contains more than two diffracting edges (corresponding to more than three segments) the screen must be simplified to include the two most efficient diffracting edges, only. The determination of which edges are the most efficient depends on the given source and receiver position but whenever possible, it must be recommended to let the user simplify the screen as much as possible (to ensure reliability and to reduce computation time). Figure 6 shows the principle for determining the two most efficient edges.

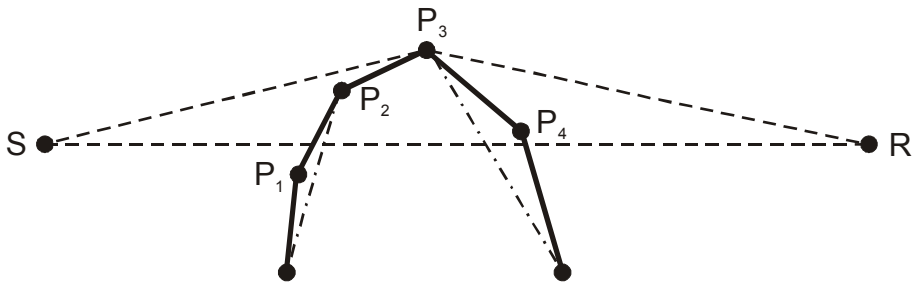

Figure 6
Determination of the two most significant edges of a multi-edge screen.

In the first step the path length difference |SP| + |RP| - |SR| is calculated for each of the edges P_1 to P_4. The most efficient edge corresponds to the largest path length difference (when the edges are above the line-of-sight). In Figure 6 P_3 has been found to be the most efficient edge. In the next step the path length difference is calculated for the remaining edges but in this case the receiver is replaced by P_3 on the source side of P_3 while the source is replaced by P_3 on the receiver side of P_3. The second most efficient edge corresponds to the largest path length difference calculated this way. As an example, for the edge P_2 which has been found to be the second most efficient edge in Figure 6 the path length difference is equal to $|SP_2| + |P_3P_2| - |SP_3|$ (but in this case multiplied by –1 because P_2 is below the line SP_3). When the two most efficient edges have been determined the screen shape given by the solid line in Figure 6 will be replaced by the simplified shape shown by the dot-and-dash line. When the diffracting edges are below the line-of-sight or when more screens are involved the principle becomes a little more complicated than described above. However, in Section 4.4.4.3 where the transition between different models are dealt with, the principle for simplifying screen shapes is further described for these complicated cases.

After the simplification of the screens the segmented terrain and screens are combined as shown in Figure 7. The segmented terrain is shown by a solid line and two screens are shown by dashed lines (one double edge and one single edge screen).

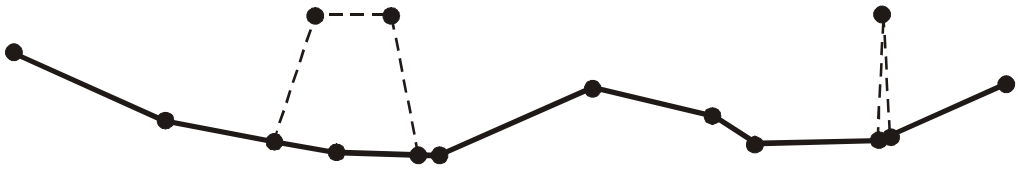

Figure 7
Combination of segmented terrain and screens.

4.2 Fresnel-Zones

The concept of Fresnel-zones is widely used within the comprehensive propagation model. The use is inspired by an approximate solution to predict sound propagation over flat terrain with varying surface types proposed by Hothersall and Harriott [6]. In this method the sound field at the receiver is assumed to be determined by the surface conditions in a region around the reflection point denoted the Fresnel-zone.

The Fresnel ellipsoid is defined by the locus of the points P defined by Eq. (6) where S is the source point, R is the receiver point, and F_λ is a fraction of the wavelength λ. The foci of the ellipsoid are placed at S and R.

$$|SP| + |RP| - |SR| = F_\lambda \lambda \tag{6}$$

When the sound field is reflected by a plane surface, the elliptically shaped Fresnel-zone is defined by the intersection between the plane and the Fresnel ellipsoid with foci at the image source point S' and the receiver R as shown in Figure 8.

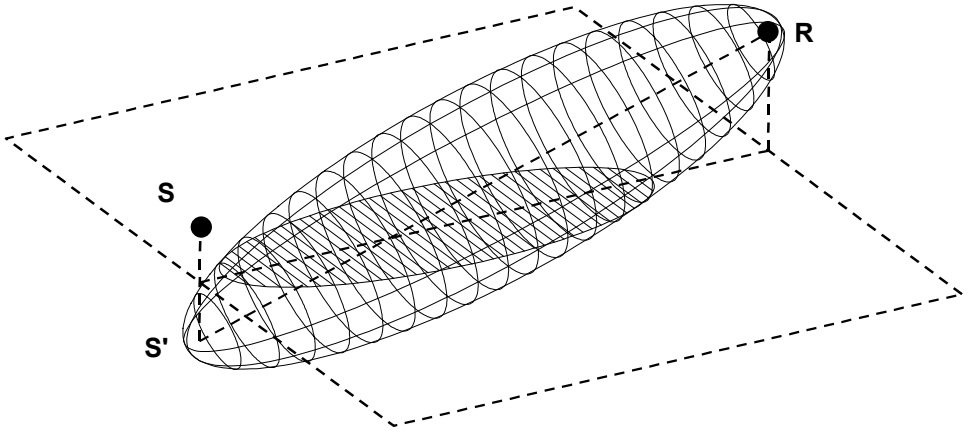

Figure 8
Definition of Fresnel ellipsoid and Fresnel-zone.

For practical purposes this elliptical shape is very inconvenient to work with when calculating sub-areas within the Fresnel-zone. Instead it has been chosen to use the circumscribed rectangle. The size of the rectangular Fresnel-zone is defined by the size of the elliptic Fresnel-zone in the direction of propagation and perpendicular to this direction. The area of the rectangle is $4/\pi$ (= 1.27) times the area of the ellipse which is a small difference taking into account the overall uncertainty in the Fresnel-zone method including the selection of the correct value of F. In principle the Fresnel-zone includes terrain outside the section from source ground point S_G to receiver ground point R_G. However, as the size of the Fresnel-zone behind the source and receiver will only be a fraction of the wavelength, it is permissible to truncate the Fresnel-zone at the source and receiver, unless the horisontal propagation distance becomes comparable with this fraction of the wavelength. Such a truncation will be an advantage in a “point-to-point” computer implementation where the user has to specify the terrain profile manually.

In a two-dimensional propagation model the Fresnel-zone becomes one-dimensional as shown in Figure 9.

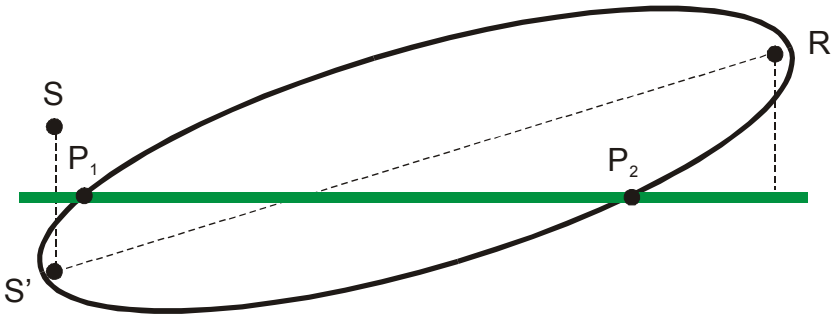

Figure 9
One-dimensional Fresnel-zone (P_1P_2) in a two-dimensional propagation model.

Algorithms for the calculation of the size of the Fresnel-zone are given in Appendix A.

The size of a sub-surface within the Fresnel-zone relative to the size of entire Fresnel-zone is used to determine the Fresnel-zone weight w_i which expresses the relative importance of the sub-surface. The Fresnel-zone weight is calculated according to Eq. (7) where S_i is the area of the i'th sub-surface within the rectangular Fresnel-zone and S_{Fz} is the area of the entire Fresnel-zone as shown in Figure 10. In a two-dimensional propagation model S_i and S_{Fz} are replaced by the lengths d_i and d_{Fz}.

$$w_i = \frac{S_i}{S_{Fz}} \tag{7}$$

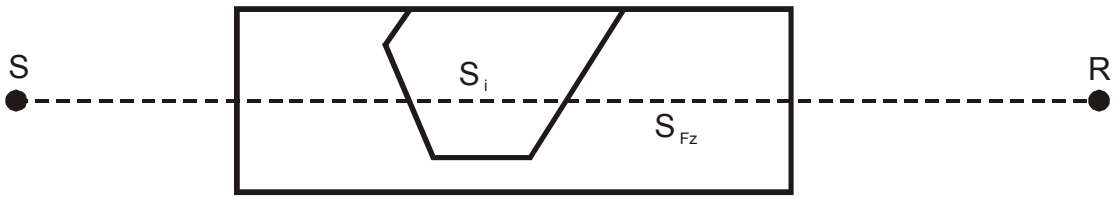

Figure 10
Top view of a Fresnel-zone.

In the present work it has been found that a fraction F_λ equal to 1/16 of the wavelength will provide the best fit when using the Fresnel-zone interpolation method in case of non-flat terrain as described in Section 4. However, when determining the efficiency of a scattering zone with a finite size (see Section 5) or the efficiency of a vertical reflecting obstacle (see Section 6) a F-value of 1/8 is considered appropriate. In the model for flat terrain with varying surface properties described in Section 4.4.1.2 a value of ¼ is used. The reason for selecting this value is mainly that the model follows the recommendation in [6]

of a value between ½ and ¼ and has been completed before the work with the non-flat terrain model was carried out. As modified weights were introduced for low source and receiver to improve the accuracy of the model it would require a time consuming reanalysis to change the model to use a value of 1/16. Furthermore, a preliminary study for a few geometries indicates that it is doubtful whether the use of 1/16 will improve the accuracy.

4.3 Classification of Ground Surfaces

In the comprehensive model, the ground surface properties are defined by the normalised acoustic impedance Z and by a roughness parameter σ_r. Each straight terrain segment in the model determined according to the procedure described in Section 4.1 is assigned a value of Z (or mix of values) and of σ_r. The roughness parameter σ_r is used to quantify the unevenness of the terrain segment and is the standard deviation of the random height variations within the segment.

In the comprehensive model, the ground is generally characterised by the ground flow resistivity and ground impedance is calculated using the Delany and Bazley one-parameter impedance model [3]. The determination of the impedance according to this model is described in Appendix B. However, impedances determined by other models or means can also be used in the comprehensive model. The ground impedance is used for calculation of the spherical wave reflection coefficient Q for coherent propagation described in Section 4.4.1 and the reflection coefficient $\Re$ for incoherent propagation described in Section 4.5.2.

For use in the final prediction model a classification has been made which include a number of ground types representing typical surfaces. The classification which is based on the Nordtest flow resistivity classes ([15], [28], [34]) is shown in Table 1.

Impedance class	Representative flow resistivity σ (kNsm^{-4})	Range of Nordtest flow resistivity classes	Description
A	12.5	10, 16	Very soft (snow or moss-like)
B	31.5	25, 40	Soft forest floor (short, dense heather-like or thick moss)
C	80	63, 100	Uncompacted, loose ground (turf, grass, loose soil)
D	200	160, 250	Normal uncompacted ground (forest floors, pasture field)
E	500	400, 630	Compacted field and gravel (compacted lawns, park area)
F	2000	2000	Compacted dense ground (gravel road, parking lot, ISO 10844)
G	20000	-	Hard surfaces (most normal asphalt, concrete)
H	200000	-	Very hard and dense surfaces (dense asphalt, concrete, water)

Table 1
Classification of ground impedance types.

The roughness parameter σ_r is a quantification of terrain unevenness characterised by random height variations. The variations are in general smaller than the height variation leading to segmentation of the terrain as described in Section 4.1. The effect of terrain roughness can be interpreted as a transformation from coherent propagation into incoherent propagation and is therefore taken into account in the model for incoherent effects described in Section 4.5.

For use in the final prediction model a classification has been made which include four roughness classes. The classification is shown in Table 2.

***Note**: No outdoor propagation measurements over uneven terrain have been found which can be used for validation. Therefore, the accuracy of the predictions is still an open question and it is possible that better agreement with measurements could be obtained by scaling the parameter σ_r.*

Roughness class	Representative σ_r	Range of heights
N: Nil	0	±0.25 m
S: Small	0.25 m	±0.5 m
M: Medium	0.5 m	±1 m
L: Large	1 m	±2 m

Table 2
Classification of ground roughness types.

In the comprehensive model allowance has been made for another kind of roughness which is denoted small scale roughness in [25]. Small scale roughness is characterised by relatively small irregularities (compared to the wavelength) and leads to a modification of the acoustic impedance in the low frequency range. The model for small scale roughness is described in Appendix C. As small scale roughness model is causing modification of the impedance, the modified impedance can be used directly in the comprehensive model. Consequently it has not been necessary to make small scale roughness an integrated part of the comprehensive model as it has been necessary with the roughness described by the parameter σ_r.

4.4 Coherent Model

The coherent model for predicting the effect of ground and screens is divided into three basic propagation models:

1) The *flat terrain model* which includes all cases with insignificant deviations from a flat terrain.

2) The *valley model* which includes all non-flat cases with insignificant screening effect.

3) The *hill model* which includes all cases with significant screening effect. The hill model consists of sub-models for one or two screens with single edges and one screen with two diffracting edges.

Each of the models are described below in Section 4.4.1 through 4.4.3 and the principles for combining the three models are described in Section 4.4.4.

4.4.1 Flat Terrain

If the surface of the flat terrain is homogeneous, the calculation is made according to the basic geometrical ray theory model described in Section 4.4.1.1. If the surface properties

vary with respect to impedance or surface roughness the method described in Section 4.4.1.2 is used instead. The calculation is in both cases based on the three geometrical parameters h_S, h_R and d which are the source and receiver heights and the source-receiver distance along the terrain surface, respectively, as shown in Figure 11.

If the terrain is uneven but considered flat according to the principle described in Section 4.4.4.1, the geometrical parameters are measured relative to the equivalent flat terrain instead. The determination of the equivalent flat terrain is also described in Section 4.4.4.1.

4.4.1.1 Homogeneous Surface

When sound propagates close to the ground, the direct sound interacts with the sound reflected from the ground. A simple approach to model this interaction when the terrain is flat with a homogeneous surface characterized by its specific acoustic impedance Z, is to represent the sound field by geometrical rays [1] as shown in Figure 11.

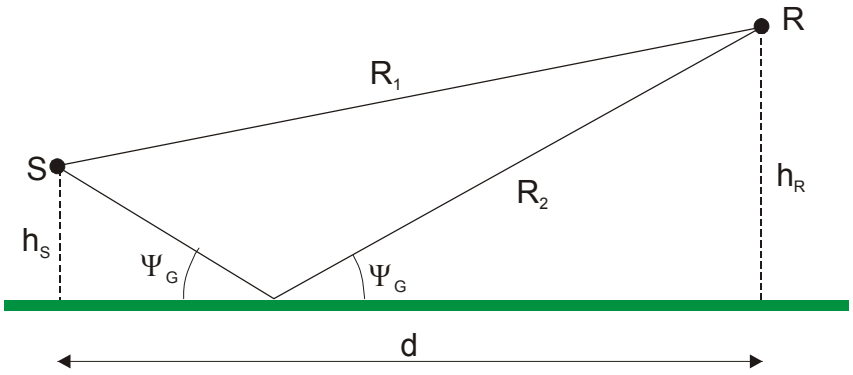

Figure 11
Propagation over flat ground.

The acoustic pressure at the receiver is calculated according to Eq. (8), where R_1 and R_2 are the path lengths of the direct and reflected ray, k is the wave number, and Q is the spherical wave reflection coefficient. Q is a function of the ground impedance Z, the grazing angle ψ_G, and the distance R_2. The calculation of Q is described in Appendix D (from [2]). The first term in Eq. (8) is the sound pressure of the direct field (equal to the free-field sound pressure) and the second term is the sound pressure of the reflected field.

$$p = \frac{e^{jkR_1}}{R_1} + Q\frac{e^{jkR_2}}{R_2} \qquad (8)$$

where

$$R_1 = \sqrt{d^2 + (h_S - h_R)^2} \tag{9}$$

$$R_2 = \sqrt{d^2 + (h_S + h_R)^2} \tag{10}$$

The ground effect ΔL_{flat} is determined the sound pressure p at the receiver relative to the free-field sound pressure p_0 as shown in Eq. (11).

$$\Delta L_{flat} = 20 \log \left| \frac{p}{p_0} \right| = 20 \log \left| 1 + \frac{R_1}{R_2} Q \, e^{jk(R_2 - R_1)} \right| \tag{11}$$

If the terrain surface include roughness this is taken into account as an incoherent effect as described in Section 4.5.

4.4.1.2 Varying Surface Properties

If the terrain is flat with varying surface properties (impedance and roughness) the ground effect is predicted by a modified Fresnel-zone model developed in [16]. The original Fresnel-zone model has been found to work well at low frequencies but poorer at high frequencies in case of small source and receiver heights. In the modified Freznel-zone model special weighting has been introduced in the high frequency range to improve the accuracy of the model. This is particularly important in cases where low sources are placed over an acoustically hard surface and the propagation takes place over porous ground leading to an impedance discontinuity (e.g. road traffic noise).

As already mentioned in Section 4.2 a F-value of ¼ is used when calculating the size of the Fresnel-zone which is a deviation from other parts of the comprehensive model. The main reason for selecting this value is that a value between ½ and ¼ has been recommended in [6] and the model has been completed before the work with the non-flat terrain model was carried out. As modified weights were introduced for low source and receiver to improve the accuracy of the model it would require a time consuming reanalysis to change the model to use another value. Furthermore, preliminary calculations indicate that it is doubtful whether the use of another F-value would improve the accuracy.

In the modified high frequency Fresnel-zone model the Fresnel-zone is divided into a source and receiver region as shown in Figure 12. The two regions are separated by a line perpendicular to the source-receiver line through the ground reflection point O. The area $S_{i,j}$ within the entire Fresnel-zone (with area S_{Fz}), the area $S_{i,j,S}$ within the source region (with area $S_{Fz,S}$) and the area $S_{i,j,R}$ within the receiver region (with area $S_{Fz,R}$) is determined for each combination of impedance (i) and surface roughness (j).

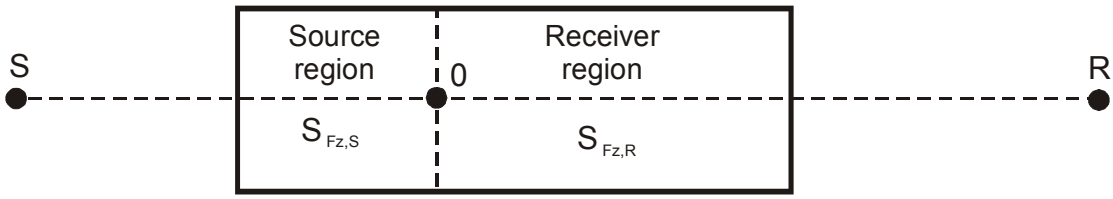

Figure 12
Fresnel-zone definitions for flat terrain and varying surface properties. Top view.

In the low frequency range the Fresnel-zone weight $w_{i,j,L}$ is calculated by Eq. (12) in agreement with the original Fresnel-zone model described in Section 4.2.

$$w_{i,j,L} = \frac{S_{i,j}}{S_{Fz}} \tag{12}$$

In the high frequency range a modified Fresnel-zone weight $w_{i,j,H}$ is calculated according to Eqs. (13) through (18). ψ_G in Eq. (17) is the grazing angle of the reflected ray.

$$r_{i,j} = 0.5\left(\frac{S_{i,j,S}}{S_{Fz,S}} + \frac{S_{i,j,R}}{S_{Fz,R}}\right) \tag{13}$$

$$r_i = \sum_j r_{i,j} \tag{14}$$

$$r_i'' = 8.78\, r_i^5 - 21.95\, r_i^4 + 21.76\, r_i^3 - 10.69\, r_i^2 + 3.1\, r_i \tag{15}$$

$$r_{i,j}' = \frac{r_i''}{\sum_i r_i''}\frac{r_{i,j}}{r_i} \tag{16}$$

$$r_h = \begin{cases} 1 & \tan\psi_G \geq 0.04 \\ \dfrac{\log\left(200\tan\psi_G\right)}{\log\left(8\right)} & 0.005 < \tan\psi_G < 0.04 \\ 0 & \tan\psi_G \leq 0.005 \end{cases} \tag{17}$$

$$w_{i,j,H} = \left(r_{i,j} - r_{i,j}'\right) r_h + r_{i,j}' \tag{18}$$

The low frequency weight $w_{i,j,L}$ is used below a frequency f_L and the high frequency weight $w_{i,j,H}$ above a frequency f_H. In the frequency range f_L to f_H a transition is used. The modified weight $w'_{i,j,}$ is calculated according to Eq. (19).

$$w'_{i,j} = \begin{cases} w_{i,j,L} & f \le f_L \\ \dfrac{\log f_H - \log f}{\log f_H - \log f_L}\left(w_{i,j,L} - w_{i,j,H}\right) + w_{i,j,H} & f_L < f < f_H \\ w_{i,j,H} & f \ge f_H \end{cases} \tag{19}$$

f_L and f_H are determined on basis of the difference in phase $\Delta\alpha$ between the direct and the reflected wave. $\Delta\alpha$ is determined for the surface type with smallest flow resistivity by Eq. (20). k, R_1 and R_2 are as defined in Section 4.4.1.1 and $\Re_p$ is the plane-wave reflection coefficient. To calculate $\Delta\alpha$ accurately the spherical wave reflection coefficient Q should have been used instead of $\Re_p$. However, the determination of the frequency corresponding to a specified value of $\Delta\alpha$ by Eq. (20) can only be solved by iteration. As the calculation of Q is very time consuming compared to calculation of $\Re_p$, it is desirable to use $\Re_p$ and this approach has been found sufficiently accurate.

$$\Delta\alpha = k\left(R_2 - R_1\right) + Arg\left(\Re_p\right) \tag{20}$$

f_H is determined as the smallest frequency where $\Delta\alpha = \Delta\alpha_H = \pi$ and f_L is determined as the smallest frequency where $\Delta\alpha = \Delta\alpha_L$. $\Delta\alpha_L$ is calculated by Eq. (21) where h_{min} is determined by Eq. (22) and ψ_G is the angle of incidence of the reflected ray as defined in Section 4.4.1.1. However, if f_L calculated this way becomes larger than $0.8f_H$ a value of $0.8f_H$ is used instead.

$$\Delta\alpha_L = \pi - \left(1.9483 \ln\left(h_{\min}\right) + 18.052\right)\tan\psi_G \tag{21}$$

$$h_{\min} = \begin{cases} Min\left(h_S, h_R\right) & h_S > 0.01 \wedge h_R > 0.01 \\ 0.01 & h_S \le 0.01 \vee h_R \le 0.01 \end{cases} \tag{22}$$

Eventually the ground effect is determined for propagation over a terrain with varying ground surface properties using the Fresnel-zone interpolation principle shown in Eq. (23) or (24). In these equations $w'_{i,j,}$ is the modified weight, $\Delta L_{i,j}$ is the ground effect and $p_{i,j}/p_0$ is the sound pressure relative to the free-field pressure calculated for each surface type using the model for a homogeneous surface in Section 4.4.1.1.

$$\Delta L_{flat} = \sum_i \sum_j w'_{i,j}\ \Delta L_{i,j} \tag{23}$$

$$\Delta L_{flat} = 20 \log \left| \prod_i \prod_j \left(\frac{p_{i,j}}{p_0} \right)^{w'_{i,j}} \right| \tag{24}$$

If the terrain is uneven but considered flat according to the principle described in Section 4.4.4.1, the area of each impedance and roughness type is determined by their projection onto the equivalent flat terrain surface.

***Note**: As the model for flat terrain and varying surface properties appear as an encapsulated unit in the comprehensive model with a smooth transition to other parts of the model it would have been possible to use a more accurate numerical model or maybe a table look-up method to further improve the accuracy. However, the modified Fresnel-zone model has in the present work been found sufficiently accurate for engineering purposes and has been preferred due its simplicity.*

4.4.2 Valley-Shaped Terrain

The prediction model for a valley-shaped terrain has been developed in [17]. An example of a valley-shaped terrain approximated by straight segments is shown in Figure 13**.** The local source and receiver heights h_S and h_R are defined as the smallest distance from the source or receiver to the terrain (the perpendicular distance).

Figure 13
Valley-shaped segmented terrain.

In the valley-model it is necessary to distinguish between three types of the terrain segments with different procedures for calculating the ground effect. These are:

- Concave segments
- Convex segments
- Transition segments

The type of segment is determined on basis of the source and receiver heights h'_S and h'_R measured relative to the extended segment. If the source or receiver is below the segment this is indicated by a negative value**.** Figure 14 shows examples of the three types of segments from Figure 13 and how the heights h'_S and h'_R are determined for each type of segment.

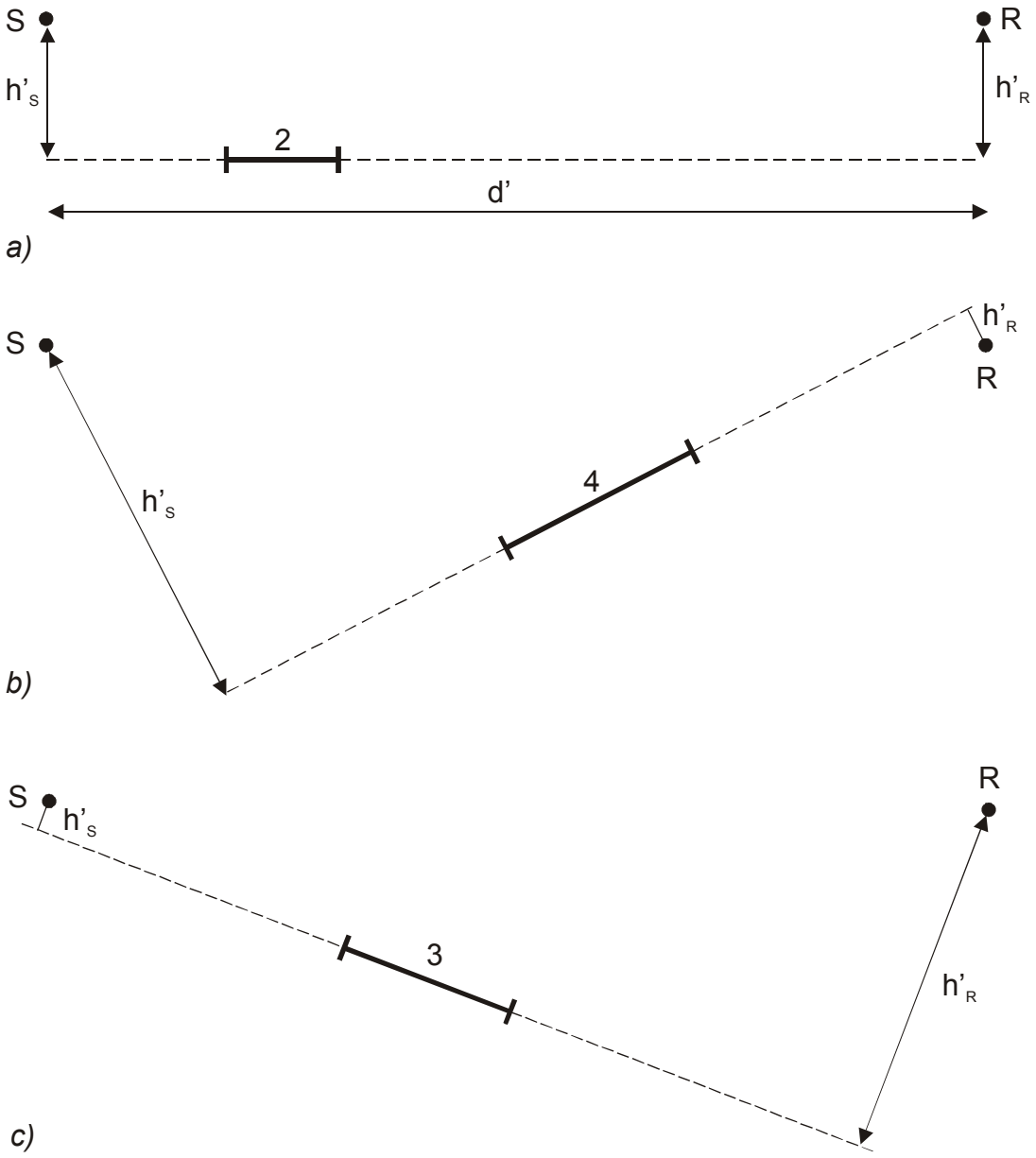

Figure 14
Determination of source and receiver heights h'_S and h'_R for a) a concave segment, b) a convex segment and c) a transition segment.

To determine the type of segment the relative source height $h_{S,rel}$ is calculated according to Eq. (25) and the relative receiver height $h_{R,rel}$ according to Eq. (26). The heights h''_S and h''_R are the minimum allowable heights for a concave segment. h''_S is determined by Eq. (27) as the minimum of the local source height h_S and the height $h_{S,Fz}$. The latter of these heights corresponds to the height of the source when the source side segment end point is

at the Freznel-zone boundary. In the same way h"$_R$ is determined by Eq. (28) as the minimum of the local receiver height h_R and the height $h_{R,Fz}$. $h_{S,Fz}$ and $h_{R,Fz}$ are calculated as shown in Appendix E.

$$h_{S,rel} = \begin{cases} 1 & h_S^{'} \geq h_S^{''} \\ \dfrac{h_S^{'}}{h_S^{''}} & 0 < h_S^{'} < h_S^{''} \\ 0 & h_S^{'} \leq 0 \end{cases} \tag{25}$$

$$h_{R,rel} = \begin{cases} 1 & h_R^{'} \geq h_R^{''} \\ \dfrac{h_R^{'}}{h_R^{''}} & 0 < h_R^{'} < h_R^{''} \\ 0 & h_R^{'} \leq 0 \end{cases} \tag{26}$$

$$h_S^{''} = \min\left(h_S, h_{S,Fz}\right) \tag{27}$$

$$h_R^{''} = \min\left(h_R, h_{R,Fz}\right) \tag{28}$$

On basis of $h_{S,rel}$ and $h_{R,rel}$ three types of segments can be defined:

Concave segment: $h_{S,rel} = 1 \wedge h_{R,rel} = 1$ (29)

Convex segment: $h_{S,rel} = 0 \vee h_{R,rel} = 0$ (30)

Transition segment: $0 < h_{S,rel} < 1 \vee 0 < h_{R,rel} < 1$ (31)

According to the definition given in Eqs. (29) to (31) a terrain segment will be a convex segment if the source or receiver is at or below the extended segment. The segment will be a concave segment if the source or receiver height is greater than or equal to the local source and receiver heights or if the segment end point is at or outside the Fresnel-zone boundary at the side where the source or receiver height is smaller than the local height. Otherwise the segment is a transition segment. The change-over from a concave segment to a transition segment may depend on $h_{S,Fz}$ and $h_{R,Fz}$ and may therefore depend on the frequency.

The over-all ground effect of a valley-shaped terrain is calculated according to Eq. (32) using the Fresnel-zone interpolation principle. The ground effect ΔL_i and the Fresnel-zone

weight w_i have to be determined for each segment (No. i). The procedure for calculating p_i/p_0 (or ΔL_i) and w_i depends on the type of segment as described in the following.

$$\Delta L_{valley,0} = \sum_i w_i \Delta L_i = 20 \log \left| \prod_i \left(\frac{p_i}{p_0} \right)^{w_i} \right| \tag{32}$$

If the ground effect calculated by Eq. (32) is less than zero and the sum of weights Σw_i is larger than one, the ground effect is modified by Eqs. (33) and (34). The reason for the modification is that if the lowest interference dip in the ground effect spectrum coincides for a number of segments the total attenuation will be unrealistic large compared to what is found in measurements. If the $\Delta L_{valley,0}$ is less -20 dB and Σw_i is larger 1 the described principle produces the weighted average of ΔL_i instead of the weigted sum (the weights w_i are normalized to $\Sigma w_i = 1$). For $\Delta L_{valley,0}$ between 0 and -20 dB a gradual transion takes place between the two principles.

$$r' = \begin{cases} 0 & \Delta L \geq 0 \\ \dfrac{\Delta L_{valley,0}}{-20} & -20 < \Delta L < 0 \\ 1 & \Delta L \leq -20 \end{cases} \tag{33}$$

$$\Delta L_{valley} = \Delta L_{valley,0} \left(1 - r' + \frac{r'}{\sum w_i} \right) \tag{34}$$

Concave Segment

In case of a concave segment the ground effect contribution ΔL_i is calculated using the method for flat terrain described in Section 4.4.1.1 Eq. (11) with source and receiver heights h'_S and h'_R and propagation distance d' as defined in Figure 14a). The Fresnel-zone weight w_i is calculated using the method described in Section 4.2, Eq. (7) and the same geometrical parameters.

If there is more than one impedance or roughness type within the common area of the straight segment and the Fresnel-zone as shown in Figure 15, the ground effect $\Delta L_{i,m}$ and Fresnel-zone weight $w_{i,m}$ is calculated for each m'th impedance or roughness type combination and combined according to Eq. (35) or (36) for each i'th straight segment before being inserted into Eq. (32).

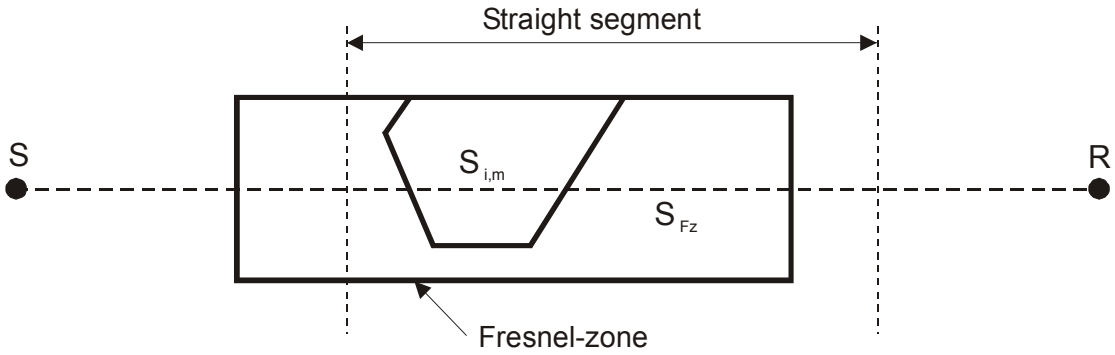

Figure 15
Top view of a Fresnel-zone for a straight segment.

$$w_i \Delta L_i = \sum_{m=1}^{N_m} w_{i,m} \, \Delta L_{i,m} \tag{35}$$

$$\left(\frac{p_i}{p_0} \right)^{w_i} = \prod_{m=1}^{N_m} \left(\frac{p_{i,m}}{p_0} \right)^{w_{i,m}} \tag{36}$$

Convex Segment

In case of a convex segment either the source or the receiver will be at or below the extended line segment. In this case neither the ground effect model in Section 4.4.1.1 nor the Fresnel-zone concept in Section 4.2 will be applicable. Instead the ground reflection effect of a convex segment is predicted using the model for a finite-impedance wedge normally used to determine the screening effect of a wedge described in Section 4.4.3.1. Also the Fresnel-zone concept has lost its meaning when the source or the receiver is below the extended segment. Instead, the Fresnel-zone weight is determined by a simple principle based on the length of the convex segment.

The ground effect of a finite impedance wedge is determined on basis of the distances r_S and r_R from the top of the wedge to the source, the diffraction angles θ_S and θ_R, the wedge angle β and the reflection coefficients Q_S and Q_R as shown in Figure 16. The calculation for a wedge is described in Appendix H.

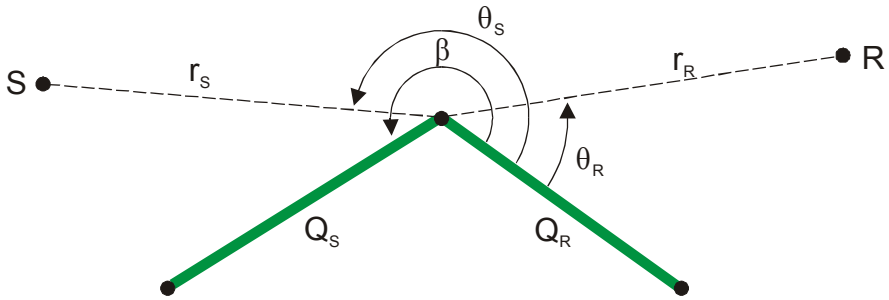

Figure 16
Ground effect of a wedge. Definition of parameters.

A convex segment will constitute one of the wedge faces or be a part of it. If the receiver is below the extended segment the source face includes the segment and if the source is below the segment the receiver face includes the segment. However, in both cases it is necessary to define what should be used as the secondary wedge face. In the first place the most natural choice would have been to use the succeeding or preceding segment. However, if such a principle was applied subdividing of segments may change the predicted ground effect although the original and subdivided terrain shape virtually is the same shape. To avoid this, another principle has been elaborated as described in the following steps where $h_{S,v}$ end $h_{R,v}$ are the local source and receiver heights measured vertically and $h'_{S,v}$ end $h'_{R,v}$ are the source and receiver heights relative to individual terrain segment measured vertically.

1) If $h_{S,rel} < h_{R,rel}$ for the considered convex segment, the segment which determines the secondary wedge face is the segment closest to the considered convex segment at the source side for which $h'_{S,v} \geq h_{S,v}$.

2) If $h_{S,rel} \geq h_{R,rel}$ for the considered convex segment, the segment which determines the secondary wedge face is the segment closest to the considered convex segment at the receiver side for which $h'_{R,v} \geq h_{R,v}$.

3) If the two segments are not adjacent the top of an equivalent wedge is determined by the intersection between the extension of the segments as shown in Figure 17. The reflection coefficients Q_S and Q_R of the two wedge faces is calculated using the impedance of the considered segment (also for the secondary face). The determination of the equivalent wedge is given in Appendix F.

4) Finally the ground effect $\Delta L_i = f(R_S,R_R,\theta_S,\theta_R,\beta,Q_S,Q_R)$ is calculated for the equivalent wedge using the calculation procedure described in Appendix H.

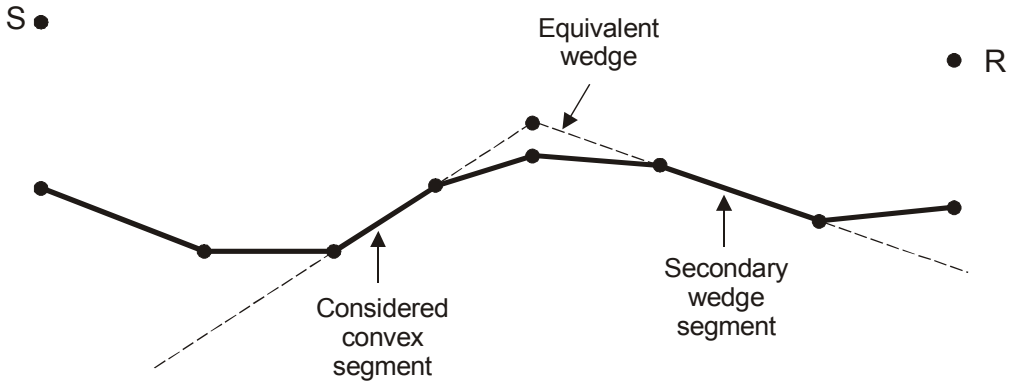

Figure 17
Definition of an equivalent wedge used for predicting the ground effect of a convex segment.

The Fresnel-zone weight $w_{x,i}$ for a convex segment is calculated using a simple principle without a particular physical foundation, but having the quality of being stable and producing correct results at borderline cases. If the top point of the wedge (the intersection between wedge faces) is at or above the terrain base line defined in Section 4.1, the projection of the convex segment onto the base line is used when determining the Fresnel-zone weight (similar to a concave segment). If the top point is below the base line the projection on a line parallel with the base line through the top point is used instead as shown in Figure 18. If the considered segment is P_1P_0 the segment used in the determination of the Fresnel-zone weight is P'_1P_0 and if the considered segment is P_0P_2 the segment to be used is $P_0P'_2$.

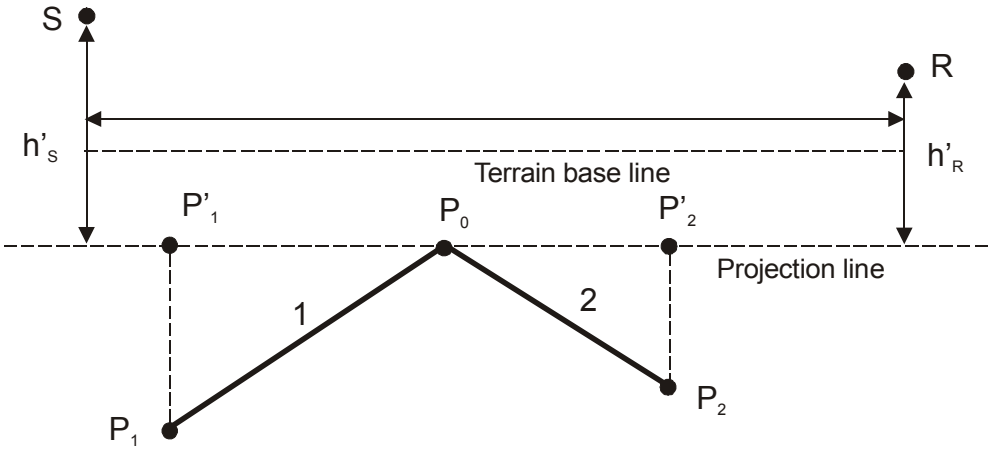

Figure 18
Definition of the Fresnel-zone weighting principle for convex segments.

If the extension of a convex segment on the source side of the equivalent wedge ($h_{S,rel} \geq h_{R,rel}$) is above source ground ($h_{S,rel} < 1$) the weight is further modified according to Eq. (37).

$$w_i = \begin{cases} w_{x,i} & h_{S,rel} \geq 1 \\ w_{x,i}\ h_{S,rel} & 0 < h_{S,rel} < 1 \\ 0 & h_{S,rel} \leq 0 \end{cases} \tag{37}$$

If the extension of a convex segment on the receiver side of the equivalent wedge ($h_{S,rel} < h_{R,rel}$) is above receiver ground ($h_{R,rel} < 1$) the weight is modified according to Eq. (38).

$$w_i = \begin{cases} w_{x,i} & h_{R,rel} \geq 1 \\ w_{x,i}\ h_{R,rel} & 0 < h_{R,rel} < 1 \\ 0 & h_{R,rel} \leq 0 \end{cases} \tag{38}$$

If a transition segment includes more than one impedance or roughness the combined effect is predicted according to Eq. (35) or (36) as for a concave segment.

Transition Segment

In cases where a segment is neither concave nor convex according to the definitions above the segment is considered a transition segment. However, as the transition from segments of concave type depends on $h_{S,rel}$ or $h_{R,rel}$, the type may therefore vary with the frequency. For a transition segment a calculation is performed using the procedure for a concave segment as well as for a convex segment. However, the former calculation is modified compared to the concave segment. The Fresnel-zone weight is calculated using the source and receiver heights h'_S and h'_R in the same way used for concave segments, but in the calculation of the ground effect, h'_S is replaced by h''_S if h'_S is less than h''_S and h'_R is replaced by h''_R if h'_R is less than h''_R. The transition is the defined between the two solution using the $h_{S,rel}$ or $h_{R,rel}$ as a transition parameter as shown in Eqs. (39) and (40).

$$\Delta L_i w_i = \Delta L_i(concave)\ w_i(concave)\ r + \Delta L_i(convex)\ w_i(convex)(1-r) \tag{39}$$

where

$$r = \begin{cases} h_{R,rel} & h_{S,rel} \geq h_{R,rel} \\ h_{S,rel} & h_{S,rel} < h_{R,rel} \end{cases} \tag{40}$$

If a transition segment includes more than one impedance or roughness the combined effect is predicted according to Eq. (35) or (36) as for a concave segment.

4.4.3 Hill-Shaped Terrain and Terrain with Screens

As defined in the introduction of Section 4.4 the hill model include all propagation cases with significant screening effect. When accounting for the effect of screening objects it is in principle not necessary to distinguish between man-made structures such as screens or embankments and natural barriers which are a screening part of the terrain surface. However, for practical reasons it is recommended in an implementation of the comprehensive model to distinguish between "natural" screens and "artificial" screens added to the terrain by man. One reason is that man-made screens normally have a well-defined finite length which terrain screens have not. Another reason is that it is appropriate in the procedure for determining the equivalent flat terrain (see Section 4.4.4.1) to disregard screens. Finally, the definition of screens and reflecting obstacles require a spatial resolution that is higher than normally required for terrain information. However, when using the hill model outlined in the following it is assumed that the segmented terrain and screens are combined into one broken line representation as shown in Figure 7 in Section 4.1.

The hill model is basically a two-dimensional model where the terrain shape used in the calculations is determined by a vertical cross section from source to receiver. In the model it is assumed that the screen has an infinite length perpendicular to the direction of propagation. This limitation is determined by the basic diffraction solutions used in the model. However, in an approximate manner the method is extended to include finite length screens as described in Section 4.6.

In the hill model diffraction effects are based on the wedge diffraction solution of Hadden and Pierce [5]. The solution is modified to include an absorbing wedge by assuming that each wedge face has finite impedance. Diffraction of the finite impedance wedge is described in Section 4.4.3.1.

If two single edge screens contribute to the diffraction effect the combined effect is calculated according to a proposal by Salomons [23] as described in Section 4.4.3.2. If more than two screens appear along the propagation path only the two most significant screens are included and the line segments of the remaining screens are considered reflecting surfaces. In principle the method outlined in Section 4.4.3.2 could be extended to any number of screens but the complexity of the implementation would increase substantially and most likely without a resulting significant gain in accuracy. In the two screen case only the most efficient edge of each screen will be considered.

If a single screen contains two diffracting edges the combined effect of the two edges is calculated according to a proposal by Salomons [23] as described in Section 4.4.3.3. If the screen contains more than two edges the screen is simplified to include the two most significant edges as described in Sections 4.1 and 4.4.4.3. In principle the method outlined in Section 4.4.3.3 could be extended to any number of edges but again the complexity of the implementation would increase substantially without a significant gain in accuracy.

The ground effect of a hill-shaped terrain is predicted by the image method proposed by Jonasson [9] for combining the diffraction effect of a wedge-shaped screen with ground effects. In the image method it is assumed that the terrain before and after the screen, as well as between screens in case of double screens, can be approximated by a flat terrain. If the terrain cannot be considered flat, Fresnel-zone interpolation is used to obtain the over-all ground effect. The principles for combining diffraction and ground effect are described in Section 4.4.3.4 for a single screen and in Section 4.4.3.5 for double screens.

By limiting the number of screens and total number of edges to two, three different cases will be possible:

1) One screen with one edge
2) One screen with two edges
3) Two screens with one edge

In some cases the significance of a secondary screen or secondary edge is disappearing and in such cases transition between the cases has to be defined to avoid discontinuities in the prediction. The transition between the cases is described in Sections 4.4.4.2, 4.4.4.3 and 4.4.4.4.

4.4.3.1 Diffraction of a Finite Impedance Wedge.

The diffraction effect of a wedge-shaped screen is determined on basis of the distances R_S and R_R from the top of the wedge to the source and receiver, the diffraction angles θ_S and θ_R, the wedge angle β, the length of the entire diffracted path ℓ ($=R_S+R_R$ for a single wedge), and the reflection coefficients Q_S and Q_R as shown in Figure 19.

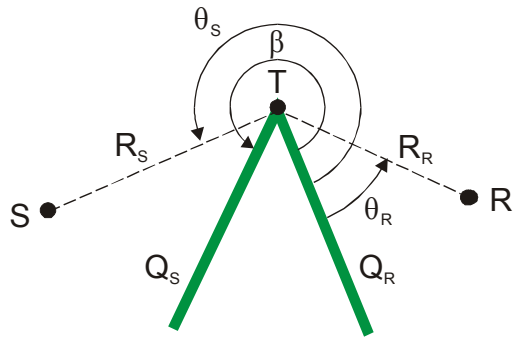

Figure 19
Diffraction effect of a wedge-shaped screen with finite surface impedance. Definition of parameters.

The calculation of the diffracted sound pressure at the receiver p_{diffr} is described in Appendix H. The diffraction coefficient D of the wedge is defined by Eq. (41) where $\ell = R_S + R_R$.

$$p_{diffr} = D\frac{e^{jk\ell}}{\ell} \tag{41}$$

A thin screen corresponds to a wedge with wedge angle $\beta = 2\pi$.

4.4.3.2 Diffraction of Two Wedge-Shaped Screens

The method for predicting the diffraction effect of two wedge-shaped screens as shown in Figure 20 is an approximate method based on the solution for one wedge-shaped screen.

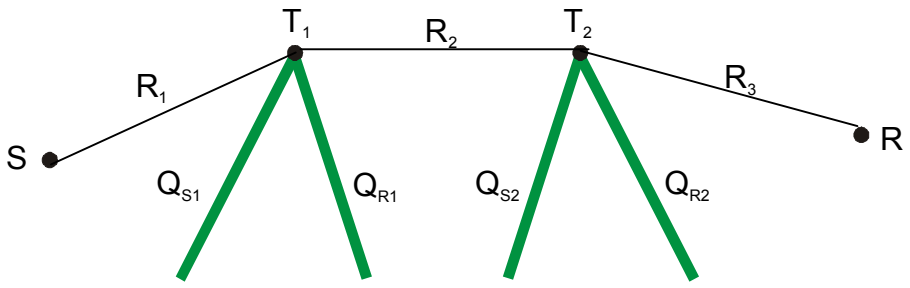

Figure 20
Diffraction by two wedge-shaped screens.

The procedure for predicting the total diffraction effect of the two screens depends on which edge is the primary edge and which is the secondary edge. This will be determined as described in Sections 4.4.4.2 and 4.4.4.3.

When calculating the diffraction coefficient D_1 of the first wedge with the top point T_1 the receiver is replaced by the top T_2 of the other wedge as shown in Figure 21. However, if T_2 is below the line T_1R the diffraction angle θ_{R1} at the receiver side is determined by the direction T_1R instead.

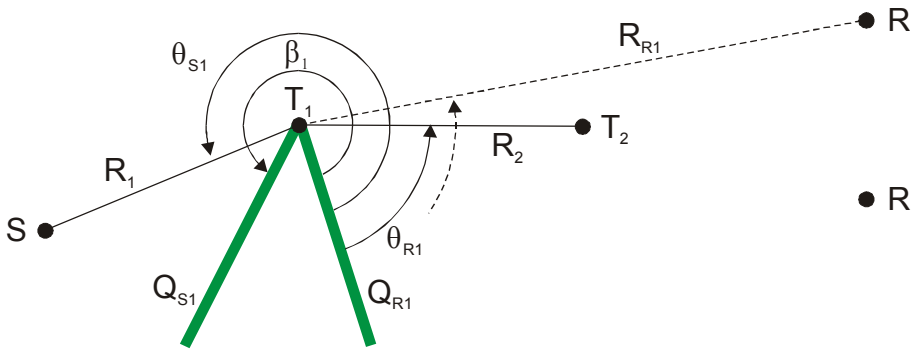

Figure 21
Calculation of the diffraction coefficient of the first wedge. Definition of parameters.

If T_1 is the primary edge the pressure p_1 is calculated as described in Appendix H for a single edge using the following parameters:

$$R_S = R_1$$
$$R_R = R_2 + R_3$$
$$\theta_S = \theta_{S1}$$
$$\theta_R = \theta_{R1} \quad \begin{cases} to\ T_1T_2\ if\ T_2\ is\ at\ or\ above\ T_1R \\ to\ T_1R\ if\ T_2\ is\ below\ T_1R \end{cases}$$
$$\beta = \beta_1$$
$$\ell = R_1 + R_2 + R_3$$
$$Q_S = Q_{S1}$$
$$Q_R = Q_{R1}$$

If T_1 is the secondary edge the pressure p_1 is instead calculated using the following parameters:

$$R_S = R_1$$
$$R_R = R_2$$
$$\theta_S = \theta_{S1}$$
$$\theta_R = \theta_{R1} \quad \begin{cases} to\ T_1T_2\ if\ T_2\ is\ at\ or\ above\ T_1R \\ to\ T_1R\ if\ T_2\ is\ below\ T_1R \end{cases}$$
$$\beta = \beta_1$$
$$\ell = R_1 + R_2$$
$$Q_S = Q_{S1}$$
$$Q_R = Q_{R1}$$

The diffraction coefficient D_1 is then calculated by Eq. (42) where $\ell_1 = \ell$ defined above.

$$D_1 = p_1\ \ell_1\ e^{-jk\ell_1} \tag{42}$$

When calculating the diffraction coefficient D_2 of the second wedge with the top point T_2 the source is replaced by the top T_1 of the other wedge as shown in Figure 22. However, if T_1 is below the line T_2S the diffraction angle θ_{S2} at the source side is determined by the direction T_2S instead.

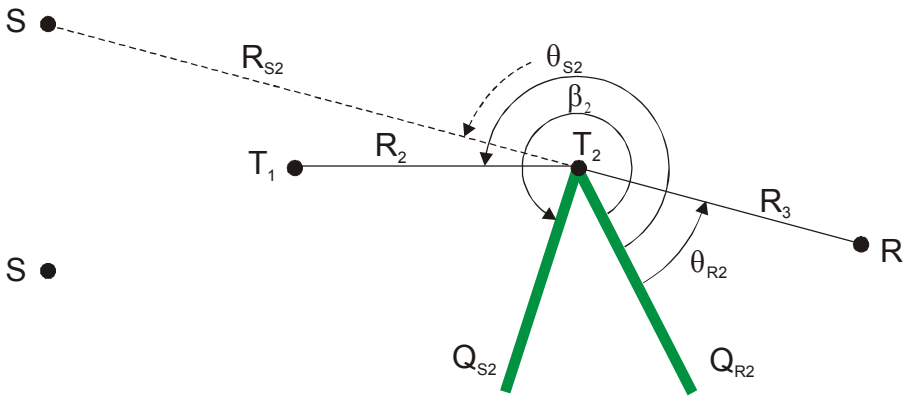

Figure 22
Calculation of the diffraction coefficient of the second wedge. Definition of parameters.

If T_2 is the primary edge the pressure p_2 is calculated as described in Appendix H for a single edge using the following parameters:

$$R_S = R_1 + R_2$$
$$R_R = R_3$$
$$\theta_S = \theta_{S2} \quad \begin{cases} to\ T_2T_1\ if\ T_1\ is\ at\ or\ above\ T_2S \\ to\ T_2S\ if\ T_1\ is\ below\ T_2S \end{cases}$$
$$\theta_R = \theta_{R2}$$
$$\beta = \beta_2$$
$$\ell = R_1 + R_2 + R_3$$
$$Q_S = Q_{S2}$$
$$Q_R = Q_{R2}$$

If T_2 is the secondary edge the pressure p_2 is instead calculated using the following parameters:

$$R_S = R_2$$
$$R_R = R_3$$
$$\theta_S = \theta_{S2} \quad \begin{cases} to\ T_1T_2\ if\ T_1\ is\ at\ or\ above\ ST_2 \\ to\ ST_2\ if\ T_1\ is\ below\ ST_2 \end{cases}$$
$$\theta_R = \theta_{R2}$$
$$\beta = \beta_2$$
$$\ell = R_2 + R_3$$
$$Q_S = Q_{S2}$$
$$Q_R = Q_{R2}$$

The diffraction coefficient D_2 is then calculated by Eq. (43) where $\ell_2 = \ell$ defined above.

$$D_2 = p_2\ \ell_2\ e^{-jk\ell_2} \tag{43}$$

Finally the diffracted sound pressure p at the receiver expressing the combined effect of the two wedges are calculated according to Eq. (44) where $\ell = R_1+R_2+R_3$.

$$p = D_1 D_2 \frac{e^{jk\ell}}{\ell} \tag{44}$$

4.4.3.3 Diffraction of a Two-Edge Screen

The method for predicting the diffraction effect of a screen with two diffracting edges as shown in Figure 23 is an approximate method based on the solution for a wedge-shaped

screen. The method follows by and large the same scheme as used in the double screen case described in the previous section.

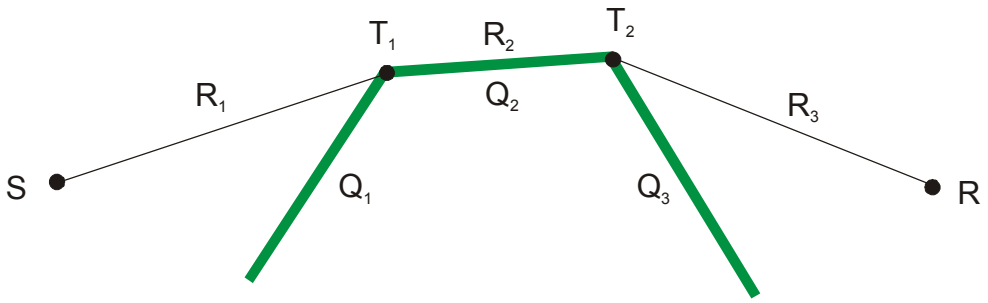

Figure 23
Diffraction by a screen with two edges.

The procedure for predicting the total diffraction effect of the two screens depends on which edge is the primary edge and which is the secondary edge. This will be determined as described in Sections 4.4.4.2 and 4.4.4.3. The calculation the diffraction coefficient D_1 of the first edge T_1 and D_2 of the second edge T_2 is based on almost the same calculation parameters as used in Section 4.4.3.2 for two wedges. The calculation parameters are defined in Figure 24 and Figure 25. The only difference is that $Q_2 = 1$ when calculating for the first edge and $Q_1 = 1$ when calculating for the second edge.

Note: *The use of $Q_2 = 1$ and $Q_1 = 1$ for the first and second edge respectively instead of the real values of Q constitutes a modification compared to the original method described in [31], [23]. It has been found that the original proposal by Salomons [23] works well if the segment between the edges is a hard surface (Q = 1). However, in the presence of finite impedance a substantial unrealistic attenuation is found at high frequencies. The reason is that Q_2 will become –1 at high frequencies and the 4 rays in the wedge model therefore will cancel each other two by two. Different procedures to solve the problem has been analysed but it has not been possible within the project to find a proper solution to the problem. BEM calculations [22] indicate that the chosen solution is acceptable in case of limited width of the screen top segment (T_1T_2) but also that some underestimation of the attenuation will be found at high frequencies if the width is large. It must be recommended to study this more closely in connection with future revisions.*

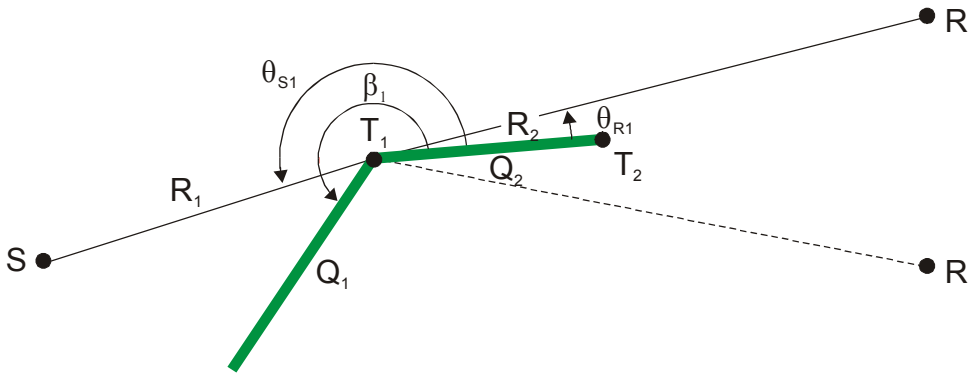

Figure 24
Calculation of the diffraction coefficient of the first edge. Definition of parameters.

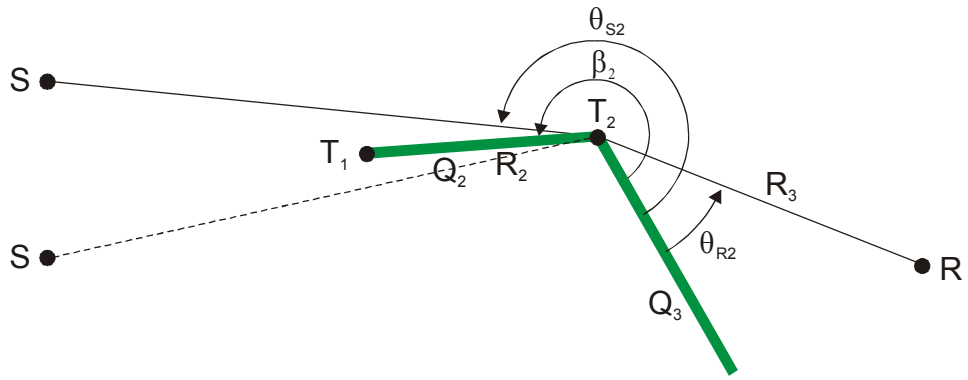

Figure 25
Calculation of the diffraction coefficient of the second edge. Definition of parameters.

Finally the diffracted sound pressure p at the receiver expressing the combined effect of the two edges is calculated according to Eq. (45) where $\ell = R_1+R_2+R_3$.

$$p = 0.5\, D_1 D_2\, \frac{e^{jk\ell}}{\ell} \tag{45}$$

4.4.3.4 Terrain with a Single Screen

In the hill prediction models it is generally assumed that any terrain segment in the simplified terrain shape which has not been identified as being a part of a significant screen shall be considered a reflecting surface. This also includes segments of "artificial" screens added to the terrain as described in Section 4.1.

According to this definition the terrain before and after a single screen may consist of more than one segment forming a non-flat terrain. By example, a terrain is shown in

Figure 26 where the two segments denoted 4 and 5 form a wedge-shaped screen. The remaining five segments will be considered reflecting surfaces. Segments 1–3 will form the surface on the source side of the screen while segments 6–7 form the surface on the receiver side.

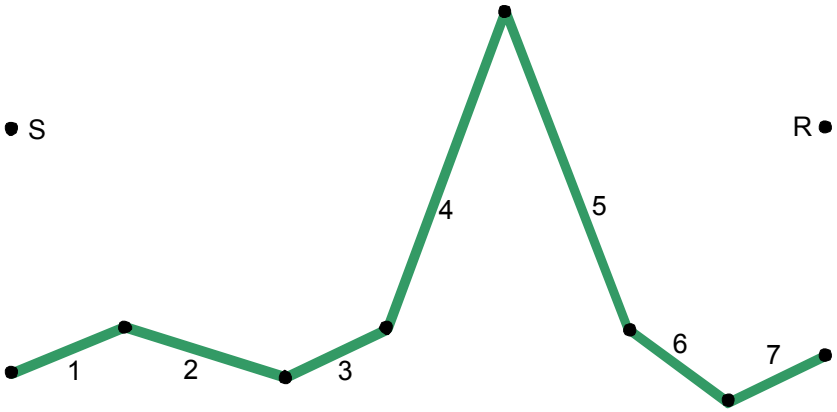

Figure 26
Example of non-flat terrain with one significant screen.

When a screen is placed on the ground, the effect of ground reflections from a finite-impedance plane before and after the screen is combined with the effect of diffraction according to the image method proposed by Jonasson [9]. Figure 27 shows the four rays considered in the image method in the case of a single thin screen placed on a flat impedance plane.

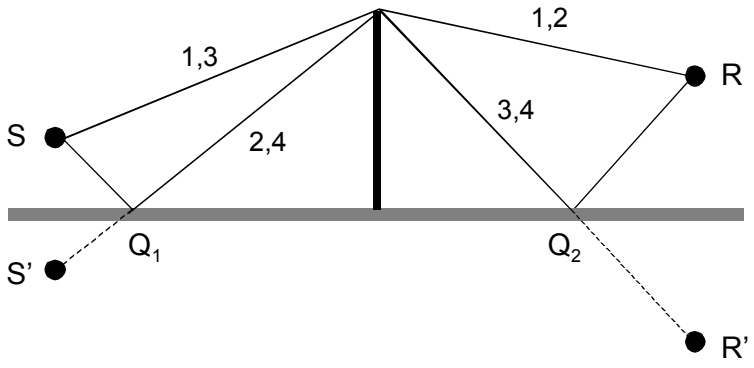

Figure 27
Combined ground and screen effect. Image method.

The total sound pressure at the receiver is sum of contributions from the four rays as expressed by Eq. (46). p_1 is the sound pressure at the receiver from the source diffracted over the screen. p_2 is the pressure at the receiver from the image source, p_3 is the pressure at the image receiver from the source and p_4 is the pressure at the image receiver from the image source. The spherical wave reflection coefficients Q_1 and Q_2 on the source and receiver side of the screen, respectively, are calculated as if the source (Q_2) or the receiver (Q_1) is located at the screen top.

$$p = p_1 + Q_1 p_2 + Q_2 p_3 + Q_1 Q_2 p_4 \tag{46}$$

The problem when trying to apply this method in case of a non-flat terrain as shown in Figure 26 is that there will be not only one image source and one image receiver but one image source for each surface segment on the source side and one image receiver for each surface segment on the receiver side.

To solve the problem the effect of screen and ground expressed by the sound pressure p in Eq. (46) relative to the free-field sound pressure p_0 has to be expressed as shown in Eq. (47). In this equation p_1/p_0 is the effect of the screen alone and the term in brackets is the effect of the ground in excess of the screen effect. In this way the screen effect part ΔL_S of the propagation effect and the ground effect part ΔL_G can be separated as shown in Eqs. (48) to (50).

$$\frac{p}{p_0} = \frac{p_1}{p_0}\left(1 + Q_1 \frac{p_2}{p_1} + Q_2 \frac{p_3}{p_1} + Q_1 Q_2 \frac{p_4}{p_1}\right) \tag{47}$$

$$\Delta L = \Delta L_S + \Delta L_G = 20 \log \left| \frac{p}{p_0} \right| \tag{48}$$

$$\Delta L_S = 20 \log \left| \frac{p_1}{p_0} \right| \tag{49}$$

$$\Delta L_G = 20 \log \left| \frac{p}{p_1} \right| = 20 \log \left| 1 + Q_1 \frac{p_2}{p_1} + Q_2 \frac{p_3}{p_1} + Q_1 Q_2 \frac{p_4}{p_1} \right| \tag{50}$$

The Fresnel-zone interpolation principle previously used in this report for a valley-shaped terrain and for a flat terrain with varying surface properties will again be used to obtain the combined ground effect of all the reflecting surfaces in a non-flat terrain with a screen. The ground effect part ΔL_G of the propagation effect is determined according to Eq. (51) by performing a calculation for all combinations of reflecting surfaces on each side of the screen. $\Delta L_{G,i,j}$ is the calculated result for the i'th segment on the source side of the screen

and the j'th segment on the receiver side. $w_{i,j} = w_{1i}\, w_{2j}$ is the product of the Fresnel-zone weight w_{1i} of the source segment and w_{2j} of the receiver segment. On the source side the size of the Fresnel-zone is determined using the position of the image source S' and a "receiver" located at the screen top. Figure 28 shows an example of the use of this principle for segment no. 2 on the source side of the screen. In the same way the size of the Fresnel-zone on the receiver side is determined by the position of the image receiver R' and a "source" located at the screen top.

$$\Delta L_G = \sum_i \sum_j w_{i,j}\ \Delta L_{Gi,j} \tag{51}$$

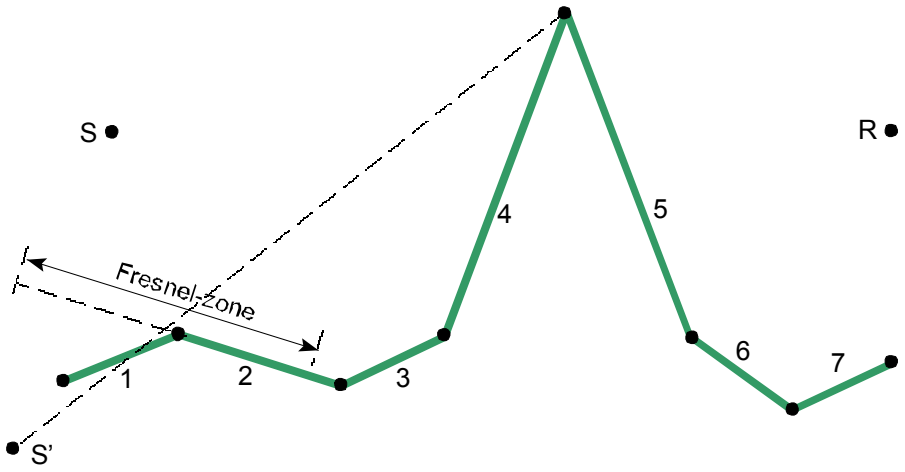

Figure 28
Principle for determining the Fresnel-zone on the source side of the screen.

If the source (or receiver, respectively) or the top of screen is at or below the segment the Fresnel-zone weight is defined as being 0. Such a segment may well contribute to the sound pressure at the receiver but as the finite size of the faces of a wedge-shaped screen on the other hand is not taken into account, when including the reflection in the screen surface, these two insufficiencies will to some extent compensate each other. To ensure a smooth transition between this case and the full contribution according to the Fresnel-zone principle a modified Fresnel-zone weight must be determined. For a segment on the source side of the screen the modified weight w_{1i} is calculated according to Eqs. (52) to (56) on the basis of the weight $w_{1i,org}$ determined by the original Fresnel-zone principle. In these equations h'_S and h'_{SCR} are the height of source and screen top measured perpendicular to the segment and d'_{SCR} is the distance between the source and screen top projections onto the segment. h_S is the height of the source above local ground as defined in Section 4.1.

$$w_{1i} = w_{1i,org}\, r_S\, r_{SCR1} \tag{52}$$

$$r_S = \begin{cases} 1 & h'_S \geq h''_S \\ \dfrac{h'_S}{h''_S} & 0 < h'_S < h''_S \\ 0 & h'_S \leq 0 \end{cases} \tag{53}$$

$$h''_S = \begin{cases} h_S & h_S < h''_{SCR1} \\ h''_{SCR1} & h_S \geq h''_{SCR1} \end{cases} \tag{54}$$

$$r_{SCR1} = \begin{cases} 1 & h'_{SCR1} \geq h''_{SCR1} \\ \dfrac{h'_{SCR1}}{h''_{SCR1}} & 0 < h'_{SCR1} < h''_{SCR1} \\ 0 & h'_{SCR1} \leq 0 \end{cases} \tag{55}$$

$$h''_{SCR1} = \begin{cases} 0.005\, d'_{SCR1} & d'_{SCR1} < 400 \\ 2 & d'_{SCR1} \geq 400 \end{cases} \tag{56}$$

For a segment on the receiver side of the screen the modified weight w_{2j} is calculated according to Eqs. (57) to (61) on the basis of the weight $w_{2j,org}$ determined by the original Fresnel-zone principle. In these equations h'_R and h'_{SCR2} are the height of receiver and screen top measured perpendicular to the segment and d'_{SCR2} is the distance between the receiver and screen top projections onto the segment. h_R is the height of the receiver above local ground.

$$w_{2j} = w_{2j,org}\, r_R\, r_{SCR2} \tag{57}$$

$$r_R = \begin{cases} 1 & h'_R \geq h''_R \\ \dfrac{h'_R}{h''_R} & 0 < h'_R < h''_R \\ 0 & h'_R \leq 0 \end{cases} \tag{58}$$

$$h''_R = \begin{cases} h_R & h_R < h''_{SCR2} \\ h''_{SCR2} & h_R \geq h''_{SCR2} \end{cases} \tag{59}$$

$$r_{SCR2} = \begin{cases} 1 & h'_{SCR2} \geq h''_{SCR2} \\ \dfrac{h'_{SCR2}}{h''_{SCR2}} & 0 < h'_{SCR2} < h''_{SCR2} \\ 0 & h'_{SCR2} \leq 0 \end{cases} \tag{60}$$

$$h''_{SCR2} = \begin{cases} 0.005\, d'_{SCR2} & d'_{SCR2} < 400 \\ 2 & d'_{SCR2} \geq 400 \end{cases} \tag{61}$$

The combined effect of screen and ground is calculated by Eq. (62).

$$\Delta L = 20 \log \left| \frac{p_1}{p_0} \prod_{i=1}^{N_1} \prod_{j=1}^{N_2} \left(1 + \frac{p_{2,i,j}}{p_1} Q_{1i} + \frac{p_{3,i,j}}{p_1} Q_{2j} + \frac{p_{4,i,j}}{p_1} Q_{1i} Q_{2j} \right)^{w_{1i} w_{2j}} \right| \tag{62}$$

Eq. (62) is valid when the sum Σw_{1i} and Σw_{2j} of weights on the source and receiver side is larger than or equal to 1. However, if one of these sums is approaching 0 at the same time as the other sum still is about 1 or larger Eq. (62) is no longer applicable. If either Σw_{1i} or Σw_{2j} is 0, the product $w_{1i}\, w_{2j}$ will also be 0 and there will be no contribution from the considered combination of source and receiver segments although there still is a full reflection from one of the sides.

To solve the problem of either Σw_{1i} or Σw_{2j} being smaller than 1 Eq. (62) is replaced by Eq. (63). If Σw_{1i} is larger than or equal to 1, w'_{1i} and Q'_{1i} are equal to w_{1i} and Q_{1i} used in Eq. (62) but if Σw_{1i} is smaller than 1, w'_{1i} is determined by Eq. (66) and Q'_{1i} by Eq. (68) instead. In the same way, if Σw_{2j} is larger than or equal to 1, w'_{2j} and Q'_{2j} are equal to w_{2j} and Q_{2j} used in Eq. (62) but if Σw_{2j} is smaller than 1, w'_{2j} is determined by Eq. (67) and Q'_{2j} by Eq. (69). If $w_{1t} = 0$ or $w_{2j} = 0$ Eq. (63) is replaced by Eq. (70) and (71), respectively, and if $w_{1t} = 0$ and $w_{2j} = 0$ by Eq. (72).

Note: *The power of 2 in Eqs. (68) and (69) has been estimated as the value which gives the best agreement between the original and modified Fresnel-zone weighting principle as described in [18].*

$$\Delta L = 20 \log \left| \frac{p_1}{p_0} \prod_{i=1}^{N_1} \prod_{j=1}^{N_2} \left(1 + \frac{p_{2,i,j}}{p_1} Q'_{1i} + \frac{p_{3,i,j}}{p_1} Q'_{2j} + \frac{p_{4,i,j}}{p_1} Q'_{1i}\, Q'_{zj} \right)^{w'_{1i} w'_{2j}} \right| \tag{63}$$

$$w_{1t} = \sum_i w_{1i} \tag{64}$$

$$w_{2t} = \sum_j w_{2j} \tag{65}$$

$$w'_{1i} = \frac{w_{1i}}{w_{1t}} \tag{66}$$

$$w'_{2j} = \frac{w_{2j}}{w_{2t}} \tag{67}$$

$$Q'_{1i} = Q_{1i}\ w_{1t}^2 \tag{68}$$

$$Q'_{2j} = Q_{2j}\ w_{2t}^2 \tag{69}$$

$$\Delta L = 20 \log \left| \frac{p_1}{p_0} \prod_{j=1}^{N_2} \left(1 + \frac{p_{3,j}}{p_1} Q'_{2j} \right)^{w'_{2j}} \right| \tag{70}$$

$$\Delta L = 20 \log \left| \frac{p_1}{p_0} \prod_{i=1}^{N_1} \left(1 + \frac{p_{2,i}}{p_1} Q'_{1i} \right)^{w'_{1i}} \right| \tag{71}$$

$$\Delta L = 20 \log \left| \frac{p_1}{p_0} \right| \tag{72}$$

In the description shown above it is assumed that there is only one impedance and roughness type within the common area of the straight line segment and the Fresnel-zone. If the impedance and roughness of the terrain is varying within this area, this is solved in a similar manner as described in Section 4.4.2 for a valley-shaped terrain (see Figure 15 and Eqs. (35) and (36)). If N_{m1} combinations of surface properties (impedance and roughness) exist for a given source side segment and N_{m2} for a given receiver side segment this can as expressed as shown in Eqs. (73) or (74). The ground effect is according to this equation calculated for the N_{m1} times N_{m2} combinations of surface properties and the segment weights w_{1i} and w_{2j} have been divided in weights $w_{1i,m1}$ and $w_{2j,m2}$ corresponding to surface property no. m1 and m2 on the source and receiver side respectively ($\Sigma w_{1i,m1} = w_{1i}$ and $\Sigma w_{2j,m2} = w_{2j}$).

$$w_{i,j} \Delta L_{G,i,j} = \sum_{m1=1}^{N_{m1}} \sum_{m2=1}^{N_{m2}} w_{1i,m1}\ w_{2j,m2}\ \Delta L_{G,i,j,m1,m2} \tag{73}$$

$$\left(\frac{p_{i,j}}{p_1}\right)^{w_{1i}w_{2j}} = \prod_{m1=1}^{N_{m1}}\prod_{m2=1}^{N_{m2}}\left(\frac{p_{i,j,m1,m2}}{p_1}\right)^{w_{1i,m1}w_{2j,m2}} \tag{74}$$

Depending on whether the screen is a single edge or a double edge screen, the diffracted sound pressures p_1 to p_4 in the method described above is calculated according to the method described in Section 4.4.3.1 or Section 4.4.3.3 respectively. When determining the spherical wave reflection coefficients Q_1 and Q_2 in the double edge case the nearest edge will be used to replace the source or receiver.

***Note**: If the nearest edge is below the line between the image source or receiver and the farthest edge it would have been physically more plausible to choose the farthest edge. However, a discontinuity will be introduced by the jump from one edge to the other and the transition principle described in Section 4.4.4.3 ensures that the solution is not used when the effect of the nearest edge becomes insignificant.*

4.4.3.5 Terrain with Double Screens

In the hill prediction model for the two screen case it is assumed similar to the one screen case that any terrain segment in the simplified terrain shape which has not been identified as being a part of one of the significant screens shall be considered a reflecting surface. According to this definition the terrain before, after and between the screens may consist of more than one segment forming a non-flat terrain.

When two screens are placed on the ground, the effect of ground reflections is combined with the effect of diffraction by extending the image method described in Section 4.4.3.4 to include a reflection between the screens. Figure 29 shows the eight rays considered in the image method in case of two thin screens placed on a flat impedance plane.

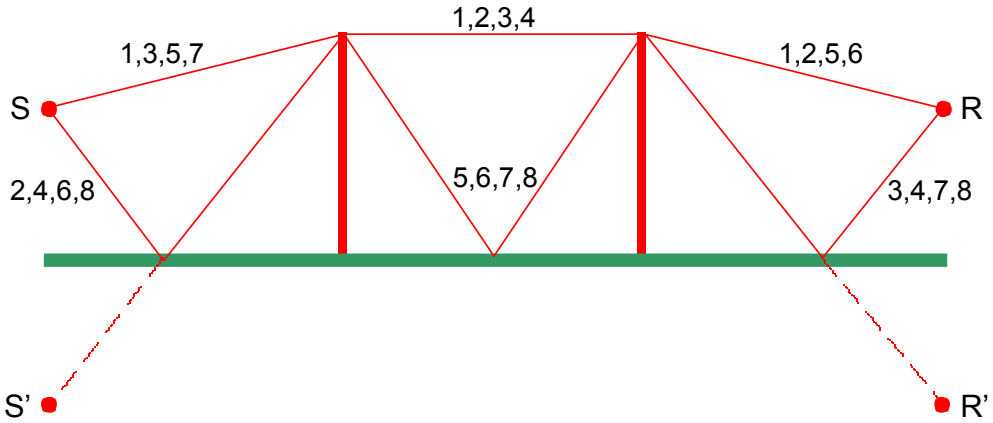

Figure 29
Definition of 8 rays in double screen calculation.

The total sound pressure at the receiver R is the sum of contributions from the eight rays as given by Eq. (75).

$$p = p_1 + Q_1\, p_2 + Q_3\, p_3 + Q_1\, Q_3\, p_4 + Q_2 p_5 + Q_1 Q_2 p_6 + Q_2 Q_3 p_7 + Q_1 Q_2 Q_3 p_8 \qquad (75)$$

In Eq. (75) p_1 is the diffracted sound pressure at the receiver from the source over the two screens, p_2 is the pressure at the receiver from the image source. p_3 is the pressure at the image receiver from the source, and p_4 is the pressure at the image receiver from the image source. p_5 to p_8 correspond to p_1 to p_4 but the rays include a reflection between the two screens. The diffracted sound pressures p_1 to p_8 is calculated according to the method described in Section 4.4.3.2. The spherical wave reflection coefficient Q_1 on the source side is calculated as if the receiver is located at the top of the first screen. The spherical wave reflection coefficient Q_2 between the screens is calculated as if the source is located at the top of the first screen and the receiver at the top of the second screen. The spherical wave reflection coefficient Q_3 on the receiver side is calculated as if the source is located at the top of the second screen.

In order to apply the method to cases of non-flat segmented terrain the same approach is used as for a single screen. Screen and ground effects are separated as shown in Eqs. (76) to (79).

$$\frac{p}{p_0} = \frac{p_1}{p_0}\left(\begin{array}{l} 1 + Q_1 \dfrac{p_2}{p_1} + Q_3 \dfrac{p_3}{p_1} + Q_1 Q_3 \dfrac{p_4}{p_1} + Q_2 \dfrac{p_5}{p_1} \\ + Q_1 Q_2 \dfrac{p_6}{p_1} + Q_2 Q_3 \dfrac{p_7}{p_1} + Q_1 Q_2 Q_3 \dfrac{p_8}{p_1} \end{array}\right) \qquad (76)$$

$$\Delta L = \Delta L_S + \Delta L_G \qquad (77)$$

$$\Delta L_S = 20 \log \left| \frac{p_1}{p_0} \right| \qquad (78)$$

$$\Delta L_G = 20 \log \left| \frac{p}{p_1} \right| = 20 \log \left| \begin{array}{l} 1 + Q_1 \dfrac{p_2}{p_1} + Q_3 \dfrac{p_3}{p_1} + Q_1\, Q_3 \dfrac{p_4}{p_1} + Q_2 \dfrac{p_5}{p_1} \\ + Q_1 Q_2 \dfrac{p_6}{p_1} + Q_2 Q_3 \dfrac{p_7}{p_1} + Q_1 Q_2 Q_3 \dfrac{p_8}{p_1} \end{array} \right| \qquad (79)$$

As in the single screen case the non-flat terrain problem with more than one terrain segment before, after, or between the screens is again solved using the Fresnel-zone interpolation principle as given by Eq. (80).

$$\Delta L_G = \sum_i \sum_j \sum_n w_{i,j,n}\ \Delta L_{G,i,j,n} \tag{80}$$

If the number of reflecting ground segments before the first screen, between the screens, and after the second screen is N_1, N_2, and N_3, respectively, the propagation effect is given by Eqs. (81) through (90). w_{1i}, w_{2j}, and w_{3n} are the modified Fresnel-zone weights of each ground segment.

$$\Delta L = 20 \log \left| \frac{p_1}{p_0} \prod_{i=1}^{N_1} \prod_{j=1}^{N_2} \prod_{n=1}^{N_3} \left(\begin{array}{l} 1 + \frac{p_{2,i,j,n}}{p_1} Q'_{1i} + \frac{p_{3,i,j,n}}{p_1} Q'_{3n} \\ + \frac{p_{4,i,j,n}}{p_1} Q'_{1i}\, Q'_{3n} + \frac{p_{5,i,j,n}}{p_1} Q'_{2j} \\ + \frac{p_{6,i,j,n}}{p_1} Q'_{1i}\, Q'_{2j} + \frac{p_{7,i,j,n}}{p_1} Q'_{2j}\, Q'_{3n} \\ + \frac{p_{8,i,j,n}}{p_1} Q'_{1i}\, Q'_{2j}\, Q'_{3n} \end{array} \right)^{w'_{1i} w'_{2j} w'_{3n}} \right| \tag{81}$$

$$w_{1t} = \sum_i w_{1i} \tag{82}$$

$$w_{2t} = \sum_j w_{2j} \tag{83}$$

$$w_{3t} = \sum_m w_{3m} \tag{84}$$

$$w'_{1i} = \begin{cases} w_{1i} & w_{1t} \geq 1 \\ \dfrac{w_{1i}}{w_{1t}} & 0 < w_{1t} < 1 \\ 1 & w_{1t} = 0 \end{cases} \tag{85}$$

$$w'_{2j} = \begin{cases} w_{2j} & w_{2t} \geq 1 \\ \dfrac{w_{2j}}{w_{2t}} & 0 < w_{2t} < 1 \\ 1 & w_{2t} = 0 \end{cases} \tag{86}$$

$$w'_{3n} = \begin{cases} w_{3n} & w_{3t} \geq 1 \\ \dfrac{w_{3n}}{w_{3t}} & 0 < w_{3t} < 1 \\ 1 & w_{3t} = 0 \end{cases} \tag{87}$$

$$Q'_{1i} = \begin{cases} Q_{1i} & w_{1t} \geq 1 \\ Q_{1i} w_{1t}^3 & w_{1t} < 1 \end{cases} \tag{88}$$

$$Q'_{2j} = \begin{cases} Q_{2j} & w_{2t} \geq 1 \\ Q_{2j} w_{2t}^3 & w_{2t} < 1 \end{cases} \tag{89}$$

$$Q'_{3n} = \begin{cases} Q_{3n} & w_{3t} \geq 1 \\ Q_{3n} w_{3t}^3 & w_{3t} < 1 \end{cases} \tag{90}$$

Note: *The power of 3 in Eqs. (88) to (90) has been estimated as the value which gives the best agreement between the original and modified Fresnel-zone weighting principle as described in [18].*

When the source, receiver or top of the screens becomes close to the extended terrain segment the effect of the segment is gradually reduced until it disappears completely below the extended segment. In the same way as for a single screen this is taken into account by modifying the Fresnel-zone weight.

The modified Fresnel-zone weight w_{1i} is determined as shown in Eqs. (91) to (95) on the basis of the original Fresnel-zone weight $w_{1i,org}$ using the same "source" and "receiver" as used to determine Q_1. h'_S and h'_{SCR1} are the heights of source and the first screen top measured perpendicular to the ground segment and d'_{SCR1} is the distance between the source and the screen top projections onto the segment. h_S is the height of the source above local ground as defined in Section 4.1.

$$w_{1i} = w_{1i,org} \; r_S \; r_{SCR1} \tag{91}$$

$$r_S = \begin{cases} 1 & h'_S \geq h''_S \\ \dfrac{h'_S}{h''_S} & 0 < h'_S < h''_S \\ 0 & h'_S \leq 0 \end{cases} \tag{92}$$

$$h''_S = \begin{cases} h_S & h_S < h''_{SCR1} \\ h''_{SCR1} & h_S \geq h''_{SCR1} \end{cases} \tag{93}$$

$$r_{SCR1} = \begin{cases} 1 & h'_{SCR1} \geq h''_{SCR1} \\ \dfrac{h'_{SCR1}}{h''_{SCR1}} & 0 < h'_{SCR1} < h''_{SCR1} \\ 0 & h'_{SCR1} \leq 0 \end{cases} \tag{94}$$

$$h''_{SCR1} = \begin{cases} 0.005\, d'_S & d'_{SCR1} < 400 \\ 2 & d'_{SCR1} \geq 400 \end{cases} \tag{95}$$

The modified Fresnel-zone weight w_{2j} is determined as shown in Eqs. (96) to (99) on the basis of the original Fresnel-zone weight $w_{2j,org}$ using the same "source" and "receiver" as used to determine Q_2. h'_{SCR21} and h'_{SCR22} are the heights of the first and second screen top measured perpendicular to the ground segment and d'_{SCR2} is the distance between the two screen top projections onto the segment.

$$w_{2j} = w_{2j,org}\, r_{SCR21}\, r_{SCR22} \tag{96}$$

$$r_{SCR21} = \begin{cases} 1 & h'_{SCR21} \geq h''_{SCR2} \\ \dfrac{h'_{SCR21}}{h''_{SCR2}} & 0 < h'_{SCR21} < h''_{SCR2} \\ 0 & h'_{SCR21} \leq 0 \end{cases} \tag{97}$$

$$r_{SCR22} = \begin{cases} 1 & h'_{SCR22} \geq h''_{SCR2} \\ \dfrac{h'_{SCR22}}{h''_{SCR2}} & 0 < h'_{SCR22} < h''_{SCR2} \\ 0 & h'_{SCR22} \leq 0 \end{cases} \tag{98}$$

$$h''_{SCR2} = \begin{cases} 0.005\, d'_{SCR} & d'_{SCR2} < 400 \\ 2 & d'_{SCR2} \geq 400 \end{cases} \tag{99}$$

The modified Fresnel-zone weight w_{3n} is determined as shown in Eqs. (100) to (104) on the basis of the original Fresnel-zone weight $w_{3n,org}$ using the same "source" and "receiver" as used to determine Q_3. h'_{SCR3} and h'_R are the heights of the second screen top and the receiver measured perpendicular to the ground segment and d'_{SCR3} is the distance

between the receiver and the screen top projections onto the segment. h_R is the height of the receiver above local ground.

$$w_{3n} = w_{3n,org}\ r_{SCR3}\ r_R \tag{100}$$

$$r_{SCR3} = \begin{cases} 1 & h'_{SCR3} \geq h''_{SCR3} \\ \dfrac{h'_{SCR3}}{h''_{SCR3}} & 0 < h'_{SCR3} < h''_{SCR3} \\ 0 & h'_{SCR3} \leq 0 \end{cases} \tag{101}$$

$$h''_{SCR3} = \begin{cases} 0.005\ d'_R & d'_{SCR3} < 400 \\ 2 & d'_{SCR3} \geq 400 \end{cases} \tag{102}$$

$$r_R = \begin{cases} 1 & h'_R \geq h''_R \\ \dfrac{h'_R}{h''_R} & 0 < h'_R < h''_R \\ 0 & h'_R \leq 0 \end{cases} \tag{103}$$

$$h''_R = \begin{cases} h_R & h_R < h''_{SCR3} \\ h''_{SCR3} & h_R \geq h''_{SCR3} \end{cases} \tag{104}$$

In the description shown above it is assumed that there is only one impedance and roughness type within the common area of the straight line segment and the Fresnel-zone. If the impedance and roughness of the terrain is varying within this area, this is solved using the same method as described in Section 4.4.3.4 for a single screen. If N_{m1}, N_{m2} and N_{m3} combinations of surface properties (impedance and roughness) exist for a given segment before, between and after the screens this can as expressed as shown in Eqs. (105) or (106). The ground effect is according to this equation calculated for the N_{m1} times N_{m2} times N_{m3} combinations of surface properties and the segment weights w_{1i}, w_{2j} and and w_{3n} have been divided in weights $w_{1i,m1}$, $w_{2j,m2}$ and $w_{3n,m3}$ corresponding to surface property no. m1, m2 and m3 on the source, middle and receiver side respectively ($\Sigma w_{1i,m1} = w_{1i}$ and $\Sigma w_{2j,m2} = w_{2j}$ and $\Sigma w_{3n,m3} = w_{3n}$).

$$w_{i,j,n}\ \Delta L_{G,i,j,n} = \sum_{m1=1}^{N_{m1}} \sum_{m2=1}^{N_{m2}} \sum_{m3=1}^{N_{m3}} w_{1i,m1}\ w_{2j,m2}\ w_{3n,m3}\ \Delta L_{G,i,j,n,m1,m2,m3} \tag{105}$$

$$\left(\frac{p_{i,j,n}}{p_1}\right)^{w_{1i}w_{2j}w_{3n}} = \prod_{m1=1}^{N_{m1}}\prod_{m2=1}^{N_{m2}}\prod_{m3=1}^{N_{m3}}\left(\frac{p_{i,j,n,m1,m2,m3}}{p_1}\right)^{w_{1i,m1}w_{2j,m2}w_{3n,m3}} \quad (106)$$

4.4.4 Combined Model

In this section principles shall be described for how to choose the appropriate prediction model between the flat, valley, or hill model and within the hill model to choose the right solution (single screen with one or two edges or two screens with one edge each). The section also contains principles for how to ensure smooth transitions from one model to another at borderline cases. In the elaboration of the transition principles special attention has been paid to the demand mentioned in the introduction of the present report that discontinuities in the prediction result should be avoided whenever possible.

4.4.4.1 Transition between Models for Flat Terrain and Non-Fflat Terrain without Screens

When deciding which model to use, the first step is to determine whether the terrain is flat or non-flat. For this purpose the equivalent flat terrain has to be estimated.

The equivalent flat terrain is defined as the flat terrain providing the best fit to the actual terrain using the least squares method (linear regression). The determination of the equivalent flat terrain line by the least squares method is described in Appendix I.

When the equivalent flat terrain has been determined, the areas of the segmented terrain above (A_+) and below (A_-) the equivalent flat terrain can calculated as shown in Appendix I ($A_+ = A_-$ if the equivalent flat terrain is determined by the least squares method). The average deviation Δh from the equivalent flat terrain above and below the terrain is calculated according to Eq. (107) where d_h is the horizontal distance between the source and receiver.

$$\Delta h = \frac{A_+}{d_h} = \frac{A_-}{d_h} \quad (107)$$

Figure 30 shows the equivalent flat terrain corresponding to a segmented terrain and the average deviation from the flat terrain above and below the terrain.

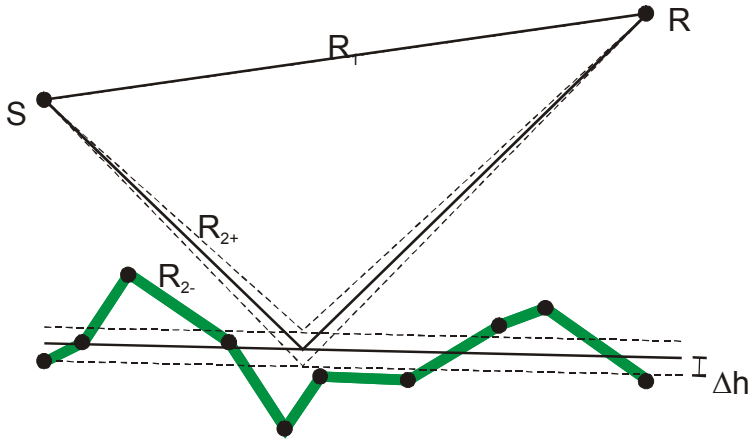

Figure 30
Equivalent flat terrain (solid line) corresponding to a segmented terrain and average deviations from the equivalent flat terrain (dashed lines).

A parallel displacement of the terrain by Δh affects the length of the reflected ray R_2 as shown in Figure 30 and therefore the difference R_2–R_1 where R_1 is the length of the direct ray. The path length difference R_2–R_1 relative to the wavelength λ determines the geometrical part of the phase shift between the direct and reflected ray. If changes in the phase shift due to the spherical wave reflection coefficient can be ignored, which is a reasonable assumption for small terrain displacements, the change in reflected path length ΔR_2 can be used to quantify the effect of a displacement. When Δh is the same below and above the equivalent flat terrain the largest effect will occur for the downward displacement. ΔR_2 is therefore calculated by Eq. (108). h_{Seq} and h_{Req} are the source and receiver heights determined perpendicular to the equivalent flat terrain and d_{eq} is the distance between the source and the receiver measured along the equivalent flat terrain. If h_{Seq} or h_{Req} becomes smaller than 0.01 m, this value is used instead.

$$\Delta R_2 = \sqrt{\left(h_{Seq} + h_{Req} + 2\Delta h\right)^2 + d_{eq}^2} - \sqrt{\left(h_{Seq} + h_{Req}\right)^2 + d_{eq}^2} \qquad (108)$$

It has been found that the terrain can be considered flat if ΔR_2 is less than 1% of the wavelength and on the other hand cannot be considered flat if ΔR_2 is greater than 3% of the wavelength. Based on these findings an interpolation parameter r_f between flat and non-flat terrain can be calculated according to Eq. (109). A value of r_f equal to 1 indicates a flat terrain whereas 0 indicates a non-flat terrain. In between, a transition is obtained between predictions by the flat and the non-flat model applying r_f as an interpolation parameter. At very high frequencies the terrain would in most cases be characterised as non-flat according to this principle. To avoid unnecessarily complicated calculations at very high frequencies the value of r_f obtained at 2000 Hz will be used for higher frequencies.

$$r_f = \begin{cases} 1 & \frac{\Delta R_2}{\lambda} \le 0.01 \\ \frac{0.03 - \frac{\Delta R_2}{\lambda}}{0.02} & 0.01 < \frac{\Delta R_2}{\lambda} < 0.03 \\ 0 & \frac{\Delta R_2}{\lambda} \ge 0.03 \end{cases} \tag{109}$$

The calculation for flat terrain (if r_f is larger that 0) according to the model described in Section 4.4.1 is based on the values of h_{Seq}, h_{Req}, and d_{eq} measured relative to the equivalent flat terrain.

In the case of a highly concavely shaped terrain the valley model will produce a ground effect that is higher than the +6 dB normally obtained for flat terrain at low frequencies. This is due to the fact that the sum of Fresnel-zone weights exceeds 1 even at low frequencies. This behaviour is in agreement with predictions by more accurate models. Unfortunately, the principle given by Eq. (109) tends to characterise such terrain as flat at very low frequencies and therefore prevents the use of the more correct valley model.

To avoid this adverse effect of the described principle the sum of "concave" weights w_{con} for all terrain segments in the valley model is calculated according to Eq. (110). $w_{con,i}$ of each terrain segment is determined by Eq. (111) depending on the type of segment defined in Section 4.4.2. w_i(concave) is the "concave" Fresnel-zone weight from Eq. (39) of the projected segment and r is given by Eq. (40).

$$w_{con} = \sum_i w_{con,i} \tag{110}$$

$$w_{con,i} = \begin{cases} w_i & \textit{concave segment} \\ 0 & \textit{convex segment} \\ w_i\,(\textit{concave})\,r & \textit{transition segment} \end{cases} \tag{111}$$

If $w_{con} \le 1.05$ Eq. (109) is sufficient for determining the flat terrain transition parameter r_{flat} but for higher values of w_{con} a modified principle is needed. Instead, r_{flat} is calculated by Eq. (112) where r_f is the transition parameter according to Eq. (109).

$$r_{flat} = \begin{cases} r_f & w_{con} \le 1.05 \\ \dfrac{1.4 - w_{con}}{0.35} r_f & 1.05 < w_{con} < 1.4 \\ 0 & w_{con} \ge 1.4 \end{cases} \qquad (112)$$

The transition parameter r_{flat} is used to combine the flat terrain model (Section 4.4.1) and the valley model (Section 4.4.2) into a model for any terrain without significant screening effects. The transition is defined by Eq. (113) where ΔL_{flat} and ΔL_{valley} is the ground effect predicted by the flat terrain model and the valley model respectively.

$$\Delta L_{nohill} = r_{flat} \Delta L_{flat} + (1 - r_{flat}) \Delta L_{valley} \qquad (113)$$

4.4.4.2 Transition between Models for Terrain with and without Screens

The next step will be to examine whether the sound propagation is affected significantly by screens. The screens may be parts of the terrain ("natural" screens) or structures added to the terrain ("artificial" screens).

To find whether a part of the terrain profile or one of the screens added to the terrain may be a significant screen the path length difference $\Delta\ell_i$ is determined for each point of discontinuity P_i in the segmented terrain including screens as illustrated in Figure 31. However, only points where the adjacent segments form a convex shape (angle larger than π) and points above the terrain baseline are considered. Furthermore the first and last points in the terrain and in every artificial screen are ignored.

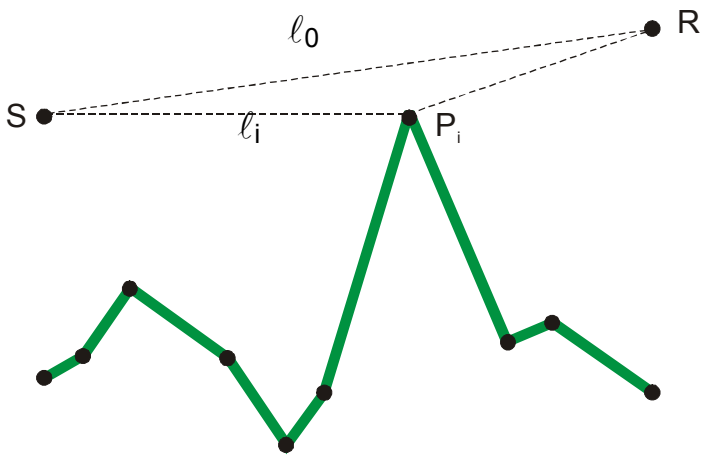

Figure 31
Determination of the screen efficiency of a terrain point.

$\Delta\ell_i$ is determined by Eq. (114). $\Delta\ell_i$ becomes positive if the line-of-sight (LOS) is blocked and negative is if the line-of-sight is unblocked.

$$\Delta\ell_i = \begin{cases} |SP_i| + |RP_i| - |SR| & P_i \text{ above LOS} \\ |SR| - |SP_i| - |RP_i| & P_i \text{ below LOS} \end{cases} \tag{114}$$

The point with the largest value of $\Delta\ell_i$ denoted $\Delta\ell_{SCR1}$ is defined as the most important diffracting edge in the most important screen.

When the most important screen has been identified this way, the efficiency of the screen has to be determined to find out whether or not the screen has a significant screening effect. Three criterions are used for this purpose:

1) $\Delta\ell_{SCR1}$ shall be sufficiently large

2) The height of the screen above the ground surface shall be sufficiently large compared to the wavelength

3) The height of the screen above the ground surface shall be sufficiently large compared to the effective width of sound field at the screen

The first criterion is based on the assumption that the screen effect ΔL_S of a semi-infinite screen can be approximated by a simple function of the path length difference as shown iny Eq. (115) when the top of the screen is just below the line-of-sight. Based on the screen effect an interpolation parameter $r_{\Delta\ell}$ is determined according to Eq. (116). A value of $r_{\Delta\ell}$ equal to 1 indicates full screening effect obtained when the line-of-sight is blocked and 0 indicates insignificant screening effect.

$$\Delta L_S = -6\left(1 - \sqrt{7.5\left|\frac{\Delta\ell}{\lambda}\right|}\right) \tag{115}$$

$$r_{\Delta\ell} = \begin{cases} 1 & \frac{\Delta\ell}{\lambda} \geq 0 \\ 1 - \sqrt{7.5\left|\frac{\Delta\ell}{\lambda}\right|} & -0.133 < \frac{\Delta\ell}{\lambda} < 0 \\ 0 & \frac{\Delta\ell}{\lambda} \leq -0.133 \end{cases} \tag{116}$$

The second criterion states that the height of the screen above the ground surface shall be sufficiently large compared to the wavelength. In [31] it has been concluded that a screen

has no effect on sound propagation below the frequency where the screen is one tenth of the wavelength, that full screen effect is obtained at a frequency 5/3 octaves higher, and that a transition should be applied between these two frequencies. On this basis an interpolation parameter r_λ is determined according to Eq. (117). A value of r_λ equal to 0 and 1 indicates no screening and full screening, respectively. h_{SCR} is the height of the screen above the terrain base line defined in Section 4.1.

$$r_\lambda = \begin{cases} 1 & \frac{h_{SCR}}{\lambda} \geq 0.3 \\ \frac{\frac{h_{SCR}}{\lambda} - 0.1}{0.2} & 0.1 < \frac{h_{SCR}}{\lambda} < 0.3 \\ 0 & \frac{h_{SCR}}{\lambda} \leq 0.1 \end{cases} \tag{117}$$

In the third criterion the height of the screen above the ground surface is compared to the effective width of sound field at the screen. The effective width of the sound field is quantified by the width of the first Fresnel-zone ($\lambda/2$). The effective width increases with increasing source-receiver distance at a given frequency and is largest midway between the source and the receiver. Therefore, the significance of a screen decreases with increasing distance from the source and receiver to the screen.

In [18] it has been found that the height h_{SCR} of the screen above the ground surface relatively to half the size of the Fresnel-zone h_{Fz} is a reasonable quantity to characterise the screen efficiency. The geometrical parameters necessary for calculation of this quantity are defined in Figure 32. In [18] it was found that screens with a height below 1.3% of h_{Fz} should be ignored whereas full screen efficiency was obtained for screen heights above 4.1% of h_{Fz}. These values have later on in the work been doubled to obtain optimum performance of the model leading to the transition parameter r_{Fz} in Eq. (118). In this equation h_{SCR} is the same quantity as used in Eq. (117). h_{Fz} is calculated using the method in Appendix A (with values $r_S = |P_S P_{SCR}|$ and $r_R = |P_R P_{SCR}|$ where P_{SCR} is the projection of the screen edge onto the terrain base line, $\theta = \pi/2$, $F_\lambda = 0.5$).

$$r_{Fz} = \begin{cases} 1 & \frac{h_{SCR}}{h_{Fz}} \geq 0.082 \\ \frac{\frac{h_{SCR}}{h_{Fz}} - 0.026}{0.056} & 0.026 < \frac{h_{SCR}}{h_{Fz}} < 0.082 \\ 0 & \frac{h_{SCR}}{h_{Fz}} \leq 0.026 \end{cases} \tag{118}$$

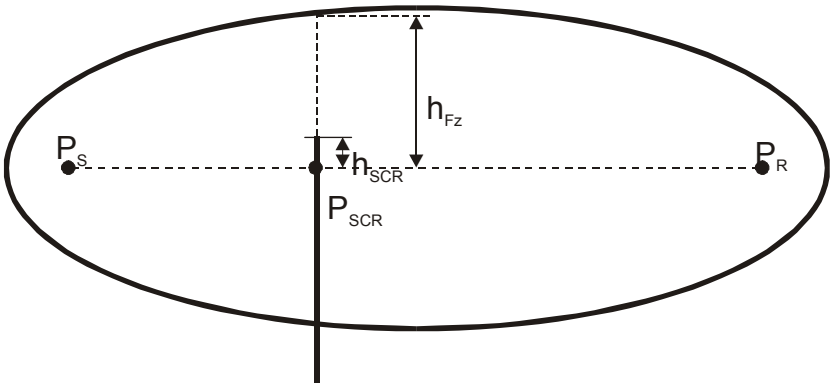

Figure 32
Geometrical parameters used to determine the efficiency of a screen based on the height of the screen compared to the effective width of sound field at the screen.

The three transition parameters are finally combined into the hill transition parameter r_{hill} as given by Eq. (119).

$$r_{hill} = r_{\Delta\ell}\ r_{\lambda}\ r_{Fz} \tag{119}$$

For screens below the line-of-sight the parameter $r_{\Delta\ell}$ will reduce the efficiency of a screen a high frequencies whereas r_{λ} and r_{Fz} will reduce the efficiency at low frequencies.

The transition parameter r_{hill} is used to combine the "nohill" model from Eq. (113) and the hill model described in Section 4.4.4.3 into the final comprehensive terrain and screen model. The transition is defined by Eq. (120) where ΔL_{hill} and ΔL_{nohill} are the ground effect predicted by the hill model and the "nohill" model respectively.

$$\Delta L_t = r_{hill}\Delta L_{hill} + (1 - r_{hill})\Delta L_{nohill} \tag{120}$$

4.4.4.3 Transitions within the Model for Terrain with Screens

In the model for terrain with screens (denoted the hill model) the number of screens is limited to two and the number of diffracting edges to two in the single screen case and to one in the double screen case as already mentioned in the introduction of Section 4.4.3. By this limitation three different cases are possible:

1) One screen with one edge
2) One screen with two edges
3) Two screens with one edge

The screen and ground effect may in each case be calculated by the models described in Sections 4.4.3.1 through 4.4.3.5.

In this section it shall be described how the three models are combined into the hill model by defining suitable transition parameters.

The most important diffracting edge has already been determined in Section 4.4.4.2 for the use of calculating the hill transition parameter. This edge constitutes one of the points in the primary screen. The next step will be to determine if there is a secondary screen with a significant screening effect. However, before doing so it will be necessary to determine which terrain points are parts of the primary screen shape because these points cannot be a part of the secondary screen.

Around the most important diffracting edge at least the preceding and the succeeding segment will be part of the screen. However, in excess of that adjacent segments are considered a part of the screen as long as they intersect convexly (wedge angle greater than π) with the last identified screen segment. The screen is this way expanded to a multi-edge screen until the point where the preceding and succeeding segment intersects concavely (wedge angle less than π). This principle is illustrated in Figure 33.

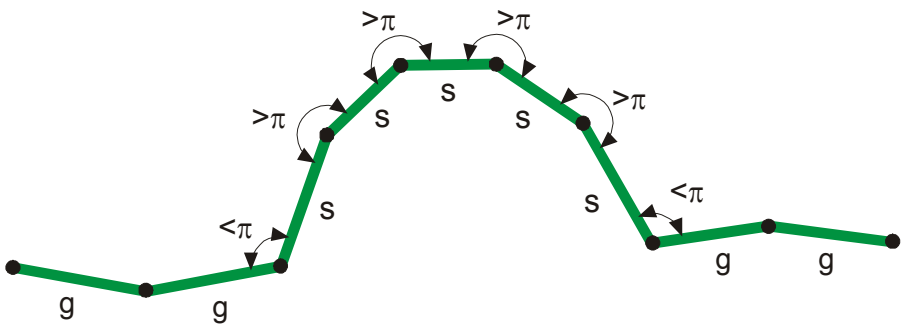

Figure 33
Definition of screen shape, s: screen segments, g: ground segments.

Note: *By the described principle a screen will always consist of at least two segments corresponding to a simple wedge. A thin screen is therefore in the description assumed to be a special case of the simple wedge with a wedge angle of 2π (two identical wedge segments). This definition has been found expedient in the present description. However, this does not necessarily mean that the use of two segments to represent a thin screen will be an expedient solution in the implementation of the method.*

To determine whether a secondary screen with a significant screening effect exists and if so to obtain a transition between predictions by the single and double screen method, a method developed in [19] is described in the following for calculation of a transition parameter r_{SCR2} which is used to quantify the efficiency of a secondary screen.

To find the most efficient edge of a secondary screen the path length difference $\Delta\ell_i$ is determined for each point of discontinuity P_i in the segmented terrain considered when finding the most significant edge of the primary screen ignoring the terrain points which are part of the primary screen shape. If the line-of-sight is blocked by the primary screen the path length difference is calculated between the source and the top of the primary screen on the source side and between the receiver and the top of the primary screen on the receiver side according to Eq. (114) where S or R is replaced by the top of the screen. The point with the largest value of $\Delta\ell_i$ denoted $\Delta\ell_{SCR2}$ is defined as the most important diffracting edge in the second most important screen. If the line-of-sight is unblocked by the primary screen a modified principle is applied to avoid undesirable effects due to possible low position of the primary screen top as described in [19]. For unblocked line-of-sight the point T' on the line-of-sight vertically above top of the screen is used instead of the screen top T as shown in Figure 34.

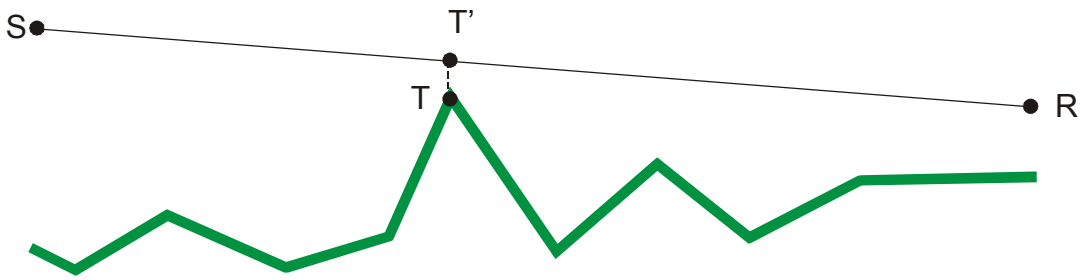

Figure 34
Principle for determining the efficiency of a secondary screen when the primary screen is below the line-of-sight.

As described in Section 4.4.4.2 the efficiency of the primary screen is based on the path length difference of the diffracting edge of the screen and the height of the screen compared to the wavelength and compared to the effective size of the sound field. Similar

quantities are used when determining the efficiency of the secondary screen but in addition to that the effect of distance between the two diffracting edges has to be included.

The efficiency of the secondary screen is determined by the parameter r_{SCR2} which is a product of four parameters $r_{\Delta\ell 2}$, $r_{\lambda 2}$, r_{Fz2}, and r_w as shown in Eq. (121). The first three parameters are calculated by Eqs. (116) to (118) where $\Delta\ell$ is the path length difference $\Delta\ell_{SCR2}$ of the secondary screen and h_{SCR} is the height h_{SCR2} above the terrain base line.

$$r_{SCR2} = r_{\Delta\ell 2}\, r_{\lambda 2}\, r_{Fz2}\, r_w \tag{121}$$

The transition parameter r_w depends on the distance between the screens and is calculated by Eq. (122) where d_{12} is the distance between the most important edges of the two screens.

$$r_w = \begin{cases} 1 & d_{12} \geq \lambda \\ \dfrac{\dfrac{d_{12}}{\lambda} - 0.3}{0.7} & 0.3\lambda < d_{12} < \lambda \\ 0 & d_{12} \leq 0.3\lambda \end{cases} \tag{122}$$

The transition between the single and double screen case can now be obtained by interpolation between the single screen solution ΔL_{SCR1} and the double screen solution ΔL_{SCR2} as shown in Eq. (123).

$$\Delta L_{hill} = \Delta L_{SCR2}\, r_{SCR2} + \left(1 - r_{SCR2}\right) \Delta L_{SCR1} \tag{123}$$

When doing the calculation of ΔL_{SCR1} in the single screen case with one diffracting edge all points of the primary screen shape are removed from the terrain shape except the start and end point and the most important edge. When doing the calculation of ΔL_{SCR2} in the double screen case the same is done for both screen shapes. When simplifying the screen shapes, the impedance and roughness closest to the edge are used.

If two significant screens have been found ($r_{SCR2} > 0$ at at least one frequency), only the most efficient edge of each screen is taken into account. However, if only one screen has been found the next step will be to consider if a significant secondary edge exists in the screen shape which should be included when determining ΔL_{SCR1}.

The efficiency of the secondary edge is by and large determined the same way as for the most important edge of a secondary screen. For each point in the screen shape (except the first and last point and the most important edge) the path length difference $\Delta\ell_i$ is calculated by the same method used for the secondary screen using the primary edge T as

source or receiver when the primary edge is above the line-of-sight and the modified point T' when the primary edge is below the line-of-sight. The point with the largest value of $\Delta\ell_i$ denoted $\Delta\ell_{SCR12}$ is defined as the secondary diffracting edge in the primary screen. After the determination of the secondary edge the screen shape is simplified to contain only the first and last point in the shape and the primary and secondary edges. In the simplified screen the impedance and roughness closest to the edges are used and closest to the primary edge between the edges.

$\Delta\ell_{SCR12}$ will together with the height h_{SCR12} of the secondary edge above the terrain base line and the distance d_{12} between the primary and secondary edge enter into the determination of the efficiency r_{SCR12} of the secondary edge. The quantities are used to determine $r_{\Delta\ell 12}$, $r_{\lambda 12}$, r_{Fz12}, and r_{w12} according to Eqs. (116) through (118) and (122), respectively. However, the determination of r_{SCR12} in Eq. (124) contains two supplementary modifiers $r'_{\lambda 12}$ and r'_{Fz12}.

$$r_{SCR12} = r_{\Delta\ell 12}\ r_{\lambda 12}\ r_{Fz12}\ r'_{\lambda 12}\ r'_{Fz12}\ r_{w12} \tag{124}$$

The modifiers $r'_{\lambda 12}$ and r'_{Fz12} are used to prevent that a secondary edge where the adjacent segments virtually forms a straight line (wedge angle close to π) is interpreted as being an efficient edge. $r'_{\lambda 12}$ and r'_{Fz12} are based on the height h'_{SCR12} determined as illustrated in Figure 35 for the case where the secondary edge is on the source side of the primary edge.

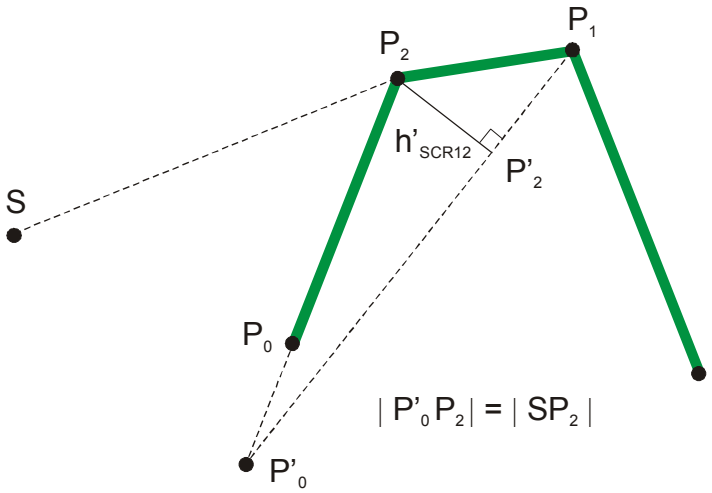

Figure 35
Definition of h'_{SCR12} used for determination of $r'_{\lambda 12}$ and r'_{Fz12}.

In the figure P_1 is the primary edge, P_2 is the secondary edge, P_0 is the first point in the screen and S is the source. P'_0 is the point on the extension of the segment P_2P_0 with a distance to P_2 equal to the distance between S and P_2 as given by Eq. (125).

$$\overrightarrow{P_2P'_0} = \frac{|P_2S|}{|P_2P_0|}\overrightarrow{P_2P_0} \tag{125}$$

h'_{SCR12} is determined as the perpendicular distance to the line $P_1P'_0$ and P'_2 is the projection of P_2 onto the line. In the calculation of the efficiency of the secondary edge it is then assumed that h'_{SCR12} has to be sufficiently large compared to the wavelength and to the effective size of the sound field (same idea as previously used for the height of a screen above the ground). The effective size of the sound field h_{Fz} is calculated by replacing P_S, P_R and P_{SCR} in Figure 32 by P'_0, P_1 and P'_2. $r'_{\lambda 12}$ and r'_{Fz12} is calculated by Eqs. (117) and (118).

In the case where the secondary edge is on the receiver side of the primary edge a similar approach is used but the source S is replaced by the receiver R in Figure 35 and in Eq. (125) and P_0 will be the last point in the screen.

The transition between the single and double edge case for a single screen can be obtained by interpolation between the single edge solution ΔL_{SCR11} and the double edge solution ΔL_{SCR12} as shown in Eq. (126).

$$\Delta L_{SCR1} = \Delta L_{SCR12}\, r_{SCR12} + (1 - r_{SCR12})\Delta L_{SCR11} \tag{126}$$

4.4.4.4 Combining Flat Terrain, Valley and Hill Models, Overview

The combined model for predicting the effect ΔL_t of propagation over terrain and screens has thoroughly been described in the previous Sections 4.4.4.1 through 4.4.4.3. In this section an overview of the model shall be given.

The prediction results by the flat terrain, valley and hill models are

- ΔL_{flat}: Flat terrain model
- ΔL_{valley}: Valley model
- ΔL_{SCR11}: Hill model, one screen with one edge
- ΔL_{SCR12}: Hill model, one screen with two edges
- ΔL_{SCR2}: Hill model, two screens with one edge each

The transition parameters r_{flat}, r_{hill}, r_{SCR2}, r_{SCR12} are described in Section 4.4.4.1 to 4.4.4.3.

The terrain effect ΔL_t is predicted according to Eqs. (127) through (130).

$$\Delta L_t = r_{hill}\Delta L_{hill} + (1 - r_{hill})\,\Delta L_{nohill} \tag{127}$$

where

$$\Delta L_{nohill} = r_{flat}\Delta L_{flat} + \left(1 - r_{flat}\right)\Delta L_{valley} \tag{128}$$

and

$$\Delta L_{hill} = r_{SCR2}\ \Delta L_{SCR2} + \left(1 - r_{SCR2}\right)\Delta L_{SCR1} \tag{129}$$

If $r_{SCR2} > 0$ at at least one frequency then $\Delta L_{SCR1} = \Delta L_{SCR11}$, otherwise ΔL_{SCR1} is determined by Eq. (130).

$$\Delta L_{SCR1} = r_{SCR12}\ \Delta L_{SCR12} + \left(1 - r_{SCR12}\right)\Delta L_{SCR11} \tag{130}$$

4.5 Incoherent Effects

In the sound propagation model described in Section 4.4 it is assumed that contributions from interacting rays are added coherently. However, such a model produces much stronger phase effects at high frequencies, than is observed in outdoor measurements. The use of the attenuation at the centre frequency as representative of the attenuation in the entire one-third octave band will further increase such an effect. In practice, incoherent and averaging effects will smooth out the interference pattern in the attenuation spectrum. The development of a model for including incoherent and averaging effects is described in [18].

The incoherent and averaging effects that are taken into account are:

- Effect of frequency band averaging
- Effect of fluctuating refraction
- Effect of turbulence
- Effect of surface roughness
- Effect of scattering zones

The effect of frequency band averaging covers the averaging within each one-third octave band.

The effect of fluctuating refraction covers the averaging due to fluctuations in atmospheric refraction in excess of what is included in the effect of turbulence.

The effect of turbulence covers the reduction in coherence between different rays due to turbulence.

The effect of surface roughness covers the effect that is observed when a reflecting surface is not perfectly even but contains random height variations.

Finally, the effect of scattering zones covers the reduction in coherence obtained when the sound field is passing a scattering zone. The scattering zone may be a housing area or a forest. The effect of scattering zones are described in general in Section 5 but as already mentioned in Section 2 scattering may influence the propagation effect of terrain and screens by reducing the coherence.

4.5.1 General Principle

The general principle that has been chosen to account for incoherent effects when predicting the ground effect $|p/p_0|$ is shown in Eq. (131). In this principle a coefficient of coherence F is defined for each ray in excess of the primary ray. F_i expresses the coherence between the i'th ray and the primary ray (i=1). In Eq. (131) the first term within the outer brackets is the coherent part and the second term the incoherent part of the sound pressure.

$$\left|\frac{p}{p_0}\right|^2 = \left|\frac{p_1}{p_0}\right|^2 \left(\left| 1 + \sum_{i=2}^{N} F_i \frac{p_i}{p_1} \right|^2 + \sum_{i=2}^{N} \left(1 - F_i^2\right) \left|\frac{p_i}{p_1}\right|^2 \right) \tag{131}$$

For flat terrain the primary ray is the direct ray and for terrain with screens the primary ray is the diffracted ray from source to receiver via the screen edge(s). F will be a real value between 0 and 1, with 0 and 1 indicating full incoherence and full coherence, respectively. The principle defined in Eq. (131) is not a rigorous mathematical solution when the number of rays exceeds two because only the reduction in coherence compared to the primary ray is considered. However, the principle has been found adequate in an engineering model taking into account the large uncertainty involved in describing incoherent effects.

In the two-ray case for flat terrain Eq. (131) will change to Eq. (132) where R_1 and R_2 are the path lengths of the direct and reflected ray, respectively.

$$\begin{aligned} \left|\frac{p}{p_0}\right|^2 &= \left| 1 + F \frac{p_2}{p_1} \right|^2 + \left(1 - F^2\right) \left|\frac{p_2}{p_1}\right|^2 \\ &= \left| 1 + FQ \frac{R_1}{R_2} e^{jk(R_2 - R_1)} \right|^2 + \left(1 - F^2\right) \left| Q \frac{R_1}{R_2} \right|^2 \end{aligned} \tag{132}$$

The first term in Eq. (132) is the coherent part and the second term the incoherent part. The incoherent part is determined by |Q| and R_1/R_2 and is therefore independent of the phase. When propagation becomes very incoherent, it is not likely that Q keeps its physi-

cal relevance. It has therefore been decided in the incoherent part of Eqs. (131) and (132) to replace |Q| by a reflection coefficient $\Re$ based on the random incidence absorption coefficient as described in Section 4.5.2.

4.5.2 Incoherent Reflection Coefficient

The incoherent part of the sound pressure level in Eqs. (131) and (132) is only determined by the numerical value of the spherical wave reflection coefficients and the path lengths and is therefore independent of the phase. The spherical wave reflection coefficient Q is not a "true" reflection coefficient, but has been derived from a mathematical solution for a spherical field reflected by an impedance surface. When propagation becomes significantly incoherent, it is not likely that Q keeps its physical relevance. It has therefore been decided in the incoherent part of Eq. (131) to replace |Q| by a reflection coefficient $\Re$ based on the random incidence absorption coefficient α_{ri} as given by Eq. (133).

$$\Re = \sqrt{1-\alpha_{ri}} \tag{133}$$

α_{ri} is calculated by Eq. (134) (from [14]) where X and Y is the real and imaginary part of the ground impedance Z as defined in Eq. (135).

$$\alpha_{ri} = 8\frac{X}{X^2+Y^2}\left(1-\frac{X}{X^2+Y^2}\ln\left((1+X)^2+Y^2\right)+\frac{X^2-Y^2}{\left(X^2+Y^2\right)Y}\arctan\left(\frac{Y}{1+X}\right)\right) \tag{134}$$

$$Z = X + jY \tag{135}$$

By this approach it will be possible to save a lot of significant calculation time. The calculation of Q is very time-consuming and determines to a high extent the overall calculation time in the model. Q is a function of the reflection angle, propagation distance, and ground impedance whereas $\Re$ only depends on the impedance. It is therefore possible to pre-calculate $\Re$ for each impedance type in the prediction model and insert it in a table. At high frequencies where the ray contributions become fully incoherent in most cases (F = 0) the calculation time will decrease considerably as the calculation of the reflection coefficient can be replaced by a table look-up.

4.5.3 Coefficients of Coherence

The overall coherence coefficient F determining the coherence between two rays is the product of a number of coherence coefficients as shown in Eq. (136). F_f, $F_{\Delta\tau}$, F_c, F_r, F_s are

coherence coefficients corresponding to frequency band averaging, averaging due to fluctuating refraction, partial incoherence, surface roughness, and scattering.

$$F = F_f F_{\Delta\tau} F_c F_r F_s \tag{136}$$

The determination of four of these coefficients is described in the following Sections 4.5.3.1 through 4.5.3.4 whereas F_s is described in Section 5.

4.5.3.1 Frequency Band Averaging

A solution to F_f has been given in [1] which can be used to determine the effect of averaging within one-third octave frequency bands. However, in the present model the solution has been practically modified to obtain $F_f = 0$ for arguments of sine above B as shown in Eq. (137). k is the wave number, R_1 is the length of the primary ray and R_2 of the length secondary ray.

$$F_f = \begin{cases} \dfrac{\sin\left(0.115\, k\left(R_2 - R_1\right)\right)}{0.115\, k\left(R_2 - R_1\right)} & 0.115\, k\left(R_2 - R_1\right) < \pi \\ 0 & 0.115\, k\left(R_2 - R_1\right) \geq \pi \end{cases} \tag{137}$$

4.5.3.2 Averaging Due to Fluctuating Refraction

A similar solution can be found for fluctuating refraction as described in [18]. At a fixed frequency f it is assumed that the path lengths of the rays and therefore the travel time difference τ_2-τ_1 is varying within the range $\Delta\tau_2$-$\Delta\tau_1$ and is uniformly distributed within this range. τ_1 is the travel time corresponding to the primary ray and τ_2 to the secondary ray. The solution is shown in Eq. (138). Again, the solution has been practically modified to obtain $F_{\Delta\tau} = 0$ for arguments of sine above π.

$$F_{\Delta\tau} = \begin{cases} \dfrac{\sin\left(\pi f \left|\Delta\tau_2 - \Delta\tau_1\right|\right)}{\pi f \left|\Delta\tau_2 - \Delta\tau_1\right|} & f\left|\Delta\tau_2 - \Delta\tau_1\right| < 1 \\ 0 & f\left|\Delta\tau_2 - \Delta\tau_1\right| \geq 1 \end{cases} \tag{138}$$

It is generally assumed that τ_2-τ_1 will increase monotonically with an increasing degree of refraction. Therefore, $\Delta\tau_2$-$\Delta\tau_1$ may on this basis be determined by τ_2-τ_1 for the outmost refraction cases as expressed by Eq. (139). τ_{1+} and τ_{2+} are the travel times of the primary and secondary ray in the most downward refraction case and τ_{1-} and τ_{2-} are the corresponding travel times in the least downward refraction case. How the travel times are calculated is described in the companion report for prediction of propagation in refracting atmospheres [20] and shall not be repeated in the present report.

$$\Delta\tau_2 - \Delta\tau_1 = \tau_{2+} - \tau_{1+} - \tau_{2-} + \tau_{1-} \tag{139}$$

For practical reasons it has been found expedient to calculate $\Delta\tau_2$-$\Delta\tau_1$ according to Eq. (140) assuming symmetry in distribution of τ_2-τ_1 around the average meteorological condition. τ_{1m} and τ_{2m} is the travel times corresponding to the average meteorological condition. The advantage of this approach is that τ_{1-} and τ_{2-} shall not be calculated which saves calculation time (τ_{1m} and τ_{2m} have already been calculated for other purposes) and difficulties in the approach would occur when τ_{1-} and τ_{2-} correspond to a shadow zone case.

$$\Delta\tau_2 - \Delta\tau_1 = 2\left(\tau_{2+} - \tau_{1+} - \tau_{2m} + \tau_{1m}\right) \tag{140}$$

In practice, the distribution of τ_2-τ_1 will not be uniform but be more Gaussian-like as the variations are determined by fluctuations in wind speed and temperature. However, a good approximation to account for Gaussian variation in wind speed and temperature gradient is obtained if τ_{1+} and τ_{2+} are calculated for a wind speed of $u_+ = u_m + 1.7\ \sigma_u$ and temperature gradient of $dt/dz_+ = dt/dz_m + 1.7\ \sigma_{dt/dz}$. u_m and σ_u is the mean value and standard deviation of the wind speed, and dt/dz_m and $\sigma_{dt/dz}$ is the mean value and standard deviation of the temperature gradient. 1.7 is the value where the Gaussian distribution and the uniform distribution will have the same standard deviation.

4.5.3.3 Partial Incoherence

The effect of partial incoherence between rays includes the reduction in coherence due to turbulence. It has also been considered also to include a source-related reduction in coherence (from differences in the emission direction of the rays) but this has not been found possible on a general basis. The coherence coefficient defined by Eq. (141) is identical to the mutual coherence function given in [4]. C_v^2 and C_T^2 are the turbulence strength corresponding to wind and temperature, T_0 is the mean temperature in Kelvin, c_0 is the mean sound speed, k is the wave number, ρ is the transversal separation ($\rho = 2h_Sh_R/(h_S+h_R)$ for flat ground where h_S and h_R are heights of source and receiver above the ground and d is the horizontal distance).

$$F_c = \exp\left(-\frac{3}{8}0.364\left(\frac{C_T^2}{T_0^2} + \frac{22}{3}\frac{C_v^2}{c_0^2}\right)k^2\rho^{5/3}d\right) \tag{141}$$

The exponential function in Eq. (141) suffers from the weakness that F_c will never be zero even for very large arguments and as mentioned earlier the calculation time will benefit by having $F_c = 0$. Therefore Eq. (141) is practically modified as shown in Eq. (142) where x is the argument of the exponential function.

$$F_c = \begin{cases} \exp(x) & -1 \le x \le 0 \\ (2+x)\exp(-1) & -2 < x < -1 \\ 0 & x \le -2 \end{cases} \qquad (142)$$

4.5.3.4 Terrain Surface Roughness

The effect of terrain surface roughness covers the effect that is observed when the reflecting terrain surface is not perfectly even but contains random height variations. A method to include this effect has been described in [25]. In the method F_r is a function of the Rayleigh roughness parameter X defined in Eq. (143) where Φ_r is the rms-value of surface height variations, and ψ_G is the grazing ground reflection angle.

$$X = k\sigma_r \sin\psi_G \qquad (143)$$

The coherence coefficient F_r is calculated by Eqs. (144) and (145). The function g(X) is slightly modified compared to [25] to achieve that F_r becomes exactly 1 at X = 0.

$$F_r = \exp\left(0.5\, g\,(x)\right) \qquad (144)$$

where

$$g(x) = \begin{cases} 0 & X \le 0.026686 \\ 0.55988\,(0.115448 - X) - 0.049696 & 0.026686 < X < 0.115448 \\ -0.066 + 1.066X - 8.543X^2 + 4.71X^3 - 0.83X^4 & X \ge 0.115448 \end{cases} \qquad (145)$$

Note: *The method described above is not fully in agreement with the method described in [25] where F_r is used to modify the plane wave reflection coefficient $\Re_p$ which is used in the calculation of the spherical* wave *reflection coefficient Q in the coherent part of the solution. However, it has been found that the simplified method produce results which agree well with the original method within acceptable limits considering the uncertainty of the method. Due to a complete lack of outdoor measurements over terrain with roughness, it must be recommended in the future to validate this part of the model.*

4.6 Finite screens

In the method for predicting screen effects described in Section 4.4.3 it is assumed that the screens have an infinite length. In practice, screens will have a finite length and it is therefore possible that the screen effect will be reduced significantly when sound is diffracted around the vertical edges of the screen. The method for taking into account finite

length of screens is based on [33] but modified slightly to avoid discontinuities. The method is used only for screens with well-defined ends which comprise man-made screens and embankments ("artificial" screens). Screens with less well-defined ends such as natural screens formed by the terrain are instead taken into account by the method for irregularly shaped screens described in Section 4.7.

The contribution from diffraction around vertical edges is in an approximate manner taken into account by adding additional transmission paths as shown in Figure 36. The solid line in the figure is the transmission path from the source S to the receiver R over the screen considered in Section 4.4.3 while the dashed lines are two subsidiary transmission paths introduced to account for diffraction around the vertical edges. The sound pressure is calculated for of each path using the comprehensive propagation model with propagation parameters measured along the vertical propagation planes and added incoherently after a correction for the screening effect of the vertical edges.

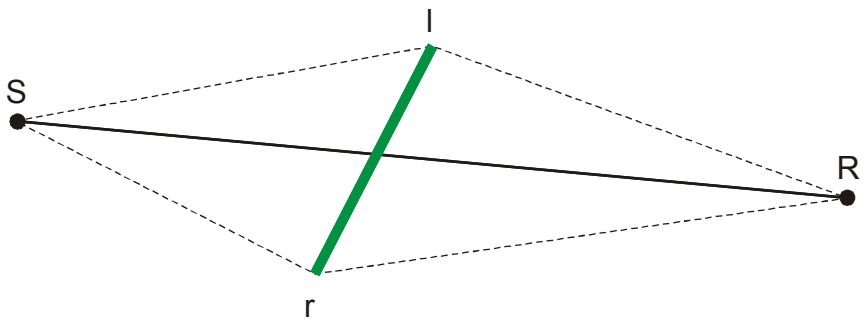

Figure 36
Definition of additional transmission paths in case of a finite screen (top view, l: left edge, r: right edge).

The method for taking into account the contribution of sound diffracted around the vertical edges is based on the diffraction model in Appendix H but reflections in the wedge faces are ignored by including only the principal term (n=1) in Eq. (H1). The principal case is shown in Figure 37 where the screen represented by the line P_1 to P_2 is blocking the propagation plane from the source S to the receiver R. In this case P_1 is on the left side and P_2 on the right side of the propagation plane. The subsidiary case is the case where the propagation plane is not blocked by the screen but where the screen is sufficiently close to the propagation plane to affect the sound pressure level at the receiver. In this case P_1 and P_2 is on the same side of the propagation plane. Figure 38 shows the case where the screen is on the left side.

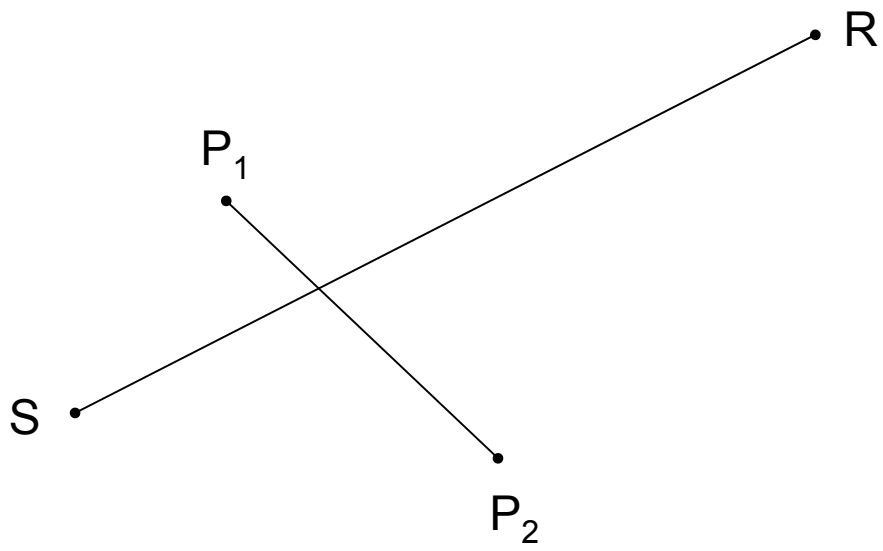

Figure 37
Finite screen with vertical edges at P_1 to P_2 blocking the propagation plane from the source S to the receiver R (top view).

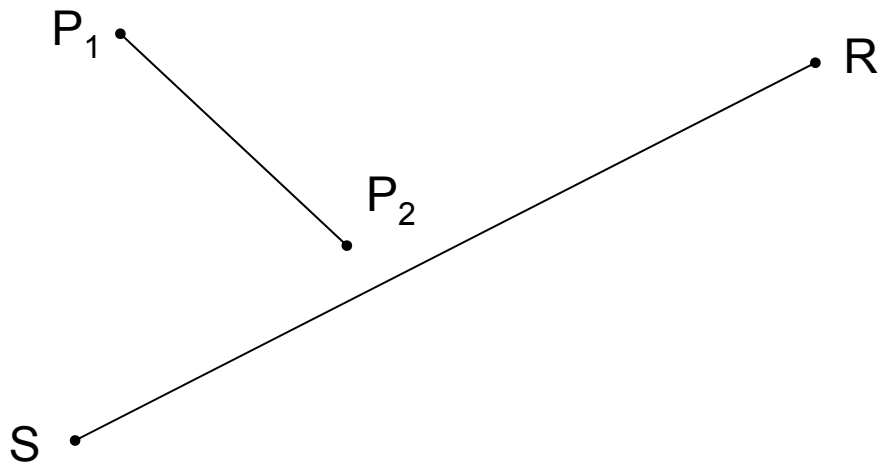

Figure 38
Finite screen with vertical edges at P_1 to P_2 outside the propagation plane from the source S to the receiver R (top view).

In the principal case the sound pressure is calculated for the three vertical propagation planes defined in Figure 39. Plane SR is the direct propagation plane from the source to the receiver and Plane 1 and Plane 2 are the propagation planes around the left and the

right edge of the screen. Plane 1 and 2 are passing just outside the screen so that the screen is not included in the propagation planes. The corresponding sound pressures are denoted p_{SR}, p_1 and p_2 and will be calculated using the two-dimensional reference model.

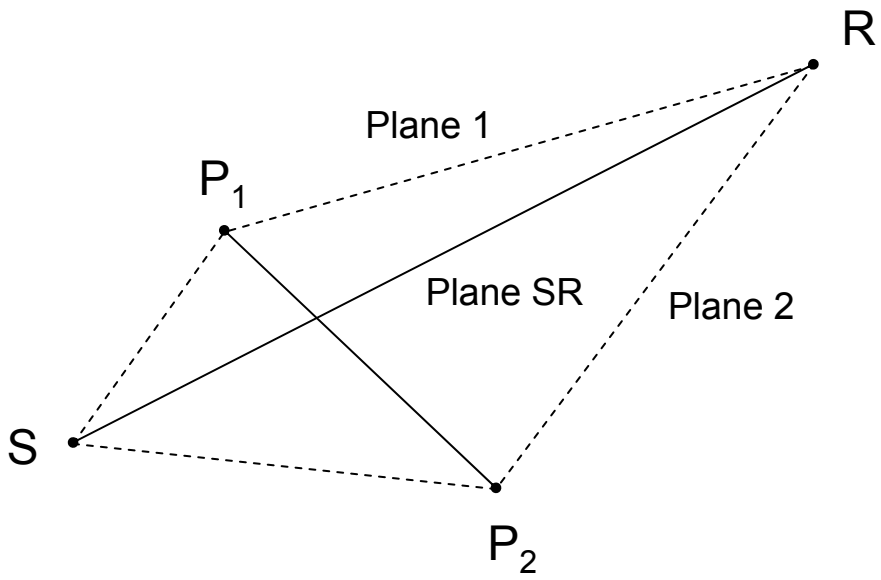

Figure 39
D Definition of vertical propagation planes in case of a blocked direct propagation plane (top view).

If propagation planes 1 and 2 are far away from the direct propagation plane it is reasonable to assume as proposed in [33] that the contributions from the three propagation planes are incoherent. In this case the results have to be added on an energy basis after the results have been weighted as shown in Eq. (146).

$$|p|^2 = |w_{SR} p_{SR}|^2 + |w_1 p_1|^2 + |w_2 p_2|^2 \tag{146}$$

However, this approach will not produce correct results if the planes are very close to each other. In this case the contributions will be coherent and the results have to be added according to Eq. (147).

$$p = w_{SR} p_{SR} + w_1 p_1 + w_2 p_2 \tag{147}$$

The problem is to establish a reasonable transition between the principles given in Eqs. (146) and (147). The principle used in Section 4.5 for combining coherent and incoherent effects has been adopted for this purpose. According to this principle the sound pressure

can be calculated by Eq. (148). F_i is a coherence coefficient which accounts for the reduction in coherence between the i'th propagation plane and the direct propagation plane and possibly for averaging effects. F will be a real value between 0 and 1, with 0 and 1 indicating full incoherence and full coherence, respectively.

$$|p|^2 = |w_{SR} p_{SR} + F_1 w_1 p_1 + F_2 w_2 p_2|^2 + (1 - F_1^2)|w_1 p_1|^2 + (1 - F_2^2)|w_2 p_2|^2 \qquad (148)$$

F_1 and F_2 are calculated by Eq. (149) where F_f is the coherence coefficient due to frequency band averaging (see Section 4.5.3.1) and F_c is the coherence coefficient due to turbulence (see Section 4.5.3.3).

$$F = F_f F_c \qquad (149)$$

To determine the weights w_{SR}, w_1 and w_2 the sound pressure reduction from diffraction around the vertical edges has to be calculated.

Figure 40 defines the geometry used to calculate the contribution of sound diffracted around the left vertical edge of the screen. P_S, P_R, and P_1 are the horizontal projections of the source, receiver and left edge and r_S, r_R, θ_S, θ_R, β, are the parameters used in Appendix H. The weight w_1 is calculated by Eq. (150) where the diffracted sound pressure $p_{diffr,1}$ as a function of frequency is calculated by the Appendix H but with the simplification that the screen faces are assumed to be non-reflecting as mentioned above. r_S, r_R, θ_S, θ_R, β can be determined according to Eqs. (151) to (157). p_0 is the free-field pressure ($p_0 = 1/r_{SR}$).

$$w_1 = \left| \frac{p_{diffr,1}(r_S, r_R, \theta_S, \theta_R, \beta, f)}{p_0} \right| \qquad (150)$$

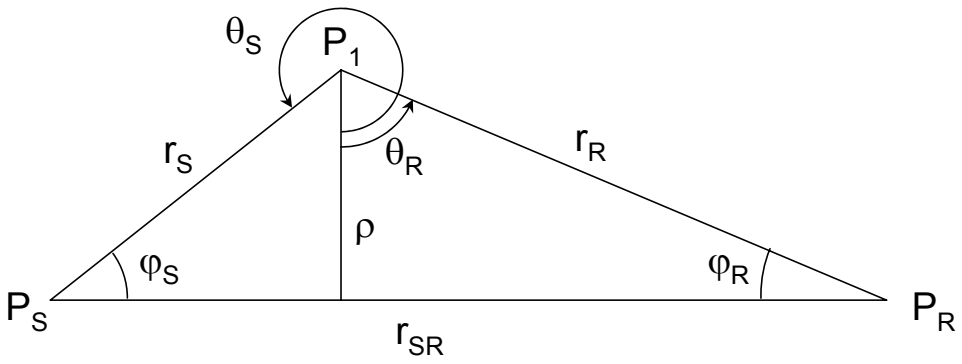

Figure 40
Definition of parameters θ_S, θ_R, β, r_S and r_R to be used in the diffraction calculation and the transversal separation ρ to be used in calculation of F_c.

$$\cos\varphi_R = \frac{\overrightarrow{P_R P_S} \cdot \overrightarrow{P_R P_1}}{\left|P_R P_S\right|\left|P_R P_1\right|} \tag{151}$$

$$\theta_R = \frac{\pi}{2} - \varphi_R \tag{152}$$

$$\cos\varphi_S = \frac{\overrightarrow{P_S P_R} \cdot \overrightarrow{P_S P_1}}{\left|P_S P_R\right|\left|P_S P_1\right|} \tag{153}$$

$$\theta_S = \frac{3\pi}{2} + \varphi_S \tag{154}$$

$$\beta = 2\pi \tag{155}$$

$$r_S = \left|P_S P_1\right| \tag{156}$$

$$r_R = \left|P_R P_1\right| \tag{157}$$

The weight w_2 corresponding to the contribution of sound diffracted around the right vertical edge of the screen can be calculated in a similar manner with the only alteration that P_1 has to be replaced by P_2.

Now w_{SR} has to be determined in a way where the w_{SR}, w_1, and w_2 add up to a value of unity. In the incoherent and coherent case Eqs. (158) and (159) have to be used, respectively.

$$w_{SR} = \sqrt{1 - w_1^2 - w_2^2} \tag{158}$$

$$w_{SR} = 1 - w_1 - w_2 \tag{159}$$

The problem is again to establish a reasonable transition between the incoherent principle given by Eq. (158) and the coherent principle given by Eq. (159). This can be done by assuming $p = p_{SR} = p_1 = p_2$ in Eq. (148) and solving the equation with respect to w_{SR}. The solution is given by Eq. (160). In the incoherent case ($F_1 = F_2 = 0$) Eq. (160) corresponds to Eq. (158) and in the coherent case ($F_1 = F_2 = 1$) to Eq. (159).

$$w_{SR} = -F_1 w_1 - F_2 w_2 + \sqrt{1 - w_1^2 - w_2^2 + \left(F_1 w_1\right)^2 + \left(F_2 w_2\right)^2} \tag{160}$$

When the screen length becomes 0 the method described above will produce a result identical to the result obtained when ignoring the screen.

In the subsidiary case of an unblocked direct propagation plane the sound pressure is calculated for the three vertical propagation planes defined in Figure 41. P_1 is the more remote of the two edges in the sense that it is the edge giving the largest sound pressure reduction. Plane SR is the direct propagation plane from the source to the receiver and Plane 1 and Plane 2 are the propagation planes around the left and the right edge of the screen. Plane 1 is passing just outside the screen so that the screen is not included in the propagation plane while plane 2 includes the screen. The corresponding sound pressures are denoted p_{SR}, p_1 and p_2 and will be calculated using the comprehensive two-dimensional propagation model.

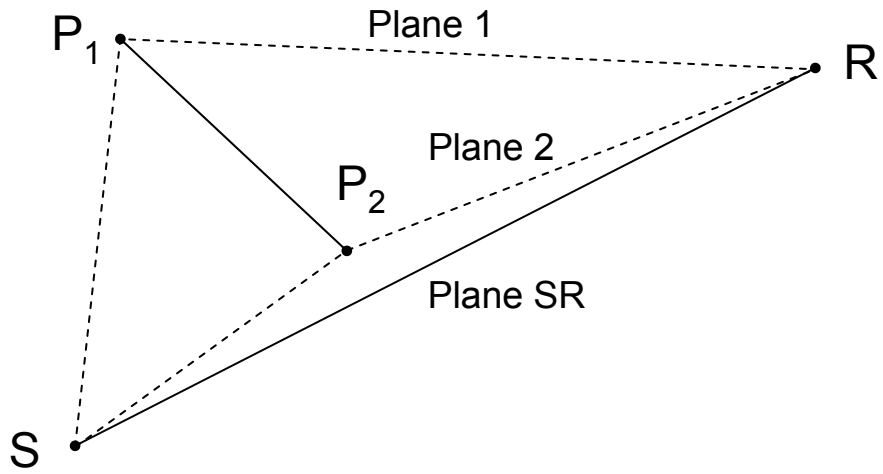

Figure 41
Definition of vertical propagation planes in case of an unblocked direct propagation plane (top view).

The sound pressure level for the unblocked case is also calculated by Eq. (148) but in this case the weights w_1 , w_{SR} are calculated by Eqs. (161) and (162), respectively. Note that instead of calculating w_{SR} using a diffraction point below the line-of-sight, w_{SR} is calculated as the inverse of the result for a point above the line-of-sight. This is done to obtain a more continuous model.

$$w_1 = \left| \frac{p_{diffr,1}(r_S, r_R, \theta_S, \theta_R, \beta, f)}{p_0} \right| \tag{161}$$

$$w_{SR} = 1 - \left| \frac{p_{diffr,2}(r_S, r_R, \theta_S, \theta_R, \beta, f)}{p_0} \right| \tag{162}$$

Finally, w_2 is calculated by Eq. (163).

$$w_2 = -F_1 w_1 - F_2 w_{SR} + \sqrt{1 - w_1^2 - w_{SR}^2 + (F_1 w_1)^2 + (F_2 w_{SR})^2} \tag{163}$$

If the uncertainties introduced by using the incoherent summation defined by Eq. (146) can be accepted in cases where one of the vertical screen edges are close to the direct propagation plane it will normally be preferable to apply this simplification due to the considerable reduction in the complexity of the calculation.

As already mentioned in Section 2.2 diffraction around vertical edges can normally be ignored in case of moving sources due to the averaging caused by the movement.

4.7 Irregularly Shaped Screens

In most cases of man-made screens and embankments the height of the screen edge is the constant along the screen. However, in some cases the height may vary for different reasons and in the case of natural screens the height will in general vary along the screen and there will be no well-defined ends.

It is not possible to account for such variations in an accurate manner but a proposal shall be given on how to deal with moderate variations in the screen height. In case of large variations it will be necessary to divide the screen in sub-screens. Also, if the variations in screen height have been introduced to obtain enhanced performance of the screen, the screen attenuation should instead be treated according to the procedure described in Section 4.8 for special screens.

For a screen with no well-defined ends the screen height is determined as the average height within the significant part of the screen. The significant part of the screen is defined by the part of the screen which is inside the horizontal limits of the Fresnel-zone around the propagation path as shown in Figure 42. The width of the Fresnel-zone defined by the points P_l and P_r is determined by the method described in Appendix A using a fraction F_λ of the wavelength of ½. The method is considered reasonable for moderate screen height variations. Moderate variations are estimated to be variations where difference between the free-field screen attenuation corresponding to the upper and lower screen height is less than 5 dB.

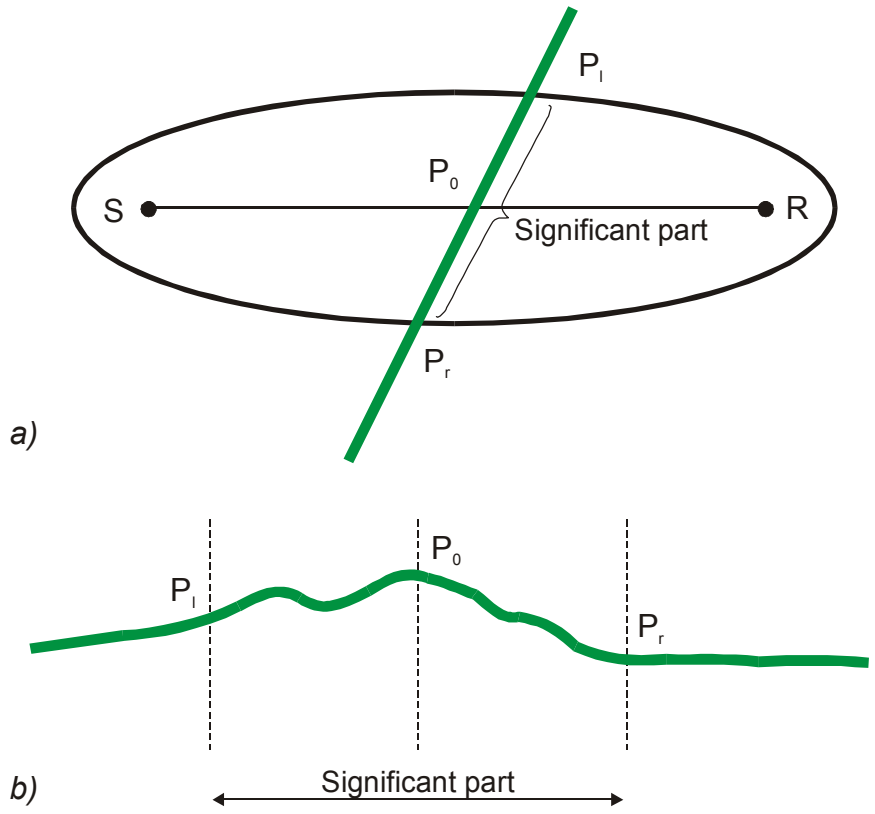

Figure 42
Significant part of screen used to calculate the average height. a) top view, b) front view.

For an irregularly shaped screen with well-defined ends the method shall be combined with the method of finite screens described in the previous section. In this case the average height is determined for the part of the finite screen which is inside the Fresnel-zone and the contribution from subsidiary paths are calculated as described in Section 4.6.

In order to avoid that the width of the significant part becomes frequency dependent which could lead to a frequency dependent screen height it is recommended to calculate to calculate the width at the centre frequency of the 250 Hz band.

For the same reason given in Section 4.6 for ignoring diffraction around vertical edges, the screen height of irregularly shaped screens can in case of moving sources be represented simply by the height of the screen at the propagation path.

4.8 Special Screens

All propagation parameters that significantly affect the noise level should be taken into account in the new Nordic prediction methods. It is particularly important that any serious

attempt at noise reduction should be reflected in the calculation result. As it has been shown that the acoustic performance of specially designed barriers (barriers with special shape or barriers made of special material) may be significantly better than the performance of a plane and reflecting barrier, the comprehensive propagation model shall make allowance for such improvement.

Unfortunately, the matter cannot be solved by simple algorithms. Very often the acoustical design of special screens is based on complicated specialist prediction tools such as BEM (Boundary Element Method). It has been found impossible to include algorithms in the comprehensive propagation model which on one hand are sufficiently accurate for any type of special screen and on the other hand fulfils the requirement of covering an acceptable degree of complexity.

Instead, it has been decided [21] to include the extra attenuation obtained by special screens in tabular form based on four geometrical parameters. The extra attenuation is defined as the difference between the attenuation of the actual screen and the attenuation that would have been obtained by a thin reflecting screen with the same height. Although it is difficult to foresee which format will be adequate for future use, it is expected that four entry parameters will be sufficient, namely the geometrical parameters shown in Figure 43. These parameters are the basic parameters for calculating the effect of a thin screen.

For each combination of these parameters, the 1/3-octave band frequency spectrum of extra attenuation has to be defined in the table. The spectrum to be applied for other parameter values can be determined by linear interpolation and extrapolation.

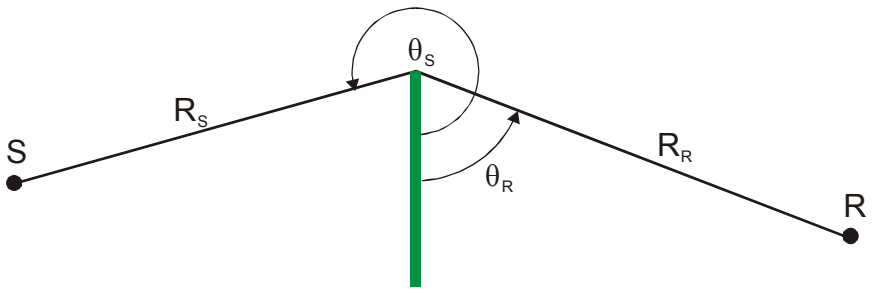

Figure 43
Definition of entry parameters in a table of extra insertion losses for special screens.

R_S	R_R	θ_S	θ_R	ΔL (25 Hz – 10 kHz)			
				25 Hz	31.5 Hz	.....	10 kHz

Table 3
Format of table of extra insertion losses for special screens.

The user of the method has to determine the extra attenuation based on BEM calculations, measurements or whatever means are suitable, and it is the responsibility of the user to demonstrate the accuracy of the estimated extra attenuation.

4.9 Effect of Atmospheric Turbulence in a Shadow Zone

The sound reduction of screens is limited by the energy scattered from atmospheric turbulence into the shadow zone of the screen. This is taken into account by a method developed by Jens Forssén and described in [4] and [32].

In the method the contribution of scattered energy depends on the R_1, R_2 and h_e where R_1 and R_2 are the distances to the normal to the source-receiver line through the top of the screen as defined in Figure 44. The wind and temperature turbulence are described by the turbulence strengths C_v^2 and C_T^2, respectively. If the top of screen is below the source-receiver line the contribution from turbulent scattering is ignored.

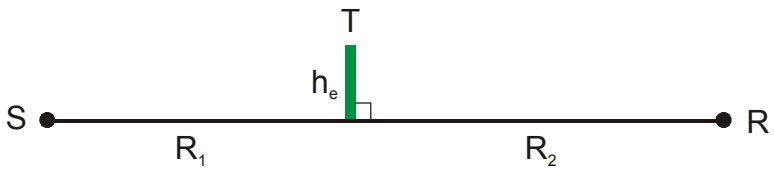

Figure 44
Definition of geometrical parameters for calculation of turbulent scattering in the shadow zone of a single screen.

Based on a comparison between predictions by the model and predictions by PE (Parabolic Equations) described in [24] it was concluded that the method by Forssén underestimates the contribution from turbulent scattering. To improve the method the effective

turbulence strength parameters C_{ve}^2 and C_{Te}^2 were introduced which are 10 times the true parameters ($C_{ve}^2 = 10\ C_v^2$ and $C_{Te}^2 = 10\ C_T^2$).

The sound pressure level contribution ΔL_{ws} from wind turbulence relative to the free field level is given by Eq. (164) where f is the frequency and H(x) is Heavisides' step function (H = 1 for x ≥ 0 and H = 0 for x < 0). f_0 is calculated by Eqs. (165) and (166) where c is the speed of sound. L_{ws0} is the normalized scattered level from the wind turbulence disregarding the ground. L_{ws0} is determined by linear interpolation in a two-dimensional table with input parameters $40R_2/R_1$ and $40h_e/R_1$. The table can be found in Appendix G. C_SC_R is a correction which shall account for reflections in the ground surface before and after the screen. C_SC_R is approximated by the ground effect part of the single screen effect $p_G = p/p_1$ which has already been calculated by the Fresnel-zone interpolation principle as described in Section 4.4.3.4. However, C_SC_R is limited downwards to a value of 1 for practical reasons. This is not fully in agreement with procedure described in [4] but it has been found that the deviations for most terrain geometries are very small and even in extreme cases will seldom exceed more than a few dB. Considering the expected uncertainty of the turbulence method, it has been found that the calculation of a more correct value of C_SC_R cannot justify the increase in time consumption.

$$\begin{aligned}\Delta L_{ws} &= L_{ws0} + 10\log(C_S C_R) + \frac{10}{3}\log\left(\frac{f}{2000}\right) + 10\log\left(C_{ve}^2\right) \\ &+ 15H\left(f_0 - f\right)\log\left(\frac{f}{f_0}\right) + 15H\left(0.5f_0 - f\right)\log\left(\frac{f}{0.5f_0}\right) + 10\log\left(\frac{R_1}{40}\right)\end{aligned} \tag{164}$$

$$\theta = \pi - \arctan\left(\frac{R_1}{h_e}\right) - \arctan\left(\frac{R_2}{h_e}\right) \tag{165}$$

$$f_0 = \frac{c}{2\sin\left(\theta/2\right)} \tag{166}$$

Similarly, the sound pressure level contribution ΔL_{ts} from temperature turbulence is given by Eq. (167). L_{ts0} is the normalized scattered level from the temperature turbulence disregarding the ground and is again determined by linear interpolation in a two-dimensional table which can be found in Appendix G.

$$\begin{aligned}\Delta L_{ts} &= L_{ts0} + 10\log(C_S C_R) + \frac{10}{3}\log\left(\frac{f}{2000}\right) + 10\log\left(C_{Te}^2\right) \\ &+ 15H\left(f_0 - f\right)\log\left(\frac{f}{f_0}\right) + 15H\left(0.5f_0 - f\right)\log\left(\frac{f}{0.5f_0}\right) + 10\log\left(\frac{R_1}{40}\right)\end{aligned} \tag{167}$$

Finally, ΔL_{ws} and ΔL_{ts} are added incoherently to ΔL_{hill} as shown in Eq. (168).

$$\Delta L_{hill,total} = 10 \log \left(10^{\Delta L_{hill}/10} + 10^{\Delta L_{ws}/10} + 10^{\Delta L_{ts}/10}\right) \quad (168)$$

If two screens are included in the calculation of ΔL_{hill} the parameters R_1, R_2 and h_e are determined for an equivalent single screen top T as shown in Figure 45 where T_1 and T_2 are the two screen tops. The point T can be determined by the method described in Appendix F. $C_S C_R$ is in this case approximated by the ground effect part of the double screen effect $p_G = p/p_1$ calculated as described in Section 4.4.3.5.

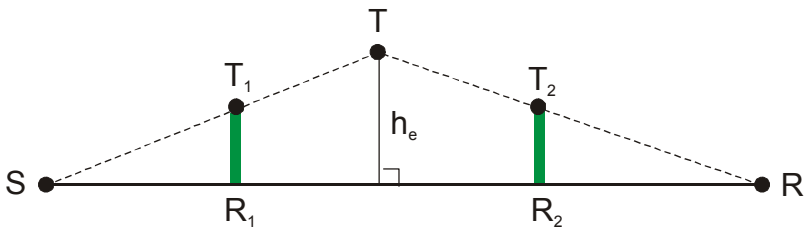

Figure 45
Definition of geometrical parameters for calculation of turbulent scattering in the shadow zone of double screens.

5. Scattering zones

A model for including scattering effects has been described in [27]. The model covers sound propagation through housing areas and forests.

According to Eq. (1) the propagation effect of terrain ΔL_t and of scattering zones ΔL_s shall be calculated separately. However, as previously mentioned in Section 2.1 the former calculation may be affected by the existence of scattering zone quantified by a reduction in the coherence coefficient.

In prediction of scattering zone propagation effects one of the fundamental parameters is the sound path length R_{sc} in the scattering volume as shown in Figure 46 and Figure 47. When the line-of-sight is not blocked by obstacles (excluding the scattering zones), R_{sc} is measured along the source-receiver sound path as shown in Figure 46. When the line-of-sight is blocked, R_{sc} is measured along the sound path over the top of the obstacles using the "rubber band" principle as shown in Figure 47. When a screen inside a scattering zone cannot be considered to constitute a natural part of the scattering zone (e. g. a house in a forest or a very large building inside a low housing area) the screen is taken into account in the calculation of ΔL_t and ignored in the calculation of ΔL_s. Therefore such a screen is taken into account when determining the sound path used to determine R_{sc}.

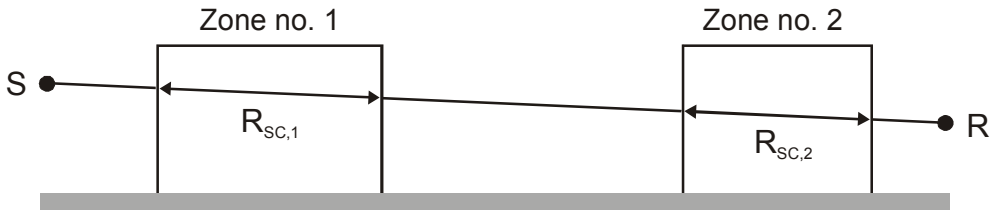

Figure 46
Propagation path used to determine the scattering zone path length R_{sc} when the line-of-sight is unblocked.

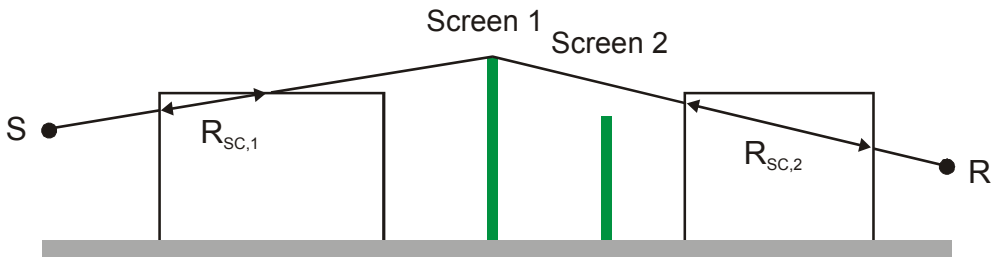

Figure 47
Propagation path used to determine the scattering zone path length R_{sc} when the line-of-sight is blocked.

5.1 Scattering Zones of Same Type

If there is only one scattering zone along the propagation path or if the scattering zones are of the same type (have the same parameters except for R_{sc}) the method described in [27] can be used.

The coherence coefficient F_s corresponding to scattering to be used in Section 4.5.3 when calculating the terrain effect ΔL_t is determined by Eq. (169).

$$F_s = 1 - k_f T \tag{169}$$

The variable T in Eq. (169) is calculated by Eq. (170) where nQ is given by Eq. (171) for housing areas and by Eq. (172) for forests. R_{sc} is the total sound path length of the scattering zones ($R_{sc} = \Sigma R_{sc,i}$ where $R_{sc,i}$ is the sound path length of the i'th scattering zone). If T is greater than 1 a value of 1 is used instead.

$$T = \left(\frac{R_{sc} nQ}{1.75} \right)^2 \tag{170}$$

k_f is given by Table 4 in case of housing areas and by Table 5 in case of forests. The parameter ka in Table 5 is the product of the wave number k and the mean stem radius a. Between the values of ka linear interpolation is used to determine k_f.

f (Hz)	k_f
25	0.000
32	0.020
40	0.040
50	0.087
63	0.180
80	0.290
100	0.360
125	0.440
160	0.510
200	0.590
250	0.630
315	0.700
400	0.790
500	0.830
630	0.860
800	0.900
1000	0.930
1250	0.950
1600	0.970
2000	0.980
2500	0.990
3150	1.000
4000	1.000
5000	1.000
6300	1.000
8000	1.000
10000	1.000

Table 4
Frequency weighting function k_f for housing areas.

ka	k_f
0	0.00
0.7	0.00
1	0.05
1.5	0.20
3	0.70
5	0.82
10	0.95
20	1.00

Table 5
Frequency weighting function k_f for forests as a function of ka where k is the wave number and a is the mean stem radius.

In case of housing areas nQ (in m^{-1}) is determined by Eq. (171) where n' is the fraction of the plan area of all buildings to the total area of the scattering zone (a value between 0 and 1), $\overline{S}$ is the surface area (sum of walls and roof surfaces) of an average building (m^2), h_{max} is the height of the highest building (m) and A_b is the average building plan area (m^2).

$$nQ = \frac{n' \, \overline{S}}{4 \, h_{\max} \, A_b} \tag{171}$$

In case of forests nQ is determined by Eq. (172) where n" is the density of trees (m^{-2}) and d is the mean trunk diameter (m).

$$nQ = n'' \, d \tag{172}$$

The propagation effect of the scattering zone ΔL_s is calculated by Eq. (173) where k_f and T are as described above and k_p is a constant of proportionality. k_p is 1.25 for forests and in the range 0.4-1.0 for housing areas (0.4 is a "safe" estimate not to overestimate the attenuation). $A_e(R_{SC})$ is a level correction due to scattering calculated by Eq. (174). ΔL_s shall be limited downwards to a value of -15 dB. The limitation is based on practical considerations without a documented foundation.

$$\Delta L_s = k_f \, T \, k_p \, A_e\left(R_{SC}\right) \tag{173}$$

$$A_e\left(R_{SC}\right) = \Delta L(h', \alpha, R') + 20\log\left(8R'\right) \tag{174}$$

In Eq. (174) h' is the normalised scatter obstacle height and h' = nQh where h is the average scatter obstacle height. α is the absorption coefficient of the scatter obstacles (normally in the range 0.1 – 0.4). R' is the normalised effective distance through the scattering zone and R' = nQR_{sc}. $\Delta L(h',\alpha,R')$ is determined from a three-dimensional table with table parameters h', α, and R' using cubic interpolation. The table is given in Appendix J.

5.2 Scattering Zones of Varying Type

If there is more than one type of scattering zone along the propagation path the method described in [27] cannot be used directly. To overcome this, a procedure will be described in the following which has not been validated but has the quality of producing the same result as the method described in Section 5.1 if all scattering zones are of the same type and produces a smooth transition between calculated results for different types of scattering zones. The general idea in the procedure is that the parameters in the method (k_f, k_p, h', and α) for all scattering zones are determined as a weighted average of the individual values of each zone using $r_i=R_{SC,i}nQ_i$ as the weight.

In the method the normalised effective distance is determined by Eq. (175) where $R_{sc,i}$ is the sound path length of the i'th scattering zone and nQ_i is the corresponding value of nQ. Besides a weighting factor r_i for each scattering zone is calculated by Eq. (176).

$$R' = \sum_i R_{sc,i} nQ_i \tag{175}$$

$$r_i = \frac{R_{sc,i} nQ_i}{R'} \tag{176}$$

In excess of R' already defined in Eq. (175) the quantities h' and α used to calculate $A_e(R_{SC})$ in Eq. (174) are calculated by Eqs. (177) and (178) instead and the quantities k_f, T and k_p used in Eqs. (169) and (173) by Eqs. (179) to (181).

$$h' = \sum_i r_i nQ_i h_i \tag{177}$$

$$\alpha = \sum_i r_i \alpha_i \tag{178}$$

$$k_f = \sum_i r_i k_{f,i} \tag{179}$$

$$k_p = \sum_i r_i k_{p,i} \tag{180}$$

$$T = \left(\frac{\sum_i R_{sc,i} n Q_i}{1.75} \right)^2 \tag{181}$$

5.3 Scattering Zones with Limited Height

In the method described in the previous sections it is assumed that the height of the scattering zone is sufficiently large to obtain the predicted attenuation. In cases with a limited height of the scattering zone this may not be fulfilled. If the scattering zone is below the sound ray any effect is automatically ignored as R_{sc} will be zero. However, if the upper end of the scattering zone is just above the sound ray it is possible to have a sudden considerable change in R_{sc} and therefore a large discontinuity. To avoid this a transition principle has been developed which will be described in the following. In the transition principle a smooth transition is obtained from the case where no effect is assumed when the scattering zone is below the sound ray to the case where the full effect is obtained when the scattering zone is sufficiently high.

In the transition principle the volume of the scattering zone within the half of the Fresnel ellipsoid above the sound ray relative to the entire volume of this half Fresnel ellipsoid is used to modify the R_{sc} as shown in Figure 48. However, as the approach is very approximate the calculation of the volumes is simplified.

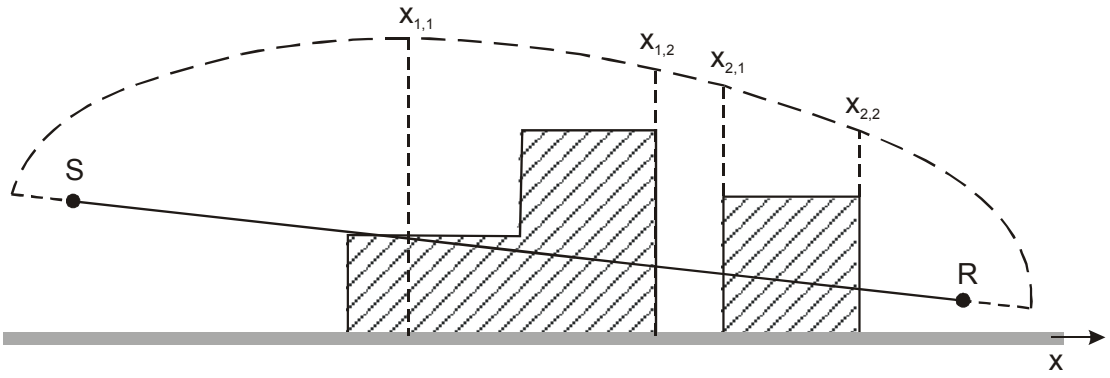

Figure 48
Limited height of the scattering zone within half of the Fresnel ellipsoid above the sound ray.

In the calculation the x-axis of the coordinate system is assumed to follow the horizontal projection of the sound ray with the source placed at $(0,0,z_S)$. The receiver is placed at

$(x_{SR},0,z_R)$ where x_{SR} is the horizontal distance between the source and receiver. Points on the sound ray as a function of x is defined by $(x,0,z_{ray}(x))$ where x is varying between 0 and x_{SR}. The intersection between the y-plane and the Fresnel ellipsoid which is an ellipse is replaced by a rectangle with height and width to each side of the sound ray of $r_{Fz}(x)$ as shown in Figure 49. $r_{Fz}(x)$ is half the width of Fresnel ellipsoid at x calculated according to Eq. (182). R_{Sx} is defined by Eq. (183) and the function f is calculated as described in Appendix A based on a fraction F=1/8.

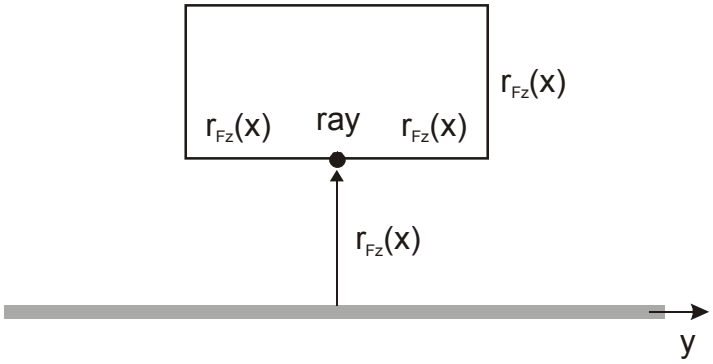

Figure 49
Simplified Fresnel shape in the y-plane.

$$r_{Fz}(x) = f\left(R_{Sx}, R_{SR} - R_{Sx}, \frac{\pi}{2}\right) \tag{182}$$

$$R_{Sx} = \frac{x}{x_{SR}} R_{SR} \tag{183}$$

The volume of the simplified Fresnel-shape V_{Fz} is calculated by Eq. (184) and the volume of the scattering zone inside the shape V_{sc} by Eq. (185) where Δz_{sc} is defined in Eq. (186). x_1 and x_2 is the start and end coordinate of the intersection between the sound ray and the scattering belt.

$$V_{Fz} = \int_{x=x_1}^{x_2} 2\, r_{Fz}^2(x)\, dx \tag{184}$$

$$V_{sc} = \int_{x=x_1}^{x_2} \left(\int_{y=-r_{Fz}(x)}^{r_{Fz}(x)} \Delta z_{sc}(x,y)\,dy \right) dx \tag{185}$$

$$\Delta z_{sc}(x,y) = \begin{cases} 0 & z_{sc}(x,y) \le z_{ray}(x) \\ z_{sc}(x,y) - z_{ray}(x) & z_{ray}(x) < z_{sc}(x,y) < z_{ray}(x) + r_{Fz}(x) \\ r_{Fz}(x) & z_{sc}(x,y) \ge z_{ray}(x) + r_{Fz}(x) \end{cases} \tag{186}$$

Finally, the modified sound path length R'$_{sc}$ can be determined by Eq. (187).

$$R'_{sc} = R_{sc} \frac{V_{sc}}{V_{Fz}} \tag{187}$$

Note: *If the shape of the scattering zone is not too complex the modified value of R_{sc} is easily determined by the equations shown above. The easiest approach will probably be to solve the problem numerically by discretizing the calculation in the x-direction. A resolution of around 10 intervals will normally be sufficient. If the shape of the scattering zone is more complex it may be necessary to use a numerical solution in the y-direction as well.*

5.4 Front Region of a Housing Area

At the front region of a scattering zone the scattering process is not fully developed and therefore the solution described above will not be valid in this region. Also in the region before the scattering zone the sound levels may be affected by the scattering zone to some extent.

In the case of forests it has been found reasonable to neglect these effects. However, in case of housing areas the calculation result in receiver points before or between the first rows of houses will be very inaccurate if only the scattering zone model is applied.

Although not described in the present report it is assumed that the propagation effect in build-up areas where it is not relevant to use the scattering model is predicted using the method described in the present report including a sufficient number of reflections from the houses.

In the front region of a housing area or in the region before the housing area it has been found more accurate to apply the method for build-up areas. To obtain a smooth transition between the calculation result by the method for build-up areas ΔL_b and the calculation result for scattering zones $\Delta L_t + \Delta L_s$ the propagation effect of the houses is determined by Eq. (188). d_{sc} is the distance to the facade of the first house measured along the propaga-

tion path and Δd_{sc2} is the typical distance from the facades of the first row of houses to the facades of the fourth row of houses (equal to the width of three rows).

$$\Delta L = \begin{cases} \Delta L_b & d \le d_{sc} \\ \left(\Delta L_t + \Delta L_s - \Delta L_B\right)\dfrac{d - d_{sc}}{\Delta d_{sc,2}} + \Delta L_b & d_{sc} < d < d_{sc} + \Delta d_{sc,2} \\ \Delta L_t + \Delta L_s & d \ge d_{sc} + \Delta d_{sc,2} \end{cases} \qquad (188)$$

6. Reflections from Obstacles

Sound reflected from an obstacle such as a building facade or a noise screen is dealt with by introducing an extra propagation path from the source via the reflection point to the receiver. The reflection point is defined by the intersection between the straight line from the image source to the receiver and the plane which contains the reflecting surface. Therefore, the reflection point may be outside the real surface.

The propagation effect of the extra propagation path is predicted by the same propagation model used for the direct path and described in Sections 2 through 5. The prediction is based on propagation parameters determined along the propagation path. The contribution of the path is corrected for the efficiency of the reflection, determined by the size and reflection coefficient of the surface as described in [30]. The reflected sound is added incoherently to the direct sound.

The efficiency of the reflection is quantified by the reflection effect ΔL_r which can be calculated by Eq. (189). The first term in the equation is a correction for the effective energy reflection coefficient ρ_E and the second term is a correction for the size of the reflecting surface. The effective size of the reflecting surface may be used, see comments given in the Note below. The reason for this is to distinguish between surfaces that are freely suspended, and surfaces placed on the ground. S_{refl} is the area of the surface within a Fresnel-zone in the plane of reflection and S_{Fz} is the total area of the Fresnel-zone. The parameters will be described more closely below. In order to avoid unnecessary calculation of S_{refl} and S_{Fz} a reflecting surface is ignored if the point of reflection hits more than 2m outside one of the surface edges. Any difference in directivity between the direct and reflected sound path is assumed to be incorporated in L_W in Eq. (1).

$$\Delta L_r = 10\log(\rho_E) + 20\log\left(\frac{S_{refl}}{S_{Fz}}\right) \qquad (189)$$

ρ_E is the energy reflection coefficient, with numeric examples given in Table 6.

***Note**: An effective size of the reflecting surface should be used. For freely suspended surfaces (i.e. the propagation of the reflected sound is not affected by the ground) the physical size of the surface is used. For surfaces on (or near to) the ground, the effective surface area is twice the physical area. This is obtained by shifting the lower edge of the surface downwards.*

Characteristics of reflecting surface	**ρ_E**
Plane and acoustically hard surface (concrete, stone, brick wall, metal sheets)	1.0
Non-absorbent building facades with windows and small irregularities, dense wooden panels	0.8
Factory walls with 50 % of the surface consisting of openings, installations or pipes	0.4

Table 6
Examples of energy reflection coefficients ρ_E.

For a reflecting surface with a frequency dependent energy reflection coefficient ρ_E is calculated by Eq. (190) where α is the absorption coefficient.

$$\rho_E = 1 - \alpha \tag{190}$$

If the surface is hard or almost hard with a rough texture of random nature, the reflection coefficient can be estimated by Eq. (191) where k is the wave number, σ is the rms-value of the random (gaussian) irregularities in the texture and θ is the angle of incidence (relative to the normal of the surface). σ can approximately be estimated by 0.3 times the peak to peak irregularities.

$$\rho_E = \exp\left(-2\left(k\,\sigma\cos\theta\right)^2\right) \tag{191}$$

In the correction for the size of the reflecting surface S_{refl} is the area of the surface within Fresnel-zone in the plane of reflection and S_{Fz} is the total area of the Fresnel-zone. The Fresnel-zone is determined by the intersection between the Fresnel ellipsoid around the sound ray from the image source to the receiver and the plane of reflection as shown in Figure 8. The intersection is an ellipse but in order to simplify the calculations the Fresnel zone has been replaced by the circumscribed rectangle symmetrically placed around the major axis of the ellipse as described in Section 4.2 (Figure 10 defines the area of the Fresnel-zone S_{Fz} and S_{refl} is equal S_i for a shape of the reflecting surface as shown in the figure). The major axis of the ellipse is the projection of the sound ray onto the reflecting plan. The size of the Fresnel-zone is calculated as described in Appendix A based on a fraction $F_\lambda = 1/8$.

Although the Fresnel-zone has been simplified to a rectangle the geometrical calculations can still be quite troublesome (examples can be found in [30]) especially when the reflecting surface is tilted. However, in case of a vertical reflector the calculation of the Fresnel-zone becomes much simpler if the sound ray is horizontal because the major axis of the

Fresnel-zone will be horizontal. The horizontal size of Fresnel-zone is determined by the distances R_S and R_R and the angles θ_1 and θ_2 to the left and right side of the reflection point respectively as shown in Figure 50 (top view) and the vertical size is determined by an angle of $\pi/2$. On this basis the size of the Fresnel-zone is easily calculated by the equations in Appendix A. When the vertical reflection angle is below 10-15° it will still be reasonable to assume that the sound ray is horizontal and use the horizontal projection of the reflection angles. This is fulfilled if the propagation distance is greater than 5 times the difference in source and receiver height which most often will be the case. For non-horizontal sound rays a guideline to an approximate calculation can be found in [30].

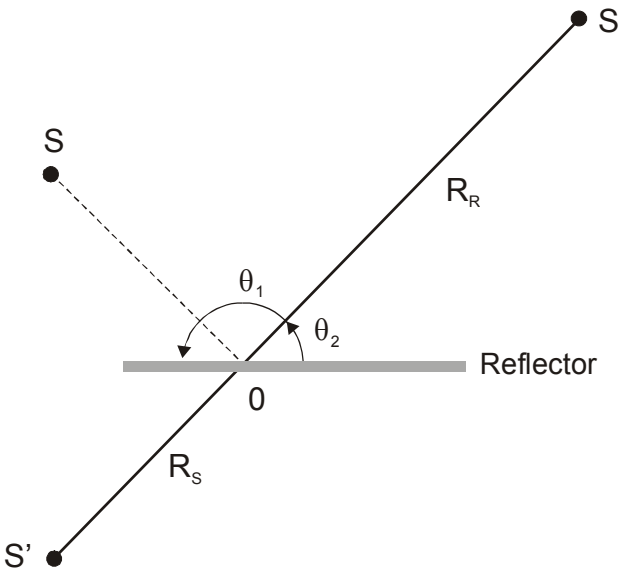

Figure 50
Distances and angles used to calculate the horizontal size of Fresnel-zone (top view) in case of a vertical reflection plane and a nearly horizontal ray path.

Irregularly shaped obstacles may be divided into a number of sub-surfaces which each fulfils the requirement of being a plane surface, and the overall effect is obtained by a simple incoherent summation of the contributions from all surfaces.

7. Conclusion

The comprehensive sound propagation model described in the present report has mainly been based on geometrical ray theory and theory of diffraction when calculating terrain and screen effects combined with a statistical approach in case of propagation through scattering zones.

The model includes only the two most significant edges along the propagation path which may be two screens with one edge each or one screen with one or two edges.

Terrain surface properties are characterised by the impedance and roughness (unevenness) of the surface. A classification has been made for impedance types and roughness types. It will be necessary to study the effect of surface roughness more closely in future before fully applying this part of the model.

Incoherent effects are introduced in the theoretical model which shall account for effect of frequency band averaging, fluctuating refraction, turbulence, surface roughness and propagation through scattering zones.

8. References

[1] C. I. Chessell: *Propagation of noise along a finite impedance boundary,* J. Acoust. Soc. Am. 62, 825-834, 1977.

[2] C. F. Chien and W. W. Soroka: *A note on the calculation of sound propagation along an impedance boundary*, J. Sound Vib. 69, 340-343, 1980.

[3] M. E. Delany and E. N. Bazley: *Acoustical properties of fibrous absorbant materials*, Appl. Acoust. 3, 105-116, 1970.

[4] J. Forssén: *Influence of atmospheric turbulence on noise reduction by barriers – an approximative method based on a scattering cross-section*, Note prepared to Nord 2000 Technical Committee, Gothenburg, 2000.

[5] J. W. Hadden and A. D. Pierce: *Sound diffraction around screens and wedges for arbitrary point source locations*, J. Acoust. Soc. Am. 69, 1266-1276, 1981.

[6] D. C. Hothersall and J. B. N. Harriott: *Approximate models for sound propagation above multi-impedance plane boundaries*, J. Acoust. Soc. Am. 97, 918-926, 1995.

[7] ISO 9613-1: *Acoustics – Attenuation of sound during propagation outdoors - Part 1: Calculation of the air absorption of sound by the atmosphere,* 1993.

[8] P. D. Joppa, L. C. Sutherland and A. J. Zuckervar: *Representative frequency approach to the effect of bandpass filters on evaluation of sound attenuation by the atmosphere*, Noise Control Eng. J. 44, 261-273, 1996.

[9] H. G. Jonasson: *Sound reduction by barriers on the ground,* J. Sound Vib. 22, 113-126, 1972.

[10] H. G. Jonasson and S. A. Storeheier: *Nord 2000. New Nordic Prediction Method for Road Traffic Noise,* SP Report 2001:10, 2001.

[11] H. G. Jonasson and S. A. Storeheier: *Nord 2000. New Nordic Prediction Method for Rail Traffic Noise,* SP Report 2001:11, 2001.

[12] J. Kragh, B. Plovsing, S. Å. Storeheier, G. Taraldsen, H. G. Jonasson: *Nordic Environmental Noise Prediction Methods, Nord2000 Summary Report. General Nordic Sound Propagation Model and Applications in Source-Related Prediction Methods*, DELTA Acoustics & Vibration, Report AV 1719/01, 2001.

[13] A. L'Espérance, P. Herzog, G. A. Daigle, and J. R. Nicolas: *Heuristic model for outdoor sound propagation based on an extension of the geometrical ray theory in the case of a linear sound speed profile,* Appl. Acoust. 37, 111-139, 1992.

[14] F. P. Mechel: *Schallabsorber*, Band 1, S. Hirzel Verlag Stuttgart 1989, p. 72.

[15] Nordtest NT ACOU 104: *Ground surfaces: Determination of the acoustic impedance*, 1999.

[16] B. Plovsing and J. Kragh: *Prediction of sound propagation in a homogeneous atmosphere over flat terrain with varying ground surface types*, DELTA Acoustics & Vibration, Report AV 496/97, 1997.

[17] B. Plovsing and J. Kragh: *Prediction of sound propagation in a homogeneous atmosphere over non-flat terrain*, DELTA Acoustics & Vibration, Report AV 907/97, 1997.

[18] B. Plovsing and J. Kragh: *Prediction of sound propagation in an atmosphere without significant refraction. Outline of a comprehensive model*, DELTA Acoustics & Vibration, Report AV 1818/98, 1998.

[19] B. Plovsing and J. Kragh: *Principles for including the effect of multiple screens in the new Nordic prediction methods for environmental noise*, DELTA Acoustics & Vibration Report AV 1820/98, 1998.

[20] B. Plovsing and J. Kragh: *Nord2000. Comprehensive Outdoor Sound Propagation Model. Part 2: Propagation in an Atmosphere with Refraction*, DELTA Acoustics & Vibration Report AV 1851/00, 2006.

[21] B. Plovsing and J. Kragh: *Nordic prediction methods for environmental noise. Proposed method for including the effect of noise barriers with special shape or barriers made of special material,* DELTA Acoustics & Vibration, Report AV 1063/97, 1997.

[22] S. Quirós-Alpera: *Validation of Nord2000 using BEM (Boundary Element Method)*. Personal communication, 2001.

[23] E. M. Salomons: *Sound propagation in complex outdoor situations with a non-refracting atmosphere: Model based on analytical solutions for diffraction and reflection*, Acoustica/ acta acoustica 83, 1997.

[24] E. M. Salomons: *Turbulence*, Harmonoise memo HAR25MO-030512-TNO01, 2003.

[25] S. Å. Storeheier: *Scattering effects in sound propagation outdoors. Scattering at terrain surfaces. N2000 Sub-project 1997-10*, SINTEF Report 40-N0 970225.

[26] S. Å. Storeheier: *Scattering effects in sound propagation outdoors. Sound Scattering in Housing Areas and Forests. N2000 Sub-project 1997-10*, SINTEF Report 40-N0 970226.

[27] S. Å. Storeheier: *Nord 2000: Sound scattering outdoors. Revised simple models*, SINTEF Memo 40-N0 990003, Trondheim 1999.

[28] S. Å. Storeheier: *Nord 2000: Acoustical classification of ground types*, SINTEF Report STF40 A98074, Trondheim 1998.

[29] S. Å. Storeheier: *Effects of reflections from obstacles. N2000 sub-project 1997-9*, SINTEF Report 40-N0 970224.

[30] S. Å. Storeheier: *Nord2000: The reflection of sound from vertically erected surfaces. A modified approach*, SINTEF Memo 402549.01, Trondheim 2001.

[31] M. Ögren: *Propagation of sound - screening and ground effect. Part 1: Non-refracting atmosphere*, SP Report 1997:44, ISBN 91-7848-713-7, 1997.

[32] M. Ögren: *Propagation of sound - screening and ground effect. Part 2: Refracting atmosphere*, SP Report 1998:44, ISBN 91-7848-746-3, 1998.

[33] M. Ögren: *Turbulence and finite screens, Environmental noise 2000*, SP Technical Note 1998:32, Borås 1998.

[34] M. Ögren and H. Jonasson: *Measurement of the Acoustic Impedance of Ground*, Nordtest Project 1365-1997, SP Report 1998:28, 1998

Appendix A

Calculation of the Size of the Fresnel-zone

The point P on the Fresnel ellipsoid is defined by Eq. (A1) where F_λ is the fraction of the wavelength λ.

$$|SP| + |PR| - |SR| = F_\lambda \lambda \tag{A1}$$

The point O in Figure A1 is the intersection between the source-receiver line SR and the Fresnel-zone plane, and $r_S = |SO|$ and $r_R = |RO|$.

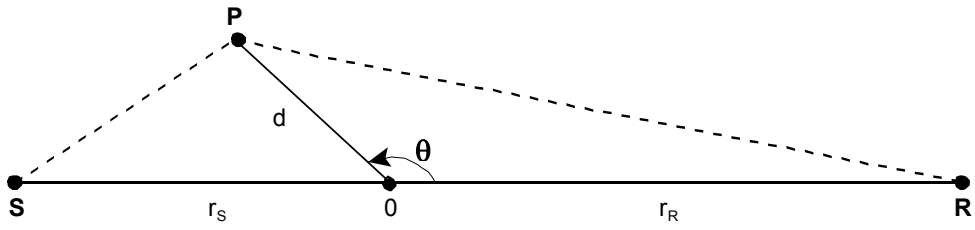

Figure A1

The distance $d = |OP| = f(r_S, r_R, \theta)$ is calculated as shown below in Eqs. (A2) to (A7).

$$r = r_S + r_R \tag{A2}$$

$$l = r + F_\lambda \lambda \tag{A3}$$

$$A = 4\left(l^2 - (r\cos\theta)^2\right) \tag{A4}$$

$$B = 4\, r\cos\theta\left(r_R^2 - r_S^2\right) + 4\left(r_S - r_R\right) l^2 \cos\theta \tag{A5}$$

$$C = -l^4 + 2\left(r_S^2 + r_R^2\right) l^2 - \left(r_S^2 - r_R^2\right)^2 \tag{A6}$$

$$d = \frac{-B + \sqrt{B^2 - 4AC}}{2A} \tag{A7}$$

If $\theta = \pi/2$, $\cos\theta$ becomes 0 and the calculation of d can be simplified to Eq. (A8).

$$d = \sqrt{\frac{\ell^2}{4} - \frac{r_S^2 + r_R^2}{2} + \frac{\left(r_S^2 - r_R^2\right)^2}{4\ell^2}} \tag{A8}$$

If $\theta = \pi/2$ and $r_S = r_R$ the calculation of d can be further simplified to Eq. (A9).

$$d = \sqrt{\frac{\left(F_\lambda \lambda\right)^2}{4} + \frac{F_\lambda \lambda}{2} r} \tag{A9}$$

When source and receiver position relative to the reflecting ground surface are described by the source and receiver heights h_S and h_R and the horizontal distance d as shown in Figure A2, the size of the Fresnel-zone is calculated as shown in the following. S' is the image source, R is the receiver and O is the reflection point.

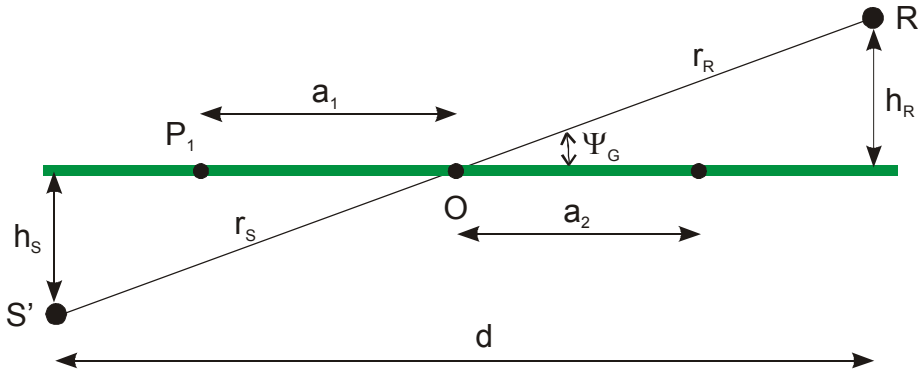

Figure A2

$$\psi_G = \arctan\left(\frac{h_S + h_R}{d}\right) \tag{A10}$$

$$r_{SR} = \sqrt{\left(h_S + h_R\right)^2 + d^2} \tag{A11}$$

$$r_S = \frac{h_S}{h_S + h_R} r_{SR} \tag{A12}$$

$$r_R = \frac{h_R}{h_S + h_R} r_{SR} \tag{A13}$$

The size of the Fresnel-zone along the propagation path is $\left| P_1P_2 \right| = a_1 + a_2$ where a_1 and a_2 are calculated by Eqs. (A14) and (A15).

$$a_1 = \left| P_1O \right| = f\left(r_S, r_R, \pi - \psi_G\right) \tag{A14}$$

$$a_2 = \left| P_2O \right| = f\left(r_S, r_R, \psi_G\right) \tag{A15}$$

The size of the Fresnel-zone perpendicular to the propagation path is 2b where b is calculated by Eqs. (A16) and (A17). In this case the simple solution in Eq. (A9) can be used to calculate b_0.

$$b_O = f\left(r_S, r_R, \frac{\pi}{2}\right) \tag{A16}$$

$$b = \sqrt{\frac{b_O^2}{1 - \left(\frac{a_2 - a_1}{a_2 + a_1}\right)^2}} \tag{A17}$$

Appendix B

Determination of the Ground Impedance based on the Flow Resistivity and the Delany and Bazley Impedance Model

According to the Delany and Bazley impedance model [3] the normalised acoustic impedance Z of the ground is calculated according to the following equation (with time dependence $e^{-j\omega t}$)

$$Z = 1 + 9.08\left(\frac{1000\ f}{\sigma}\right)^{-0.75} + j\,11.9\left(\frac{1000\ f}{\sigma}\right)^{-0.73} \qquad \text{(B1)}$$

where f is the one-third octave band centre frequency in Hz and σ is the effective flow resistivity in Nsm^{-4}.

Appendix C

Effects on Small Scale Roughness on Ground Impedance

Small scale roughness is characterised by relatively small irregularities essentially on a plain surface. The extent of the irregularities is kept below certain limits (0.5-1 m) and form groups or patterns which are characteristic of an area. The irregularities may be described as 2D- or 3D bosses. The material of the irregularities is mainly that of the base ground surface. This scattering occurs when the extent of the objects is small compared to the acoustic wavelength of interest.

The essence of recent work in this field is that the small-scale roughness acts to modify the acoustic impedance associated with the flat surface. Also 2D boss scattering algorithms are developed to include the effect of periodic structures by introducing simple diffracting grating theory as mentioned in [25].

For a high flow resistivity semi-infinite and rigid-porous material, a simple estimate of the rough surface effective admittance β_r can be approximated by Eq. (C1).

$$\beta_r = \beta_s - i\left(C + Df\right) \tag{C1}$$

where β_r is the apparent admittance of the rough surface containing the scatterers, β_s is the normalized admittance for the lower material if it were smooth and f is the frequency.

The constants C and D can be determined for simple special cases of “roughness”, like hemi-spherical (3D-) or semi-cylinders (2D-) bosses. The constants depend on the size of the elements, their packing density and the base material porosity. Details are given in [25].

The model is implemented by determining the constants C and D for the actual boss approximation, calculating β_r using the known β_s and then transforming to the specific acoustic impedance Z that enters into the propagation calculation, according to $Z = 1/\beta_r$. The model is subject to the restriction that the relevant height parameter h of the roughness should be small compared to the acoustic wavelength of interest. This means that the small scale roughness affects the low frequency part of the ground admittance. The limiting frequency of this influence is estimated in [25].

Appendix D

Calculation of the Spherical Wave Reflection Coefficient Q

The spherical wave reflection coefficient Q is a function of the path length R of the reflected ray, the reflection angle θ (equal to $\pi/2 - \psi_G$ where ψ_G is the grazing angle), the wave number k and the normalised impedance Z. Q is calculated by Eq. (D1) where $\Re_p(\theta)$ is the plane wave reflection coefficient calculated according to Eq. (D2). The function E(ρ) is calculated by Eqs. (D3) and (D4) where erfc(z) is the complementary error function extended to complex arguments.

$$Q = \Re_p(\theta) + \left(1 - \Re_p(\theta)\right) E(\rho) \tag{D1}$$

$$\Re_p(\theta) = \frac{\cos(\theta) - \frac{1}{Z}}{\cos(\theta) + \frac{1}{Z}} \tag{D2}$$

$$E(\rho) = 1 + j\sqrt{\pi}\,\rho\, e^{-\rho^2}\, erfc\left(-j\rho\right) \tag{D3}$$

$$\rho = \frac{1+j}{2}\sqrt{kR}\left(\cos(\theta) + \frac{1}{Z}\right) \tag{D4}$$

The complex function $w(\rho) = \exp(-\rho^2)\mathrm{erfc}(-j\rho)$ in Eq. (D3) can be determined by an approximate method as described in the following. x and y is the real and imaginary parts of ρ (ρ = x + jy).

|x| > 3.9 ∨ |y| > 3:

$$\rho_+ = |x| + j|y| \tag{D5}$$

$$w(\rho) = \begin{cases} w_+(\rho) & x > 0 \wedge y > 0 \\ w_+^*(\rho_+) & x < 0 \wedge y > 0 \\ 2e^{-(\rho_+^*)^2} - w_+^*(\rho_+) & y < 0 \end{cases} \tag{D6}$$

where * denotes complex conjugation and w_+ is calculated by Eq. (D7) or (D8)

$x > 6 \vee y > 6$:

$$w_+(\rho) = j\rho\left(\frac{0.5124242}{\rho^2 - 0.2752551} + \frac{0.05176536}{\rho^2 - 2.724745}\right) \tag{D7}$$

else

$$w_+(\rho) = j\rho\left(\frac{0.4613135}{\rho^2 - 0.1901635} + \frac{0.09999216}{\rho^2 - 1.7844927} + \frac{0.002883894}{\rho^2 - 5.5253437}\right) \tag{D8}$$

$|x| \le 3.9 \wedge |y| \le 3$:

$$h = 0.8 \tag{D9}$$

$$A_1 = \cos(2xy) \tag{D10}$$

$$B_1 = \sin(2xy) \tag{D11}$$

$$C_1 = e^{-2y\pi/h} - \cos(2x\pi/h) \tag{D12}$$

$$D_1 = \sin(2x\pi/h) \tag{D13}$$

$$P_2 = 2e^{-\left(x^2 + 2y\pi/h - y^2\right)}\frac{A_1C_1 - B_1D_1}{C_1^2 + D_1^2} \tag{D14}$$

$$Q_2 = 2e^{-\left(x^2 + 2y\pi/h - y^2\right)}\frac{A_1D_1 + B_1C_1}{C_1^2 + D_1^2} \tag{D15}$$

$$H = \frac{hy}{\pi\left(x^2 + y^2\right)} + \frac{2yh}{\pi}\sum_{n=1}^{5}\frac{e^{-n^2h^2}\left(x^2 + y^2 + n^2h^2\right)}{\left(y^2 - x^2 + n^2h^2\right)^2 + 4x^2y^2} \tag{D16}$$

$$K = \frac{hx}{\pi\left(x^2 + y^2\right)} + \frac{2xh}{\pi}\sum_{n=1}^{5}\frac{e^{-n^2h^2}\left(x^2 + y^2 - n^2h^2\right)}{\left(y^2 - x^2 + n^2h^2\right)^2 + 4x^2y^2} \tag{D17}$$

$$w(\rho) = H + P_2 + j\left(K - Q_2\right) \tag{D18}$$

Appendix E

Calculation of $h_{S,Fz}$ and $h_{R,Fz}$

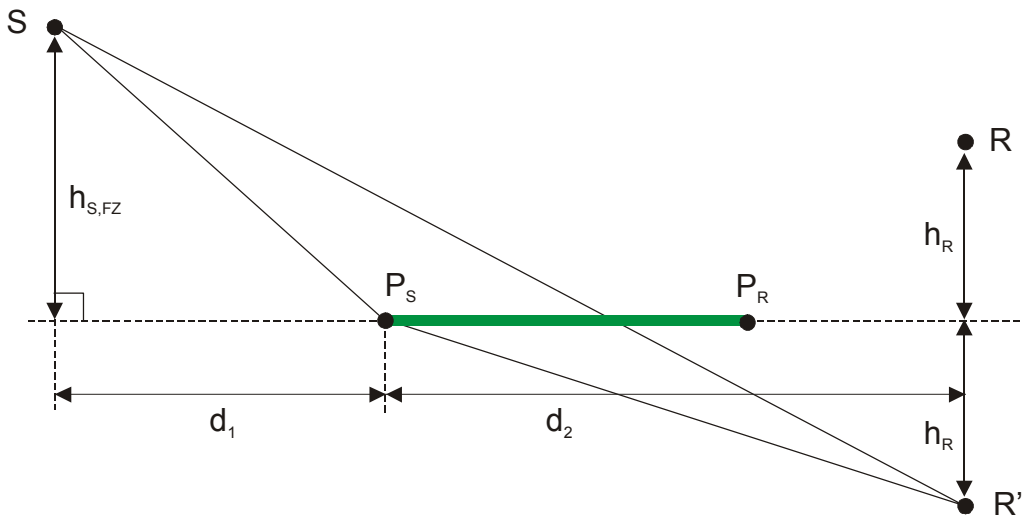

Figure E1

$h_{S,Fz}$ is the height where the following equation is fulfilled:

$$\left|SP_S\right| + \left|P_S R'\right| - \left|SR'\right| = F_\lambda \lambda \tag{E1}$$

where F_λ is the fraction of the wavelength λ used in the Fresnel-zone interpolation method.

$$x_1 = \left(\sqrt{\left(h_R^2 + d_2^2\right)} - F_\lambda \lambda\right)^2 \tag{E2}$$

$$x_2 = h_R^2 + \left(d_1 + d_2\right)^2 - d_1^2 - x_1 \tag{E3}$$

$$A = 4\, h_R^2 - 4\, x_1 \tag{E4}$$

$$B = 4\, h_R\, x_2 \tag{E5}$$

$$C = x_2^2 - 4\, d_1^2\, x_1 \tag{E6}$$

$$h_{S,Fz} = \frac{-B - \sqrt{B^2 - 4\,AC}}{2A} \qquad \text{(E7)}$$

The solution shown above for $h_{S,Fz}$ is only valid if d_2 is not to small compared to $F_\lambda\lambda$. If the following expression is fulfilled

$$\sqrt{d_2^2 + h_R^2} - h_R \leq F_\lambda \lambda \qquad \text{(E8)}$$

then $h_{S,Fz}$ is set equal to ∞.

The principle outlined above is also used to calculate $h_{R,Fz}$ by interchanging S and R in Figure E1 and in the equations.

Appendix F

Crossing of Wedge Faces

When calculating the equivalent wedge for a valley-shaped terrain as shown in Figure 17 the top point of the wedge is defined by the intersection between two line segments as defined in Figure F1. Line segment 1 is defined by the end coordinates (x_1,z_1) and (x_2,z_2) and line segment 2 by the coordinates (x_3,z_3) and (x_4,z_4). It is assumed that $x_1 < x_2 < x_3 < x_4$.

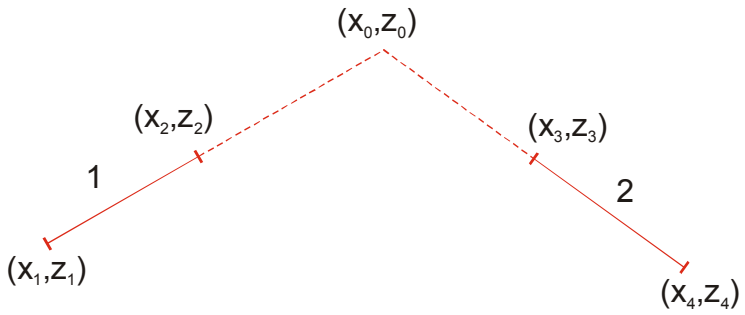

Figure F1

The top point (x_0,z_0) is determined as described in the following.

$$D = (x_2 - x_1)(z_4 - z_3) - (x_4 - x_3)(z_2 - z_1) \tag{F1}$$

$$s = \frac{(x_4 - x_1)(z_4 - z_3) - (x_4 - x_3)(z_4 - z_1)}{D} \tag{F2}$$

$$t = \frac{(x_2 - x_1)(z_4 - z_1) - (x_4 - x_1)(z_2 - z_1)}{D} \tag{F3}$$

If $s \geq 1 \wedge t \geq 1$:

$$x_0 = x_1 + (x_2 - x_1)\,s \tag{F4}$$

$$z_0 = z_1 + (z_2 - z_1)\,s \tag{F5}$$

If t < 1:

$$x_0 = x_3 \tag{F4}$$

$$z_0 = z_3 \tag{F5}$$

If s < 1:

$$x_0 = x_2 \tag{F6}$$

$$z_0 = z_2 \tag{F7}$$

Appendix G

Normalized Scattered Level Tables L_{ws0} and L_{ts0}

L_{ws0}	40 R_2/R_1									
$40h_e/R_1$	10	20	30	40	50	60	70	80	90	100
5	-41.6	-33.9	-30.2	-27.9	-26.2	-24.9	-23.9	-23.1	-22.4	-21.8
10	-49.9	-44.0	-39.5	-36.7	-34.7	-33.1	-31.8	-30.9	-30.1	-29.3
15	-52.1	-48.9	-45.8	-42.9	-40.7	-39.1	-37.7	-36.6	-35.5	-34.7
20	-53.8	-51.0	-48.8	-46.8	-45.0	-43.5	-42.1	-40.9	-39.9	-39.1
25	-55.4	-52.4	-50.4	-48.8	-47.5	-46.2	-45.1	-44.0	-43.1	-42.2
30	-57.0	-53.8	-51.5	-50.6	-48.9	-47.8	-46.8	-45.9	-45.2	-44.4
35	-58.6	-55.1	-52.7	-51.1	-49.8	-48.8	-47.9	-47.1	-46.4	-45.7
40	-59.9	-56.5	-53.9	-52.1	-50.7	-49.6	-48.7	-48.0	-47.3	-46.6

Table G1
Normalized scattered level L_{ws0} from wind turbulence.

L_{ts0}	40 R_2/R_1									
$40h_e/R_1$	10	20	30	40	50	60	70	80	90	100
5	-44.0	-39.1	-36.0	-34.0	-32.5	-31.3	-30.4	-29.6	-28.9	-28.3
10	-47.4	-44.7	-42.4	-40.5	-39.1	-37.9	-36.9	-36.0	-35.3	-34.7
15	-48.9	-46.7	-45.1	-43.6	-42.4	-41.4	-40.5	-39.7	-39.0	-38.4
20	-50.2	-48.0	-46.4	-45.2	-44.1	-43.2	-42.4	-41.7	-41.1	-40.5
25	-51.4	-49.0	-47.4	-46.2	-45.2	-44.3	-43.6	-42.9	-42.3	-41.8
30	-52.5	-50.0	-48.3	-47.0	-46.0	-45.1	-44.4	-43.7	-43.2	-42.6
35	-53.6	-51.0	-49.2	-47.8	-46.7	-45.8	-45.0	-44.4	-43.8	-43.3
40	-54.6	-52.0	-50.0	-48.5	-47.4	-46.4	-45.6	-44.9	-44.3	-43.8

Table G2
Normalized scattered level L_{ts0} from temperature turbulence.

Inside the table linear interpolation is used and outside the nearest value is used.

Appendix H

Propagation Effect of a Finite Impedance Wedge

The geometrical parameters used in the diffraction solution for a finite impedance wedge is shown in Figure H1. In the presentation of the solution shown in the following it is assumed that $0 \le \theta_R \le \theta_S \le \beta \le 2\pi$. If this is not the case the angles have to be modified as described in the end of this appendix.

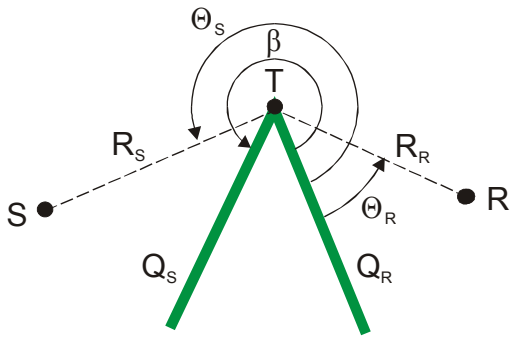

Figure H1
Definition of parameters for calculation of the propagation effect of a wedge-shaped screen with finite surface impedance.

The wedge solution shown in Eq. H1 (from [5]) contains four terms which can be interpreted as being the contribution of four rays from source or image source to receiver or image receiver. p_{diffr} is the diffracted sound pressure, k is the wave number and P is the length of the diffracted path ($P = R_S + R_R$).

$$p_{diffr} = -\frac{1}{\pi}\sum_{n=1}^{4} Q_n A(\theta_n) E_v\left(A(\theta_n)\right)\frac{e^{jk\ell}}{\ell} \qquad \text{(H1)}$$

The angle θ_n is defined by

$\theta_1 = \theta_S - \theta_R$

$\theta_2 = \theta_R + \theta_S$

$\theta_3 = 2\beta - (\theta_R + \theta_S)$

$\theta_4 = 2\beta - (\theta_S - \theta_R)$

The "reflection coefficient" Q_n is given by

$Q_1 = 1$

$Q_2 = Q_R$

$Q_3 = Q_S$

$Q_4 = Q_S Q_R$

Q_S is calculated using P as the distance parameter and $\psi_G = \beta - \theta_S$ as the grazing angle. Q_R is calculated using P as the distance parameter and $\psi_G = \theta_R$ as the grazing angle. If ψ_G becomes greater than $\pi/2$, $\psi_G = \pi/2$ is used instead.

***Note**: The use of P as the distance parameter when calculating Q_S and Q_R instead of the normally used values R_S and R_R has been preferred to avoid discontinuities when reflections in the wedge faces are included as described below. It can also be discussed which approach is correct when ψ_G exceeds $\pi/2$ where no obvious physical interpretation exists. Again, the choice has been made mainly to avoid discontinuities. However, both choices will have a very limited influence on the overall result.*

$E_\nu(A(\theta_n))$ is calculated by Eq. (H2) where $\nu = \pi/\beta$ is the wedge index. The solution is only valid for wedge angles greater than π.

$$E_\nu\left(A(\theta_n)\right) = \frac{\pi}{\sqrt{2}} \frac{\sin\left|A(\theta_n)\right|}{\left|A(\theta_n)\right|} \frac{e^{j\pi/4}}{\sqrt{1 + \left(\frac{2R_S R_R}{\ell^2} + \frac{1}{2}\right)\frac{\cos^2\left|A(\theta_n)\right|}{\nu^2}}} A_D(B) \qquad \text{(H2)}$$

In the equation $A(\theta_n)$ is given by Eq. (H3), B by Eq. (H4) and $A_D(B)$ by Eq. (H5). H(x) is Heavisides' step function (H = 1 for $x \geq 0$ and H = 0 for $x < 0$).

$$A(\theta_n) = \frac{\nu}{2}(-\beta - \pi + \theta_n) + \pi H(\pi - \theta_n) \qquad \text{(H3)}$$

$$B = \sqrt{\frac{4kR_S R_R}{\pi\ell}} \frac{\cos\left|A(\theta_n)\right|}{\sqrt{\nu^2 + \left(\frac{2R_S R_R}{\ell^2} + \frac{1}{2}\right)\cos^2\left|A(\theta_n)\right|}} \qquad \text{(H4)}$$

$$A_D(B) = sign(B)\left(f(|B|) - jg(|B|)\right) \qquad \text{(H5)}$$

In Eq. (H5) sign(x) is the signum function (sign = 1 for x > 0, sign = 0 for x = 0, sign = -1 for x < 0). f(x) and g(x) are the auxiliary Fresnel-functions. If x≥ 5 f(x) and g(x) are calculated by Eqs. (H6) and (H7). If 0 < x < 5 f(x) is calculated by the polynomial fit in Eq. (H8). The constants a_0 to a_{12} are defined in Table H1. A similar polynomial fit is used to calculate g(x) using the constants a_0 to a_{12} defined in Table H2.

$$f(x) = \frac{1}{\pi x} \tag{H6}$$

$$g(x) = \frac{1}{\pi^2 x^3} \tag{H7}$$

$$f(x) = \sum_{n=0}^{12} a_n x^n \tag{H8}$$

a_{12}	0.00000019048125
a_{11}	-0.00000418231569
a_{10}	0.00002262763737
a_9	0.00023357512010
a_8	-0.00447236493671
a_7	0.03357197760359
a_6	-0.15130803310630
a_5	0.44933436012454
a_4	-0.89550049255859
a_3	1.15348730691625
a_2	-0.80731059547652
a_1	0.00185249867385
a_0	0.49997531354311

Table H1
Constants in polynomial fit of f(x) for 0 < x < 5.

a_{12}	-0.00000151974284
a_{11}	0.00005018358067
a_{10}	-0.00073624261723
a_9	0.00631958394266
a_8	-0.03513592318103
a_7	0.13198388204736
a_6	-0.33675804584105
a_5	0.55984929401694
a_4	-0.50298686904881
a_3	-0.06004025873978
a_2	0.80070190014386
a_1	-1.00151717179967
a_0	0.50002414586702

Table H2
Constants in polynomial fit of g(x) for 0 < x < 5.

If the wedge edge is below the line from the source to the receiver ($\theta_1 < \pi$) the contribution from the direct ray shall be added to the solution as shown in Eq. (H9). R_1 which is the direct distance between the source and receiver is calculated by Eq. (H10).

$$p = p_{diffr} + \frac{e^{jkR_1}}{R_1} \tag{H9}$$

$$R_1 = \sqrt{R_S^2 + R_R^2 - 2R_S R_R \cos(\theta_1)} \tag{H10}$$

If the wedge edge is below the line from the source to the image receiver ($\theta_2 < \pi$) the contributions from the direct ray as well as the ray reflected in the receiver face of the wedge shall be added to the solution as shown in Eq. (H11). R_2 which is the direct distance between the source and image receiver is calculated by Eq. (H12). Q_R is the reflection coefficient calculated on basis of R_2 and $\psi_{G,R}$ determined by Eq. (H13).

$$p = p_{diffr} + \frac{e^{jkR_1}}{R_1} + Q_R \frac{e^{jkR_2}}{R_2} \tag{H11}$$

$$R_2 = \sqrt{R_S^2 + R_R^2 - 2R_S R_R \cos(\theta_2)} \tag{H12}$$

$$\psi_{G,R} = \arcsin\left(\frac{R_S \sin\theta_S + R_R \sin\theta_R}{R_2}\right) \tag{H13}$$

If the wedge edge is below the line from the image source to the receiver ($\theta_3 < \pi$) the contributions from the direct ray as well as the ray reflected in the source face of the wedge shall be added to the solution as shown in Eq. (H14). R_3 which is the direct distance between the image source and receiver is calculated by Eq. (H15). Q_S is the reflection coefficient calculated on basis of R_3 and $\psi_{G,S}$ determined by Eq. (H16).

$$p = p_{diffr} + \frac{e^{jkR_1}}{R_1} + Q_S \frac{e^{jkR_3}}{R_3} \tag{H14}$$

$$R_3 = \sqrt{R_S^2 + R_R^2 - 2R_S R_R \cos(\theta_3)} \tag{H15}$$

$$\psi_{G,S} = \arcsin\left(\frac{R_S \sin(\beta - \theta_S) + R_R \sin(\beta - \theta_R)}{R_3}\right) \tag{H16}$$

If $\theta_n = \pi$ numerical problems will occur when calculating the diffracted sound pressure according to Eq. (H1). This can be fixed by subtracting a small quantity ε from θ_n when $|\theta_n - \pi| < \varepsilon$. $\varepsilon = 10^{-8}$ has been found suitable but may depend on the implementation.

***Note**: The procedure described above is not valid when the source and receiver is on the same side of the wedge edge, but this case will not occur in the comprehensive model.*

In cases where the source and receiver are reflected by a ground surface before and after the wedge the calculation will also be carried out for the image source and receiver as described in Sections 4.4.3.5 and 4.4.3.6. In such cases the "source" or "receiver" may be inside the wedge. This is taken care of by modifying the angles according to the following scheme where θ'_R, θ'_S and β' are the modified angles.

$0 > \theta_R > \beta - 2\pi$:

$\theta'_R = 0$

$\theta'_S = \theta_S - \theta_R$

$\beta' \quad = \beta - \theta_R$

$\theta_R \leq \beta - 2\pi$:

$\theta'_R = 0$

$\theta'_S = 2\pi-(\beta - \theta_S)$

$\beta' = 2\pi$

$\beta < \theta_S < 2\pi$ (θ'_S and β' are used instead when modified above):

$\beta' = \theta_S$

$\theta_S \geq 2\pi$ (θ'_S is used instead when modified above):

$\theta'_S = 2\pi$

$\beta' = 2\pi$

Appendix I

Determination of the Equivalent Flat Terrain by the Least Squares Method

The start and end coordinates of each terrain segment i of n segments are:

Start coordinate: x_{i-1},z_{i-1}

End coordinate: x_i,z_i

The equivalent flat terrain to be estimated is:

$$z = \alpha + \beta x \tag{I1}$$

The parameters α and β are determined as shown in the following:

$$\bar{x} = \frac{x_n + x_0}{2} \tag{I2}$$

$$\bar{z} = \frac{1}{x_n - x_0} \sum_{i=1}^{n} \frac{\gamma_i}{2}\left(x_i^2 - x_{i-1}^2\right) + \left(z_{i-1} - \gamma_i x_{i-1}\right)\left(x_i - x_{i-1}\right) \tag{I3}$$

where γ_i is the slope of segment i:

$$\gamma_i = \frac{z_i - z_{i-1}}{x_i - x_{i-1}} \tag{I4}$$

$$t_2 = \frac{x_n^2 - x_0^2}{3} - \bar{x}\left(x_n^2 - x_0^2\right) + \bar{x}^2\left(x_n - x_0\right) \tag{I5}$$

$$t_1 = \sum_{i=1}^{n} \frac{\gamma_i}{3}\left(x_i^2 - x_{i-1}^2\right) + \frac{z_{i-1} - \bar{z} - \gamma_i\left(x_{i-1} + \bar{x}\right)}{2}\left(x_i^2 - x_{i-1}^2\right) + \bar{x}\left(\gamma_i x_{i-1} - z_{i-1} + \bar{z}\right)\left(x_i - x_{i-1}\right) \tag{I6}$$

$$\beta = \frac{t_1}{t_2} \tag{I7}$$

$$\alpha = \bar{z} - \bar{x}\beta \tag{I8}$$

The average height of the terrain Δh above the equivalent flat terrain can subsequently be calculated based on the area of each segment A_i above the equivalent flat terrain (Δh will be the same if A_i is the area of the terrain below the equivalent flat terrain):

$$\Delta h = \frac{1}{x_n - x_0} \sum_{i=1}^{n} A_i \tag{I9}$$

A_i is calculated as shown in the following.

For each segment the vertical height of the terrain relative to the equivalent flat terrain h_{i-1} at the start of the segment and h_i at the end of the segment are determined by Eqs. (I10) and (I11).

$$h_{i-1} = z_{i-1} - \alpha - \beta x_{i-1} \tag{I10}$$

$$h_i = z_i - \alpha - \beta x_i \tag{I11}$$

Depending on h_{i-1} and h_i the area A_i can be determined:

$h_i h_{i-1} \geq 0$ (h_i and h_{i-1} have same sign indicating that the segment and the equivalent flat terrain do not intersect)

$$A_i = \frac{h_i + h_{i-1}}{2}\left(x_i - x_{i-1}\right) \tag{I12}$$

If $A_i<0$, A_i is set to 0.

$h_i h_{i-1} < 0$ (h_i and h_{i-1} have opposite signs indicating that the segment and the equivalent flat terrain intersects)

The x-coordinate x_x at the point of intersection is:

$$x_x = \frac{|h_{i-1}|}{|h_i| + |h_{i-1}|}\left(x_i - x_{i-1}\right) + x_{i-1} \tag{I13}$$

$$A_i = \begin{cases} \frac{h_{i-1}}{2}\left(x_x - x_{i-1}\right) & h_{i-1} > 0 \\ \frac{h_i}{2}\left(x_i - x_x\right) & h_{i-1} < 0 \end{cases} \tag{I14}$$

Appendix J

Scattering Zone Attenuation Table $\Delta L(h', \alpha, R')$

R'	h'=0.01			h'=0.1			h'=1		
	α=0	α=0.2	α=0.4	α=0	α=0.2	α=0.4	α=0	α=0.2	α=0.4
0.0625	6.0	6.0	6.0	6.0	6.0	6.0	6.0	6.0	6.0
0.125	0.0	0.0	0.0	0.0	0.0	0.0	0.0	0.0	0.0
0.25	-7.5	-7.5	-7.5	-6.0	-7.0	-7.5	-6.0	-7.0	-7.5
0.5	-14.0	-14.25	-14.5	-12.5	-13.5	-14.5	-12.5	-13.0	-14.0
0.75	-18.0	-18.8	-19.5	-17.3	-18.0	-19.0	-16.0	-16.8	-17.7
1	-21.5	-22.5	-23.5	-20.5	-21.6	-22.8	-19.3	-20.5	-21.3
1.5	-26.3	-27.5	-29.5	-25.5	-27.2	-29.0	-24.0	-25.5	-26.3
2	-31.0	-32.5	-34.5	-30.0	-32.0	-33.3	-27.5	-29.5	-30.8
3	-40.0	-42.5	-45.5	-37.5	-40.5	-42.9	-34.2	-36.0	-37.8
4	-49.5	-52.5	-56.3	-45.5	-49.5	-52.5	-40.4	-42.8	-45.5
6	-67.0	-72.5	-78.0	-62.0	-67.0	-72.0	-52.5	-56.2	-60.0
10	-102.5	-113.0	-122.5	-94.7	-103.7	-112.0	-78.8	-84.0	-89.7

The value of $\Delta L = \Delta L\ (h', \alpha, R')$ for more general (h, α, R) may be found by tricubic interpolation:

1) From $\Delta L(h_i, \alpha_j, R_k)$ interpolate in h for each (α_j, R_k) to get $\Delta L(h, \alpha_j, R_k)$
2) From $\Delta L(h, \alpha_j, R_k)$ interpolate in α for each R_k to get $\Delta L(h, \alpha, R_k)$
3) From $\Delta L(h, \alpha, R_k)$ interpolate in R to get $\Delta L(h, \alpha, R_k)$

This should explain the term 'tri' in the above 'tricubic', when it is understood that each interpolation is a cubic interpolation through the two samples on each side of the argument. In the case of h and α this means actually a quadratic interpolation since we only have three samples, and this also applies at the boundary for R.

It can be considered to replace the cubic interpolation with for instance natural cubic spline interpolation in each dimension, but the above tricubic interpolation gives satisfactory results.